RE-ORDER NO. 66-196

ANALYSIS OF THERMAL TEST ERRORS RESULTING FROM IMPERFECTLY COLLIMATED SOLAR SIMULATION BEAMS

PHASE I

(JPL Contract 951330)

for

Jet Propulsion Laboratory
Pasadena, California

21 March 1966

MSC Project No: EC-34

Prepared by:

Edwin J. Gooze

Edwin J. Gooze

This work was performed for the Jet Propulsion Laboratory, California Institute of Technology, sponsored by the National Aeronautics and Space Administration under Contract NAS7-100.

John J. Brooks

John J. Brooks

Approved by:

Arlyn F. Winemiller

Arlyn F. Winemiller

THE MACNEAL-SCHWENDLER CORPORATION
2556 Mission Street
San Marino, California

IF 143

TABLE OF CONTENTS

TABLE OF CONTENTS

PHASE I

ANALYSIS OF THERMAL TEST ERRORS RESULTING FROM IMPERFECTLY COLLIMATED SOLAR SIMULATION BEAMS

1.0 INTRODUCTION

The document contained herein represents the final technical report on Phase I of Jet Propulsion Laboratory Contract No. 951330.

An ideal solar simulator source is considered to be an optical system which provides an incident illumination field on the surface of a test item, the properties of which are independent of position on any portion of the test item which has an unobstructed view of the source. A collimated solar simulator source provides an illumination field which is entirely within a total cone angle identical to that of the sun, 0^{o} 32' in earth's orbit. A decollimated source provides a field, the cone angle of which is larger than that of a perfectly collimated source.

One of the problems associated with thermal testing of a spacecraft in a space simulation chamber is that of evaluating errors due to non-collimation of simulated solar light beams in the chamber. This report is concerned with numerical evaluation of two of the effects of noncollimation: (1) in incident energy flux on black flat surfaces at various angles to the mean light ray; (2) in incident energy flux on black flat surfaces in the region of shadows (penumbra) cast by various surfaces due to the decollimated solar simulator sources.

The technique used to calculate the required radiation shape factors represents a departure from the standard method of double integrating a scalar function associated with the intensity distribution of the emitter (source)

and geometries of the emitter and receiver. The power transmitted from a differential element of source to a point on a receiver can be represented by a vector since the direction from which the power comes is as important as its magnitude. The double integrals which must be evaluated in conventional methods can frequently be expressed as integrals of the scalar (dot) product of a receiving surface normal vector and a power vector from a point on the source to a point on the receiver. For the sources and shading bodies considered in this report, evaluation of the vector integral is equivalent to calculating the area of the visible portion of the source and locating the centroid of that visible area.

The numerical results presented are in the form of energy flux density distributions within penumbrae for various shaded surfaces illuminated by solar simulation models corresponding to: (a) a uniformly radiating circular disc and (b) a module source with each module being a uniformly radiating circular disc. The shaded surfaces considered are:

(1) Single knife edge

(2) Knife edge with a diffuse or a specular skirt

(3) Double knife edge

(4) Rectangular "cylinder" having diffuse or specular reflective properties.

(5) Circular cylinder having diffuse or specular reflective properties.

The actual solutions were implemented through the use of digital calculating programs. However, the methods of solution outlined are applicable to other forms of calculations.

2.0 METHOD OF ANALYSIS

A detailed description of the analytic approach used in obtaining solutions is presented in Section 2.1. The application of the method detailed in Section 2.1 to the general class of unshaded and shaded surfaces considered in this report is described in Section 2.2. The solutions corresponding to particular shaded surfaces illuminated by a uniform solar simulator source are presented in Sections 2.3 through 2.7. Solutions appropriate to module solar simulator sources are presented in Section 3.0.

2.1 DESCRIPTION OF ANALYTICAL APPROACH

Energy Exchange Between Two Black Bodies

Consider two black bodies separated by nonabsorbing media. Let the hotter body, the emitter, be referred to as A_1 and the receiver be referred to as A_2. The geometry under consideration is shown in Fig. 1.

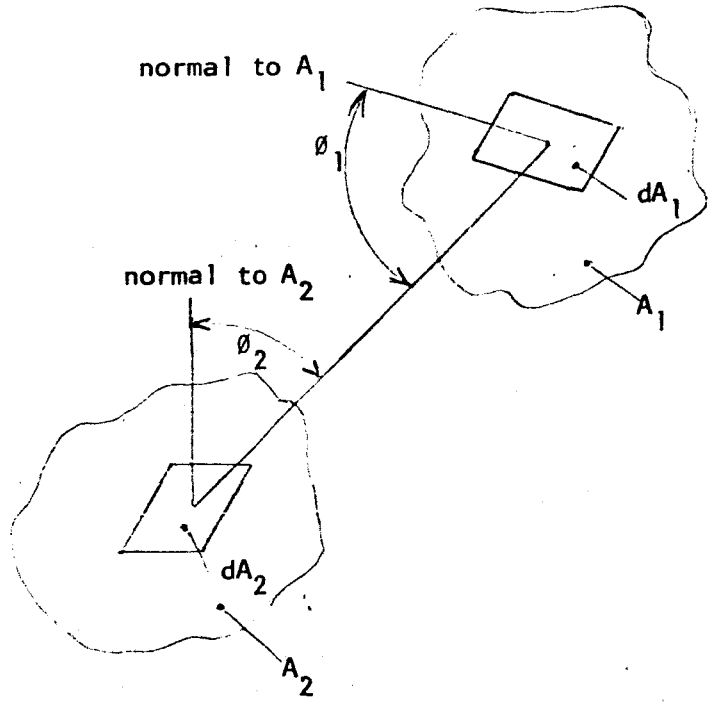

FIG. 1

The rate of radiation from a differential area on A_1, dA_1, to a differential area on the receiver, dA_2, will be proportional to the apparent area of the emitter, dA_1, viewed from dA_2 of $dA_1\cos\phi_1$, the apparent area of interceptor, dA_2, viewed from dA_1 or $dA_2\cos\phi_2$, and inversely proportional to the square of the distance separating dA_1 and dA_2 (Ref. 1). Therefore, referring to Fig. 1

$$d(dq_{12}) = \frac{I_1 dA_1 \cos\phi_1 dA_2 \cos\phi_2}{r^2} \qquad (2.1.1)$$

where

$d(dq_{12})$ = Radiation leaving surface dA_1 that is intercepted by dA_2.

I_1 = Intensity of radiation and is defined as the radiant energy propagating in a particular direction per unit solid angle per unit area dA_1 as projected on a plane perpendicular to the direction of propagation.

Now note that

$dA_1\cos\phi_1$ = projected area of dA_1 in direction ϕ_1

$\frac{dA_2\cos\phi_2}{r^2}$ = solid angle subtended by dA_2 at dA_1

$$d(dq_{12}) = \frac{I_1 dA_1 \cos\phi_1}{r^2} dA_2\cos\phi_2 \qquad (2.1.2)$$

Transition to Vector Notation

Define a vector $\overline{dE}$ that has the same direction as an arbitrary vector $\overline{r}$ and a magnitude equal to the energy flux density from an area dA_1 to an area normal to $\overline{r}$ ($dA_2\cos\phi_2$). If r is much larger than any dimension fixing A_1 or A_2, the source, A_1, can be considered on the surface of a sphere of radius, r, and centered at dA. Then $\phi_1 = 0$ and from Fig. 1 and Eq. 2.1.2

$$\left|\overline{dE}_{12}\right| = \frac{I_1 dA_1}{r^2} \qquad (2.1.3)$$

and

$$dE_{12} = \frac{I_1 dA_1}{r^2}\left\{\frac{\overline{r}}{r}\right\} \qquad (2.1.4)$$

Let

$\overline{dA_2}$ = vector having magnitude dA_2 and direction normal to plane of A_2

$$\overline{dA_2} = dA_2\left\{\frac{\overline{dA_2}}{dA_2}\right\} \qquad (2.1.5)$$

Since

$$\overline{A} \cdot \overline{B} = AB\cos(\angle \text{between } \overline{A} \text{ and } \overline{B})$$

Eq. (2.1.2) can be expressed using vector notation simply as

$$d(dq_{12}) = \frac{I_1 dA_1}{r^2}\, dA_2\left\{\frac{\overline{r}}{r}\right\} \cdot \left\{\frac{\overline{dA_2}}{dA_2}\right\} = -\overline{dA_2} \cdot \overline{dE}_{12} \qquad (2.1.6)$$

where the minus sign is due to the fact that $\overline{dA}_2$ and $\overline{dE}_{12}$ are in opposite directions as indicated in Fig. 2.

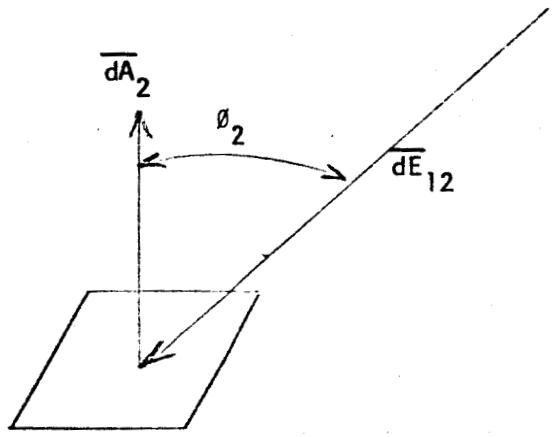

FIG. 2

The energy flux at dA_2 due to the complete source is found by integrating over A_1 and interchanging the order of scalar product and the integration. From Eq. (2.1.6)

$$dq_{12} = - \overline{dA}_2 \cdot \int_{A_2} \overline{dE}_{12} \tag{2.1.7}$$

or, in general

$$dq \triangleq - \overline{dA} \cdot \overline{E} \tag{2.1.8}$$

Equation (2.1.8) exhibits the principle that the integrated radiation from all parts of the actual source, S, to dA can be represented by radiation from a single point source. Care must be taken in using this fact, since S must be defined to include <u>all</u> areas of source "seen" on the positive side of dA and <u>only</u> those areas. This last rule is interpreted by the example in Fig. 3. The area, S, must include S_1 (the visible part of a direct source composed of S_1 and S_2) and S_4 (the visible part of a reflector "source" between the real source and dA). Area S must <u>not</u> include S_2 or S_3 (since dA cannot "see" them) nor S_5 (since S_5 is not illuminated).

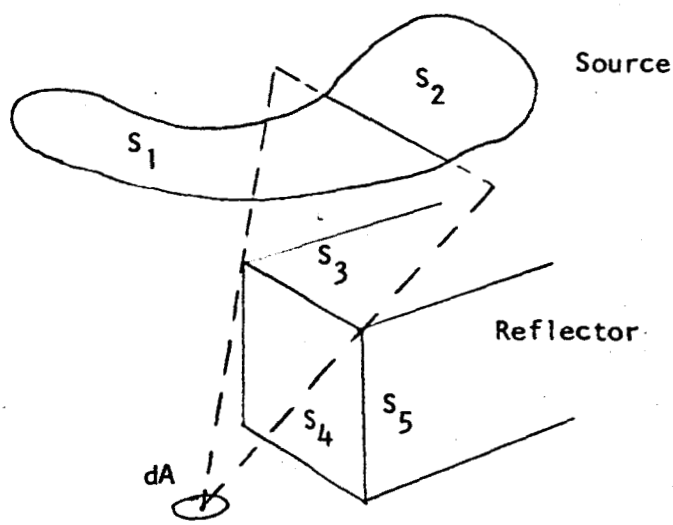

FIG. 3

Referring to Fig. 3 and Eq. 2.1.7, it is evident that S_1 and S_4 can be treated separately, so that

$$\bar{E} = \bar{E}_1 + \bar{E}_4 = \int_{S_1} \overline{dE} + \int_{S_2} \overline{dE}$$

or, in general

$$E = \sum_{i=1}^{n} \int_{S_i} \overline{dE} \tag{2.1.9}$$

where the S_i are conveniently separable areas of direct and reflected illumination.

The next question which arises is that of evaluating the effective position of a point source which represents the visible portion of an otherwise simple shape. It is obvious from symmetry considerations that the equivalent point source for a circle is at the center of the area.

For uniform intensity surfaces on a spherical source, the location of the equivalent point source is at the centroid of the visible area, and for nonuniform intensity, it is at the centroid found by weighting the differential area elements, dS, with the local intensity. For surfaces not on a sphere, the equivalent point passes through the centroid of the area weighted by $\frac{I}{r^2}$. These facts are evident from the definition of $\bar{E}$ given in Eq. 2.1.4.

$$\bar{E} \triangleq \int_{S_{visible}} \frac{I}{r^2} \left\{ \frac{\bar{r}}{r} \right\} dS \tag{2.1.10}$$

where, in Eq. 2.1.4, $dS = dA_1$ and $I = I_1$.

Equation (2.1.10) has exactly the form used in elementary mechanics to find centroids of weighted areas. The only difference is that the vector E does not have units of distance and hence does not end on the physical centroid of the surface in question. However, $\bar{E}'$, defined by

$$\bar{E}' \triangleq \frac{\bar{E}}{\int \frac{I}{r^2}\, dS} = \frac{\int \frac{I}{r^2}\left\{\frac{\bar{r}}{r}\right\} dS}{\int \frac{I}{r^2}\, dS} \qquad (2.1.11)$$

is a vector which terminates at the weighted centroid, and Eq. (2.1.11) shows that $\bar{E}$ is merely a scalar multiple of $\bar{E}'$

2.2 METHOD OF ANALYSIS FOR UNSHADED AND SHADED SURFACES - GENERAL

The method of analysis was simplified by the following assumptions

(1) The source is on the surface of a sphere centered at dA, i.e, $\overline{dE}$ is considered normal to the source for any point in the penumbra.

(2) The distance from any point in the penumbra to the source is much larger than any other characteristic dimension.

(3) Lower order trigonometric approximations are appropriate, i.e., $\sin(D/2) = \tan(D/2) = D/2$, and $\cos(D/2) = 1 - D^2/8$. where D is the solar field angle and defines the cone of radiation.

Unshaded Surface

With no umbra or penumbra present, an element area dA "sees" the entire source. Consider two different solar simulator sources each with an intensity distribution that possesses axial symmetry. Then

$$\overline{E_1}' = \overline{E_2}' \tag{2.2.1}$$

where $\overline{E}'$ is defined in Eq. (2.1.11). If it is assumed that the magnitude of the total power from each source is the same, then from Eq. (2.1.3)

$$\left|\overline{E}_1\right| = \left|\overline{E}_2\right| \tag{2.2.2}$$

or

$$\int_{S_1} \frac{I_1 dS}{r^2} = \int_{S_2} \frac{I_2 dS}{r^2} \tag{2.2.3}$$

Inspection of Eqs. (2.1.11), (2.2.1) and (2.2.3) leads to the result

$$\overline{E}_1 = \overline{E}_2 \tag{2.2.4}$$

In general, all solar simulator sources of equal power that have intensity distributions that possess axial symmetry have the same power vector. Furthermore, of most importance, for unshaded geometries all ideal solar simulator sources with the same E vector are equivalent to the same point source and produce energy flux density on a flat black

plate given by

$$\frac{dq}{dA} = \bar{E}\left\{\frac{\overline{dA}}{dA}\right\} \qquad (2.2.4a)$$

independent of the source intensity distribution within the symmetry restrictions and independent of the degree of decollimation.

The effect of incident angle on the energy flux density on unshaded surfaces is now evident since, by definition of the scalar product of two vectors, Eq. (2.2.4) is evaluated as

$$\frac{dq}{dA} = E \cos \beta \qquad (2.2.5)$$

where β = angle between $\bar{E}$ and $\overline{dA}$ vectors. Therefore, the energy flux density on unshaded surfaces varies as the cosine of the angle of incidence, B, for all symmetric sources.

Shaded Surface

When a body is placed between the source and receiver, a point on the receiver in the penumbra due to the shading body has an obstructed view of the source. If diffraction effects are ignored, then, from simple geometric considerations, it can be reasoned that for each point in the penumbra there is some plane contained in the shading body perpendicular to the mean light ray that acts as the particular shading

body to that point. That is, every shading body may be considered composed of single knife edges. It follows that the solution for a single knife edge and the other shading bodies are intimately related. The solutions for the various shading bodies are obtained using the energy flux density distribution corresponding to a single knife edge and geometric properties associated with the various penumbrae.

2.3 METHOD OF ANALYSIS - SINGLE KNIFE EDGE

Using the principle of replacement of the visible source by an equivalent point source, Eq. (2.1.8), the problem is reduced to finding the area and centroid of the circular segment of the part of the source which is visible from each point in the penumbra. The problem is described, pictorially, in Fig. 4.

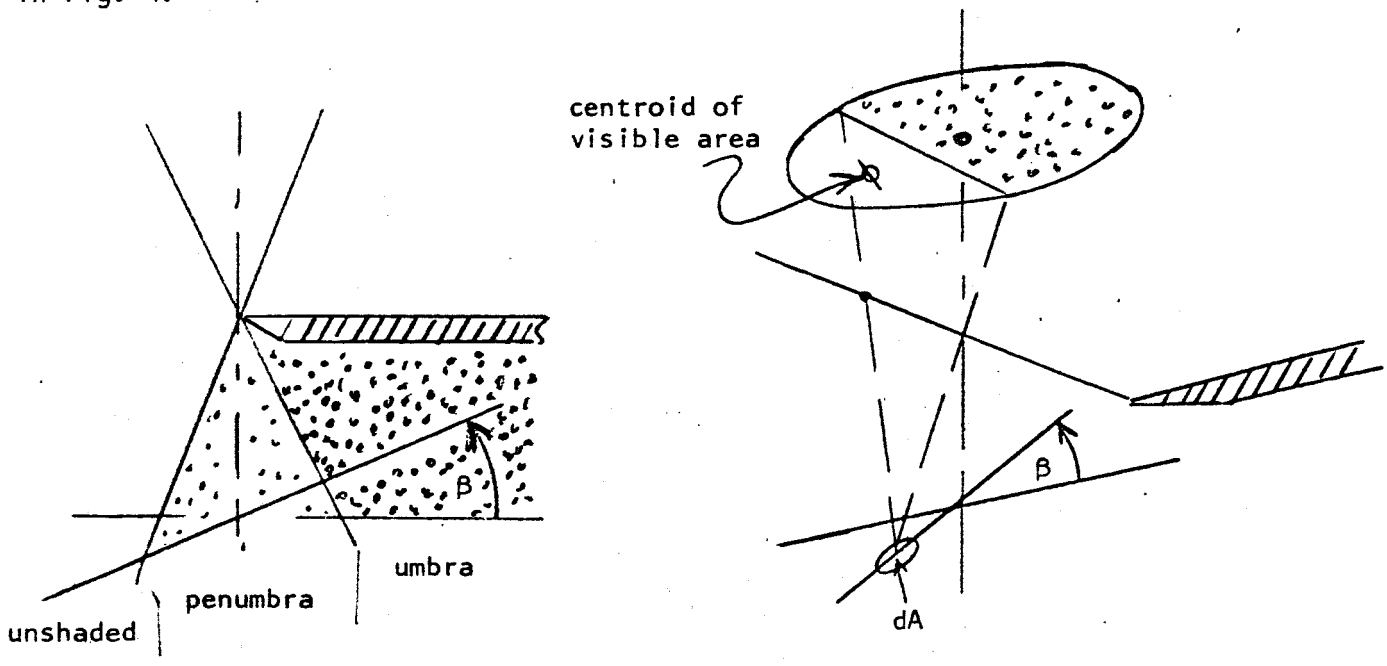

(a) (b)

FIG. 4

The detailed geometry and the natural parameters of the system are shown in Fig. 5.

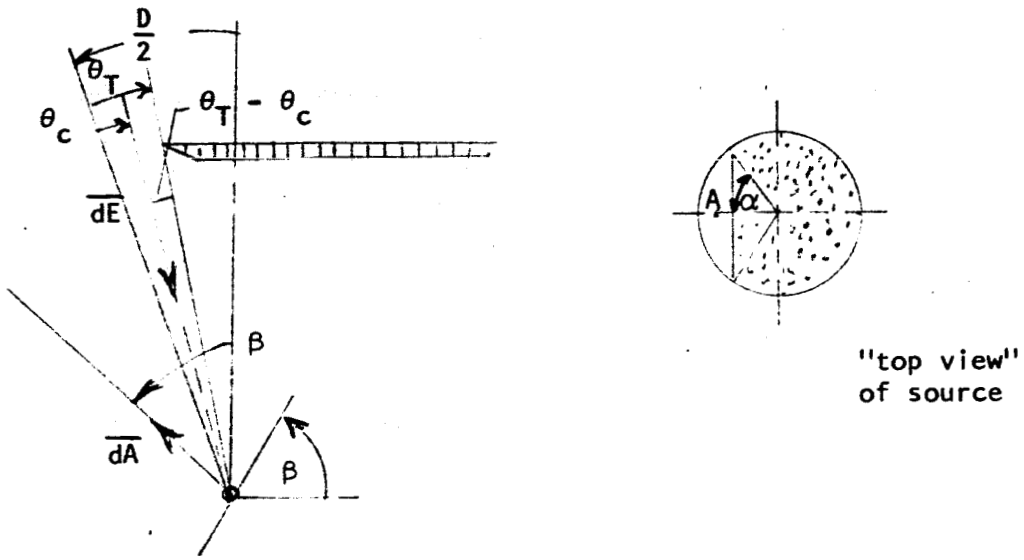

FIG. 5

The power incident on an area element dA is

$$dq = -\overline{dA} \cdot \overline{E} = E \cos\left[\beta - D\left\{\frac{1}{2} - \frac{\theta_c}{D}\right\}\right] dA \qquad (2.3.1)$$

The energy flux density is

$$\frac{dq}{dA} = E \cos\left[\beta - D\left\{\frac{1}{2} - \frac{\theta_c}{D}\right\}\right] \qquad (2.3.2)$$

Utilizing the geometrical properties of a circular segment, we find for a uniform source

$$E = \frac{(\alpha - \frac{1}{2}\sin 2\alpha)}{\pi} \int \frac{I dS}{r^2} \qquad (2.3.3)$$

The energy flux density at dA is, when normalized against the value which would be found outside the shadow,

$$Q \triangleq \frac{dq}{dA}\left[\cos\beta \int_S \frac{i dS}{r^2}\right]^{-1} = \frac{1}{\pi} \frac{\left\{\alpha - \frac{1}{2}\sin 2\alpha\right\} \cos\left[\beta - D\left\{\frac{1}{2} - \frac{\theta_c}{D}\right\}\right]}{\cos\beta} \qquad (2.3.4a)$$

or

$$Q = \frac{A \cos\left[\beta - D\left\{\frac{1}{2} - \frac{\theta_c}{D}\right\}\right]}{A_{Total}\cos\beta} \qquad (2.3.4b)$$

where

$$\alpha = \cos^{-1}\left\{1 - \frac{2\theta_T}{D}\right\} \qquad 0 < \alpha < \pi \qquad (2.3.5)$$

and

$$\frac{\theta_c}{D} = \frac{1}{2} - \frac{1}{3}\left\{\frac{\sin^3\alpha}{\alpha - \sin\alpha\cos\alpha}\right\} \qquad (2.3.6)$$

Equation (2.3.4b) shows that in calculating the relative flux density in the penumbra there are <u>two effects</u>:

(1) The magnitude of the incident $\bar{E}$ vector is reduced by $A_{visible}/A_{total}$

(2) The direction of the $\bar{E}$ vector is changed so that it passes through the centroid of the visible area rather than through the centroid of the total area of the source.

Now consider the knife edge fixed in position at the conical axis. The effect of considering the knife edge fixed as compared to a knife edge at various positions of insertion is discussed in Appendix A. The associated geometry for the fixed knife edge is shown in Fig. 6.

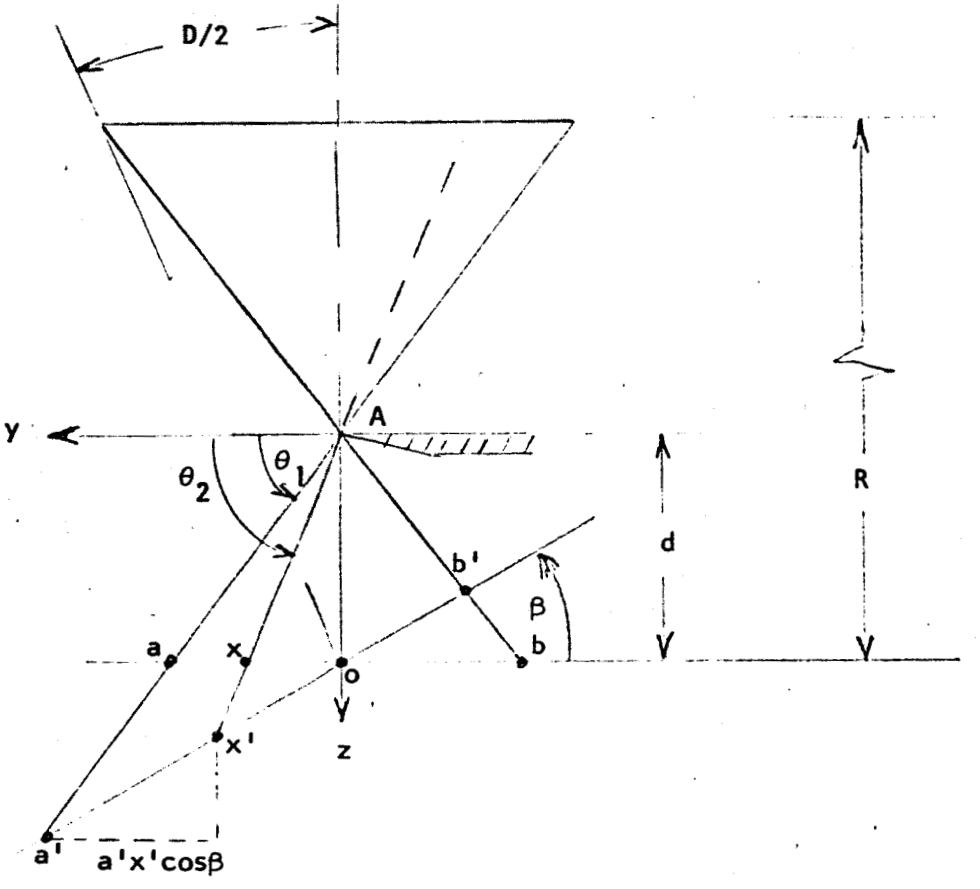

FIG. 6

In Fig. 6, R = distance from the receiver to the source. Note for

$$R >> d$$

$$\theta_2 - \theta_1 \approx D - \theta_T = D\left\{1 - \frac{\theta_T}{D}\right\} \tag{2.3.7}$$

Therefore, the position in the penumbra may be expressed in terms of θ_T/D.

The next step in the analysis involves the relationship between any given point in the penumbra and θ_T/D. Consider an orthogonal coordinate system centered at A. The equations for the ray trajectories are given as:

$$(Z)_{Aa'} = \tan \theta_1 y \tag{2.3.8}$$

$$(Z)_{Ax'} = \tan \theta_2 y \tag{2.3.9}$$

The equation for the receiving surface is given as

$$(Z)_{a'b'} = \tan \beta y + d \tag{2.3.10}$$

The y intercept of a general ray and the receiving surface is given by

$$y = \frac{d}{\tan \theta_i - \tan \beta} \tag{2.3.11}$$

so that

$$a'x'\cos\beta = y_{a'} - y_{x'} \tag{2.3.12a}$$

and from Eq. (2.3.11)

$$a'x'\cos\beta = d\left\{\frac{1}{\tan\theta_1 - \tan\beta} - \frac{1}{\tan\theta_2 - \tan\beta}\right\} \tag{2.3.12b}$$

Solving for $\tan\theta_2$

$$\tan\theta_2 = \tan\beta + \frac{1}{\frac{1}{\tan\theta_1 - \tan\beta} - \frac{a'x'}{d}\cos\beta} \tag{2.3.13}$$

Let us examine the term $\frac{a'x'}{d}$. From similar triangles

$$\frac{ab}{d} = \frac{2\sin\left\{\frac{D}{2}\right\}}{1 - \frac{d}{R}} \tag{2.3.14}$$

with the assumptions

$$\frac{d}{R} \ll 1 \tag{2.3.15a}$$

$$\sin\left\{\frac{D}{2}\right\} = \frac{D}{2} \tag{2.3.15b}$$

Equation (2.3.14) reduces to

$$ab = dD \tag{2.3.16}$$

so that

$$\frac{a'x'}{d} = D\,\frac{a'x'}{ab} = D\,\frac{a'x'}{a'b'}\left\{\frac{a'b'}{ab}\right\} \qquad (2.3.17)$$

where

$$\frac{a'x'}{a'b'} = \text{location in penumbra given as a fraction of the total length of the penumbra}$$

Using Eq. (2.3.12b)

$$a'b'\cos\beta = d\left[\frac{1}{\tan\theta_1 - \tan\beta} - \frac{1}{\tan(180-\theta_1) - \tan\beta}\right] \qquad (2.3.18)$$

Combining Eq. (2.3.16) with Eq. (2.3.18) and solving for $\frac{a'b'}{ab}$ yields

$$\frac{a'b'}{ab} = \frac{2}{D\cos\beta}\;\frac{1}{\tan\theta_1\left[1 - \left\{\frac{\tan\beta}{\tan\theta_1}\right\}^2\right]} \qquad (2.3.19)$$

Now combining Eq. (2.3.19), (2.3.17) and (2.3.13) and noting

$$\frac{1}{\tan\theta_1} = \frac{ab}{2d} = \frac{D}{2} \qquad (2.3.20)$$

yields

$$\tan\theta_2 = \tan\beta + \frac{1 - \frac{D}{2}\tan\beta}{D\left[\frac{1}{2} - \left\{\frac{1}{1 + \frac{D}{2}\tan\beta}\;\frac{a'x'}{a'b'}\right\}\right]} \qquad (2.3.21)$$

but referring to Fig. 6

$$\frac{1}{\tan \theta_2} = \frac{xo}{d} = \frac{ao - ax}{d} = \frac{1}{2}\frac{ab}{d} - \frac{ax}{d}$$

or using Eq. (2.3.16)

$$\frac{1}{\tan \theta_2} = D\left\{\frac{1}{2} - \frac{ax}{ab}\right\} \qquad (2.3.22)$$

but

$$\frac{ax}{ab} = 1 - \frac{\theta_T}{D} \qquad (2.3.23)$$

so that

$$\frac{1}{\tan \theta_2} = D\left\{\frac{\theta_T}{D} - \frac{1}{2}\right\} \qquad (2.3.24)$$

Finally, the functional relation between $\frac{\theta_T}{D}$ and the position in the penumbra is given by

$$\frac{\theta_T}{D} = \frac{1}{D \tan \theta_2} + \frac{1}{2} \qquad (2.3.25)$$

with $\tan \theta_2$ given in Eq. (2.3.21).

The position of the conical axis in the penumbra as a fraction of the total penumbra length is given as

$$\frac{a'o}{a'b'} = \frac{1}{2}\left\{1 + \frac{D}{2}\tan\beta\right\} \qquad (2.3.26)$$

The method of solution for the single knife edge is outlined as follows:

(1) For D and β = constant, calculate $\tan\theta_2$ from Eq. (2.3.21) as a function of position in penumbra, $\frac{a'x'}{a'b'}$.

(2) For a given $\frac{a'x'}{a'b'}$ with a corresponding $\tan\theta_2$, calculate $\frac{\theta_T}{D}$ from Eq. (2.3.25)

(3) Using the $\frac{\theta_T}{D}$ from step 2, calculate the relative energy flux density from Eqs. (2.3.5), (2.3.6) and (2.3.4a)

2.4 METHOD OF ANALYSIS - KNIFE EDGE WITH A SKIRT

The characteristic of the flux density distribution in the penumbra will depend on the reflective properties of the skirt (flat plate) as well as the reflectance. The possible conditions considered in this report are indicated in Table I.

TABLE I

Reflective Property	Reflectance	
Specular	0.0	1.0
Diffuse	0.0	1.0

Obviously, for reflectance = 0.0 (black body), the flux density distribution for the specular or diffuse skirt will be identical. The method of analysis for a specular skirt and diffuse skirt with reflectance = 1 is indicated in Sections 2.4.1 and 2.4.3, respectively.

2.4.1 Specular Skirt, Reflectance = 1.0

A specular reflective surface is defined as a surface that reflects incident energy according to Snell's law; i.e., the angle of reflection equals the angle of incidence. The particular geometry associated with a specular skirt is shown in Fig. 7.

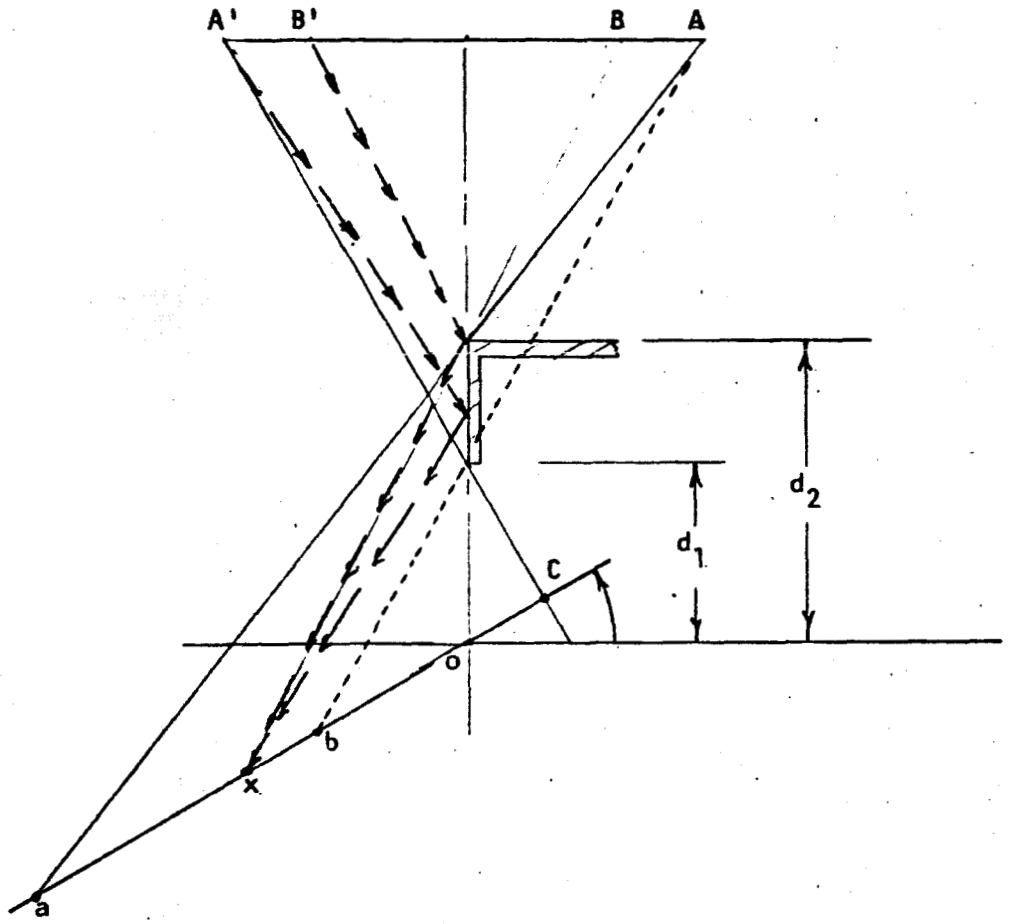

FIG. 7

Consider a point x on the receiver. Due to the skirt, the radiation from the area of the source indicated byAB in Fig. 7 is cut off. However, due to specular reflection x "sees" the mirror image of area AB, i.e., x "sees" A'B'. In fact, any point on the receiver ($0 < ax < ao$) "sees" in the specular skirt an image of the part of the source which is obscured by the skirt. Therefore, the effect of the specular skirt is the same as lowering the knife edge from d_2 to d_1.

2.4.2. Diffuse Skirt, Reflectance = 0.0

With reflectance = 0.0, the diffused skirt may be treated as parallel single knife edges. The pertinent geometry is shown in Fig. 8.

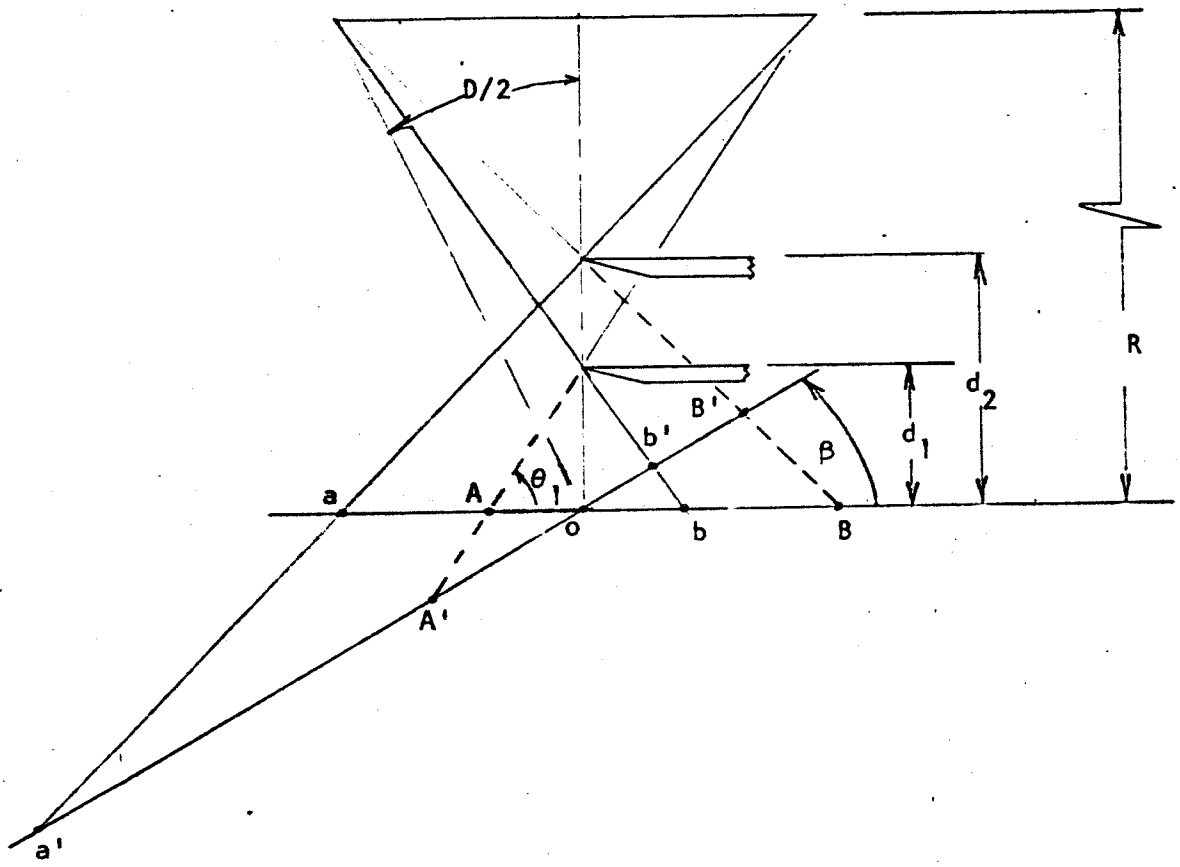

FIG. 8.

The actual length of the penumbra is defined by the region a'b' in Fig. 8. The flux density distribution in the penumbra region a'o is identical to that obtained considering a knife edge at d_2. Similarly, the distribution in the region ob' may be obtained for a single knife edge at d_1.

Let

$\frac{a'x'}{a'B'}$ = position in penumbra for a single knife edge at d_2.

and

$\frac{a'x'}{a'b'}$ = actual position in penumbra for parallel knife edges at d_1 and d_2.

Consider the condition where

$$\frac{a'x'}{a'b'} \leq \frac{a'o}{a'b'}$$

The actual position in the penumbra may be expressed as

$$\frac{a'x'}{a'b'} = \frac{a'x'}{a'B'}\left\{\frac{a'B'}{a'b'}\right\} \tag{2.4.1}$$

If it is assumed $R \gg d_2$, then referring to Fig. 8,

$$\frac{a'B'}{a'b'} = \frac{a'o + oB'}{a'o + ob'} \tag{2.4.2}$$

From similar triangles

$$\frac{a'o}{A'o} = \frac{ao}{Ao} \tag{2.4.3}$$

$$\frac{ob'}{oB'} = \frac{ob}{oB} \tag{2.4.4}$$

so that

$$\frac{a'B'}{a'b'} = \frac{1 + \left\{\frac{Ao}{A'o}\right\}\left\{\frac{ob'}{ob}\right\}\left\{\frac{oB}{ao}\right\}}{1 + \left\{\frac{Ao}{A'o}\right\}\left\{\frac{ob'}{ob}\right\}\left\{\frac{ob}{ao}\right\}} \tag{2.4.5}$$

Using the law of sines

$$\frac{Ao}{A'o} = \frac{\sin(\theta_1-\beta)}{\sin\theta_1} \tag{2.4.6}$$

and

$$\frac{ob'}{ob} = \frac{\sin\theta_1}{\sin(\theta_1+\beta)} \tag{2.4.7}$$

also.

$$\frac{oB}{ao} = 1 \tag{2.4.8}$$

and for $R >> d_2$

$$\frac{ob}{ao} = \frac{d_1\ D/2}{d_2\ D/2} = \frac{d_1}{d_2} \tag{2.4.9}$$

Substituting Eq. (2.4.6), (2.4.7), (2.4.8) and (2.4.9) into Eq. (2.4.5) yields

$$\frac{a'B'}{a'b'} = \frac{1 + \dfrac{\sin(\theta_1-\beta)}{\sin(\theta_1+\beta)}}{1 + \dfrac{\sin(\theta_1-\beta)}{\sin(\theta_1+\beta)}\ \dfrac{d_1}{d_2}} \tag{2.4.10}$$

which reduces to

$$\frac{a'B'}{a'b'} = \frac{2}{1 + \frac{D}{2}\tan\beta + (1 - \frac{D}{2}\tan\beta)\ \frac{d_1}{d_2}} \tag{2.4.11}$$

where

$$\text{ctn}\,\theta_1 = \frac{D}{2} \tag{2.4.11a}$$

Substituting Eq. (2.4.11) into Eq. (2.4.1) and solving for $\frac{a'x'}{a'B'}$ yields

$$\frac{a'x'}{a'B'} = \frac{a'x'}{a'b'}\left[\frac{1 + \frac{D}{2}\tan\beta + \left(1 - \frac{D}{2}\tan\beta\right)\frac{d_1}{d_2}}{2}\right] \tag{2.4.12}$$

$$0 \leq \frac{a'x'}{a'b'} \leq \frac{a'o}{a'b'}$$

where

$$\frac{a'o}{a'b'} = \frac{1 + \frac{D}{2}\tan\beta}{1 + \frac{D}{2}\tan\beta + \left(1 - \frac{D}{2}\tan\beta\right)\frac{d_1}{d_2}} \tag{2.4.13}$$

Equation (2.4.12) is interpreted as follows:

"The energy flux density at any point in the <u>actual</u> penumbra, $\frac{a'x'}{a'b'}$, is equivalent to the energy flux density at a point $\frac{a'x'}{a'B'}$ in the penumbra of a single knife edge at d_2."

Now consider a point in the actual penumbra where

$$\frac{a'o}{a'b'} \leq \frac{a'x'}{a'b'} \leq 1.0$$

The position in the penumbra may be expressed as

$$\frac{a'x'}{a'b'} = \frac{a'x'}{A'b'} \frac{A'b'}{a'b'} \tag{2.4.14}$$

or referring to Fig. 8

$$\frac{a'x'}{a'b'} = \left\{ \frac{a'o}{A'b'} - \frac{A'o}{A'b'} + \frac{A'x}{A'b'} \right\} \left\{ \frac{A'b'}{a'b'} \right\} \tag{2.4.15}$$

Since for $R >> d_2$

$$\frac{a'o}{ao} = \frac{A'o}{Ao} \quad . \tag{2.4.16}$$

Then from Eq. (2.4.6) and (2.4.7)

$$a'o = ao \left\{ \frac{1}{\cos\beta (1 - \frac{D}{2} \tan\beta)} \right\} \tag{2.4.17}$$

and

$$A'b' = Ab \left\{ \frac{1}{\cos\beta (1 - (\frac{D}{2} \tan\beta)^2)} \right\} \tag{2.4.18}$$

Now

$$\frac{a'o}{A'b'} = \frac{ao}{Ab} (1 + \frac{D}{2} \tan\beta) \tag{2.4.19}$$

but from Eq. (2.4.9)

$$\frac{ao}{Ab} = \frac{ao}{2ob} = \frac{1}{2}\frac{d_2}{d_1} \qquad (2.4.20)$$

so that

$$\frac{a'o}{A'b'} = \frac{1 + \frac{D}{2}\tan\beta}{2(d_1/d_2)} \qquad (2.4.21)$$

The term $\frac{A'o}{Ab}$ in Eq. (2.4.15) can be obtained by analogy from Eq. (2.4.13) with $\frac{d_1}{d_2} = 1$.

$$\frac{A'o}{A'b'} = \frac{1}{2}\left(1 + \frac{D}{2}\tan\beta\right) \qquad (2.4.22)$$

Substituting Eq. (2.4.21) and (2.4.22) into Eq. (2.4.15) and solving for $\frac{A'x'}{A'b'}$ yields

$$\frac{A'x'}{A'b'} = \frac{a'x'}{a'b'}\left\{\frac{a'b'}{A'b'}\right\} + \frac{1}{2}\left\{1 + \frac{D}{2}\tan\beta\right\}\left\{1 - \frac{d_2}{d_1}\right\} \qquad (2.4.23)$$

for $\frac{a'o}{a'b'} \leq \frac{a'x}{a'b'} \leq 1.0$

in Eq. (2.4.23)

$$\frac{a'b'}{A'b'} = \frac{a'B'}{A'b'}\frac{a'b'}{a'B'}$$

$$= \frac{aB}{Ab}\frac{a'b'}{a'B'} = \frac{2ao}{2ob}\frac{a'b'}{a'B'} \qquad (2.4.24)$$

and from Eq. (2.4.9) and (2.4.11)

$$\frac{a'b'}{A'b'} = \frac{1 + \frac{D}{2}\tan\beta + (1 - \frac{D}{2}\tan\beta)\frac{d_1}{d_2}}{2\left\{\frac{d_1}{d_2}\right\}} \qquad (2.4.25)$$

The position of the conical axis in the penumbra is given by Eq. (2.4.13).

The technique used for the solution of the diffused skirt with reflectance = 0.0 is as follows

(1) For a given d_1/d_2 determine the position of the conical axis, $\frac{a'o}{a'b}$, in the penumbra from Eq. (2.4.13).

(2) For positions in the penumbra such that

$$0 \leq \frac{a'x'}{a'b'} \leq \frac{a'o}{a'b'}$$

with $\frac{a'o}{a'b'}$ defined by Step (1). Calculate the equivalent position in the penumbra for a single knife edge, $\frac{a'x'}{a'B'}$, from Eq. (2.4.12).

(3) The energy flux density at $\frac{a'x'}{a'b'}$ is then found by substituting the equivalent $\frac{a'x'}{a'B'}$ into Eq. (2.3.21) and continuing in a manner identical to that for the solution of a single knife edge, i.e., determine θ_T/D from Eq. (2.3.25) and the relative flux density from Eq. (2.3.5), (2.3.6) and (2.3.4a). The energy flux density corresponding to $\frac{a'x'}{a'B'}$ is the required flux density at a point in the actual penumbra, $\frac{a'x'}{a'b'}$.

(4). For positions in the penumbra such that

$$\frac{a'o}{a'b'} \leq \frac{a'x'}{a'b'} \leq 1.0$$

with $\frac{a'o}{a'b'}$ defined in step (1). Calculate the equivalent position of a single knife edge, $\frac{A'x'}{A'b'}$, from Eq. (2.4.23)

(5). The required flux density is determined from step (3) replacing $\frac{a'x'}{a'B'}$ by $\frac{A'x'}{A'b'}$.

2.4.3. Diffuse Skirt, Reflectance = 1.0

Assume the skirt is located along the conical axis. The associated geometry is schematically represented in Fig. 9.

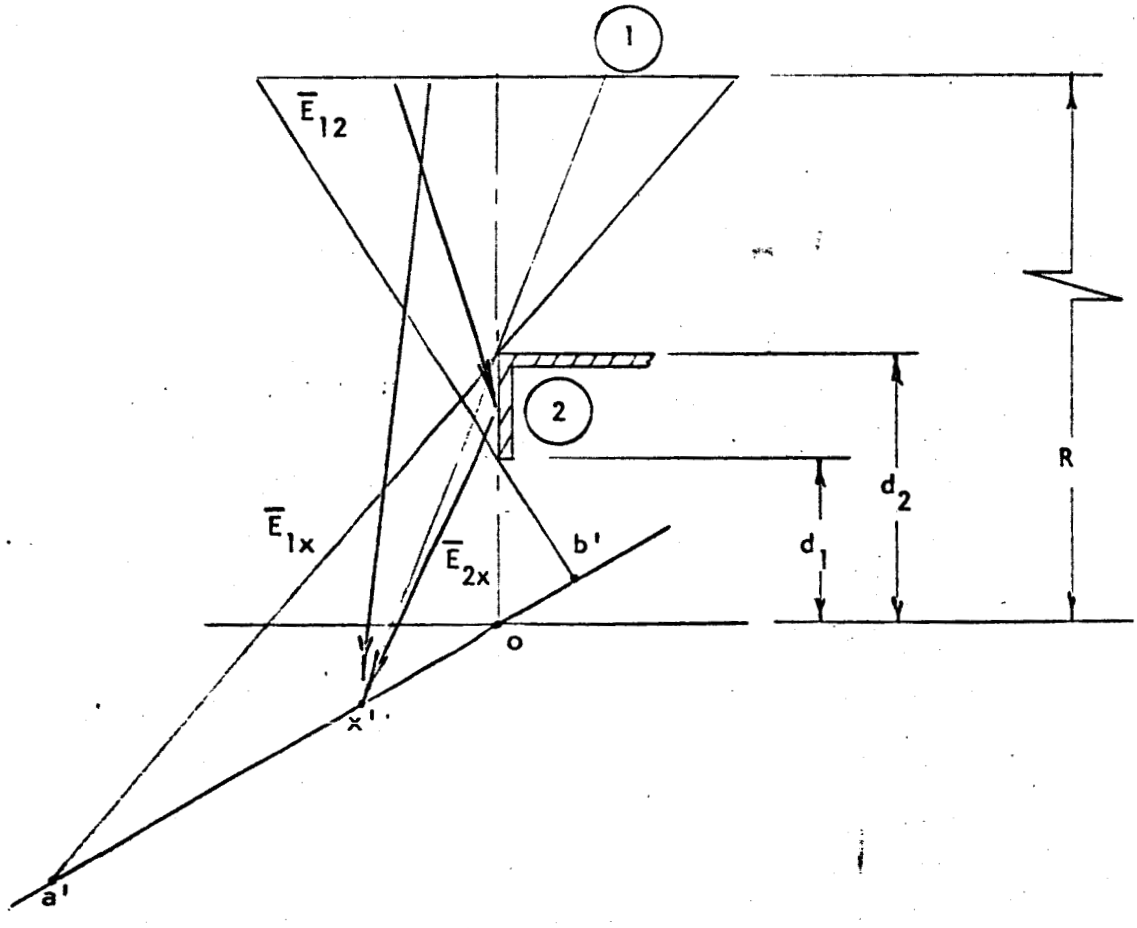

FIG. 9

First note that in the penumbra region ob' the effect of the skirt can be ignored. Furthermore, the energy flux density distribution in the penumbra can be obtained by superposition of the distribution obtained in Section 2.4.2, diffuse skirt, reflectance = 0.0 and the distribution due to the skirt.

The diffuse skirt acts as a secondary source of uniform intensity since each point on the skirt "sees" the same fraction of actual source. For notation sake, let the subscripts 1 and 2 refer to the primary and secondary source respectively. The energy incident on a differential area at a point x in the penumbra may be expressed in the form of Eq. (2.1.8) as

$$dq_x = - d\overline{A}_x \cdot (\overline{E}_{1x} + \overline{E}_{2x}) \qquad (2.4.26)$$

where

$\overline{E}_{1x}$ = power vector from part of source seen by dA_x

$\overline{E}_{2x}$ = power vector from diffuse skirt

Equation (2.4.26) can be written as

$$dq_x = dq_{1x} + dq_{2x} \qquad (2.4.27)$$

where now

$$dq_{1x} = - \overline{dA}_x \cdot \overline{E}_{1x} = \text{energy flux due to source} \qquad (2.4.27a)$$

$$dq_{2x} = - \overline{dA}_x \cdot \overline{E}_{2x} = \text{energy flux due to skirt} \qquad (2.4.27b)$$

Let us concern ourselves with the energy flux due to the skirt. The energy incident on dA_x from the diffuse skirt is some fraction of the energy incident on the skirt from the source. The energy incident on the skirt is given by

$$dq_2 = - d\bar{A}_2 \cdot \bar{E}_{12} \qquad (2.4.28)$$

where

$\bar{E}_{12}$ = power vector from part of source seen by the skirt

Since the skirt has a reflectance = 1.0, the total incident energy will be reflected in a manner not as yet specified. The skirt "sees" $\frac{1}{2}$ the total source. Therefore

$$\left|\bar{E}_{12}\right| = \frac{1}{2} \int_{A_1} \frac{I dA_1}{R^2} \quad ; \quad R \gg d_2 \qquad (2.4.29)$$

The equivalent point source seen by the skirt is located at the centroid of the visible area since the source is considered uniform. The angle between $\bar{E}_{12}$ and the normal vector, $d\bar{A}_2$, to the skirt is then

$$\psi = 90 - \tan^{-1} (.2122D) \qquad (2.4.30)$$

as indicated in Fig. 10.

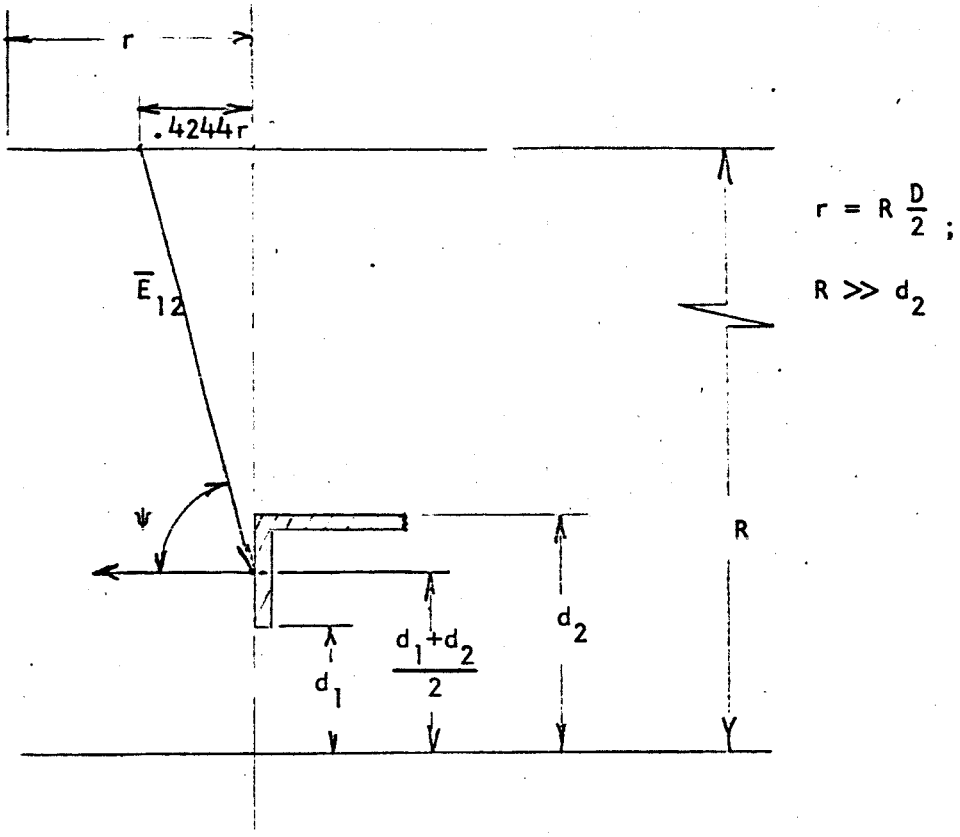

FIG. 10

The total energy incident on the skirt is then

$$(q_2)_{total} = A_2 E_{12} \cos\psi \qquad (2.4.31)$$

Substituting ψ from Eq. (2.4.30) and $E_{12} = \left|\bar{E}_{12}\right|$ from Eq. (2.4.29) into Eq. (2.4.31) yields

$$(q_2)_{total} = \frac{A_2}{2} \sin(\tan^{-1}.2122D) \int_{A_1} \frac{I dA_1}{R^2} \qquad (2.4.32)$$

where

A_2 = area of skirt

In Eq. (2.4.32), $(q_2)_{total}$ is the total energy reflected in all directions in the hemisphere surrounding the skirt. Each differential area of the skirt will distribute energy in the hemisphere surrounding the differential area according to Lambert's law of diffuse radiation (Ref. 2).

Let $d\bar{\sigma}$ = a vector defined as the maximum energy flux/unit skirt area radiated from the skirt in a direction normal to the skirt.

Since the skirt is a secondary source of uniform intensity, each differential area of the skirt radiates in a hemisphere a quantity of energy equal to

$$dA_2 \cdot \frac{(q_2)_{total}}{A_2} = \int d\bar{\sigma} \cdot \bar{r}\, dA_s \qquad (2.4.33)$$

where

$\bar{r}$ is a unit radius vector

dA_s is a differential area on the hemisphere of radiation,

$= R d\gamma_1 \cdot R \sin\gamma_1 \cdot d\gamma_2$ (see Fig. 11) (2.4.34)

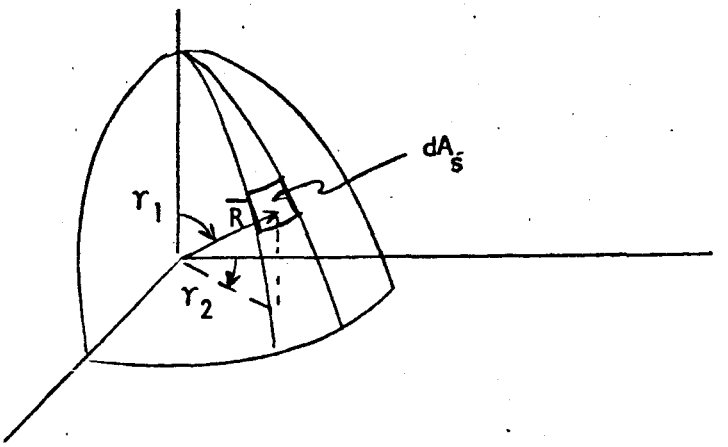

FIG. 11

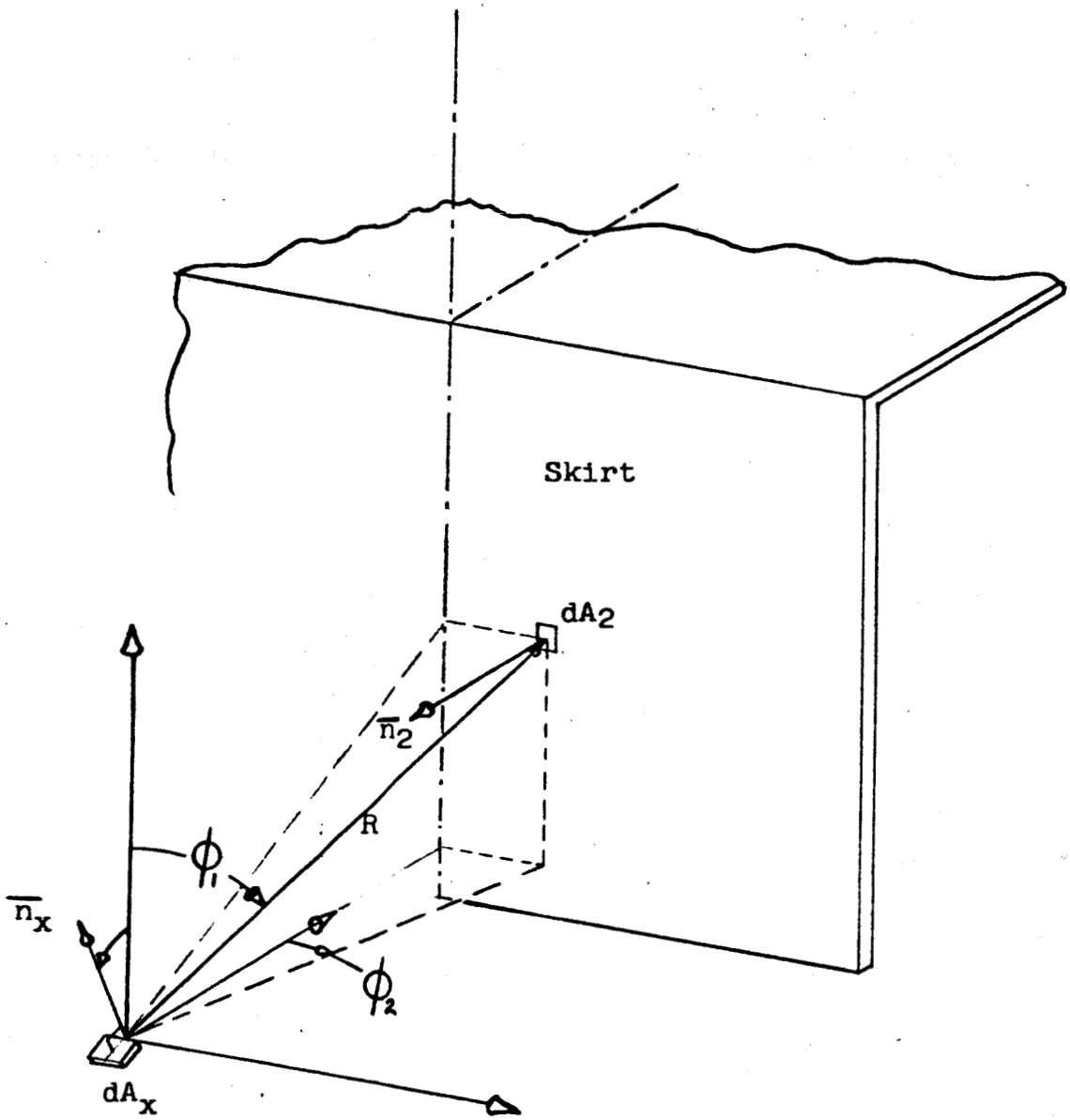

Figure 12

$$dA_2 \frac{(q_2)_{total}}{A_2} = \int_0^{\frac{\pi}{2}} \int_0^{2\pi} \overline{d\sigma} \cdot \overline{r}\, R^2 \sin\gamma_1 d\gamma_1 d\gamma_2$$

$$= d\sigma R^2 \int_0^{\frac{\pi}{2}} \int_0^{2\pi} \cos\gamma_1 \sin\gamma_1 d\gamma_1 d\gamma_2$$

$$= d\sigma\, \pi R^2 \qquad (2.4.35)$$

$$d\sigma = \frac{(q_2)_{total}}{A_2 \pi R^2} dA_2 \qquad (2.4.36)$$

Let

$\frac{dq_{2x}}{dA_x}$ = the energy received/unit area of the receiver at a point, x, on the receiver.

n_2 = unit vector normal to the skirt

n_x = unit vector normal to the receiver at x

Referring to Fig. 12, it can be seen that

$$d\left\{\frac{dq_{2x}}{dA_x}\right\} = \left\{\overline{d\sigma} \cdot \overline{r}\right\} \left\{\overline{r} \cdot \overline{n}_x\right\}$$

$$= \left\{d\sigma\, \overline{n}_2 \cdot \overline{r}\right\} \left\{\overline{r} \cdot \overline{n}_x\right\} \qquad (2.4.37)$$

The differential area on the skirt, dA_2, may be transformed into an equivalent differential area, dA_s, on a sphere of radius, R

$$dA_s = dA_2 \bar{n}_2 \cdot \bar{r} \tag{2.4.38}$$

$$\bar{n}_2 \cdot \bar{r} = \frac{dA_s}{dA_2} \tag{2.4.39}$$

Now

$$d\left\{\frac{dq_{2x}}{dA_x}\right\} = \left\{d\sigma \frac{dA_s}{dA_2}\right\} \bar{r} \cdot \bar{n}_x$$

$$= \frac{d\sigma}{dA_2} \bar{r} \cdot \bar{n}_x \, dA_s \tag{2.4.40}$$

Referring to Fig. 12, p.34a

$$dA_s = R^2 \sin\phi_1, d\phi_2 d\phi_1 \tag{2.4.41}$$

Substituting $d\sigma$ from Eq. (2.4.36) and dA_s from Eq. (2.4.41) into Eq. (2.4.40) yields

$$d\left\{\frac{dq_{2x}}{dA_x}\right\} = \frac{(q_2)_{total}}{A_2 \pi R^2} \bar{r} \cdot \bar{n}_x R^2 \sin\phi_1 d\phi_2 d\phi_1$$

$$= \frac{(q_2)_{total}}{A_2 \pi} r \cdot n_x \sin\phi_1 d\phi_2 d\phi_1 \tag{2.4.42}$$

but from Fig. 12

$$\bar{r}\cdot\bar{n}_x = \cos\beta\cos\phi_1 - \sin\beta\sin\phi_1\cos\phi_2 \qquad (2.4.43)$$

so that

$$\frac{dq_{2x}}{dA_x} = 2\,\frac{(q_2)_{total}}{A_2\pi}\int_{\phi_{11}}^{\phi_{12}}\int_{o}^{\phi_{22}} \sin\phi_1(\cos\beta\cos\phi_1 - \sin\beta\sin\phi_1\cos\phi_2)\,d\phi_2 d\phi_1 \qquad (2.4.44)$$

Symmetry about the xy-plane has been utilized to alter the limits of integration in the above expression by multiplying by 2 and integrating from 0 to ϕ_{22}. Integration of Eq. (2.4.44) yields

$$\frac{dq_{2x}}{dA_x} = \frac{2(q_2)_{total}}{A_2\pi}\left[\cos\beta\,\frac{\phi_{22}}{2}\left[\sin^2\phi_1\right]_{\phi_{11}}^{\phi_{12}} - \sin\beta\sin\phi_{22}\left[\frac{\phi_1}{2} - \frac{\sin 2\phi_1}{4}\right]_{\phi_{11}}^{\phi_{12}}\right] \qquad (2.4.45)$$

Let Q' = relative energy flux density in the penumbra contributed by diffuse reflection from the skirt

The relative energy flux density outside the penumbra being received by direct radiation from the source is

$$\cos\beta\int_{A_1}\frac{I\,dA_1}{R^2}$$

Therefore, from Eq. (2.4.32) and Eq. (2.4.45)

$$Q' = \frac{dq_{2x}/dA_x}{\cos\beta \int \frac{I dA_1}{R^2}}$$

$$= \frac{\sin(\tan^{-1}.2122D)}{\pi} \left[\frac{\phi_{22}}{2} \left[\sin^2\phi_1 \right]_{\phi_{11}}^{\phi_{12}} - \tan\beta \sin\phi_{22} \left[\frac{\phi_1}{2} - \frac{\sin 2\phi_1}{4} \right]_{\phi_{11}}^{\phi_{12}} \right]$$

$$\phi_{12} \leq \frac{\pi}{2} - \beta \qquad (2.4.46)$$

The remaining task is to define the angles ϕ_{11}, ϕ_{12} and ϕ_{22} in terms of the position in the penumbra, d_1/d_2, and the width of the skirt. These relations will be developed utilizing Fig. 13.

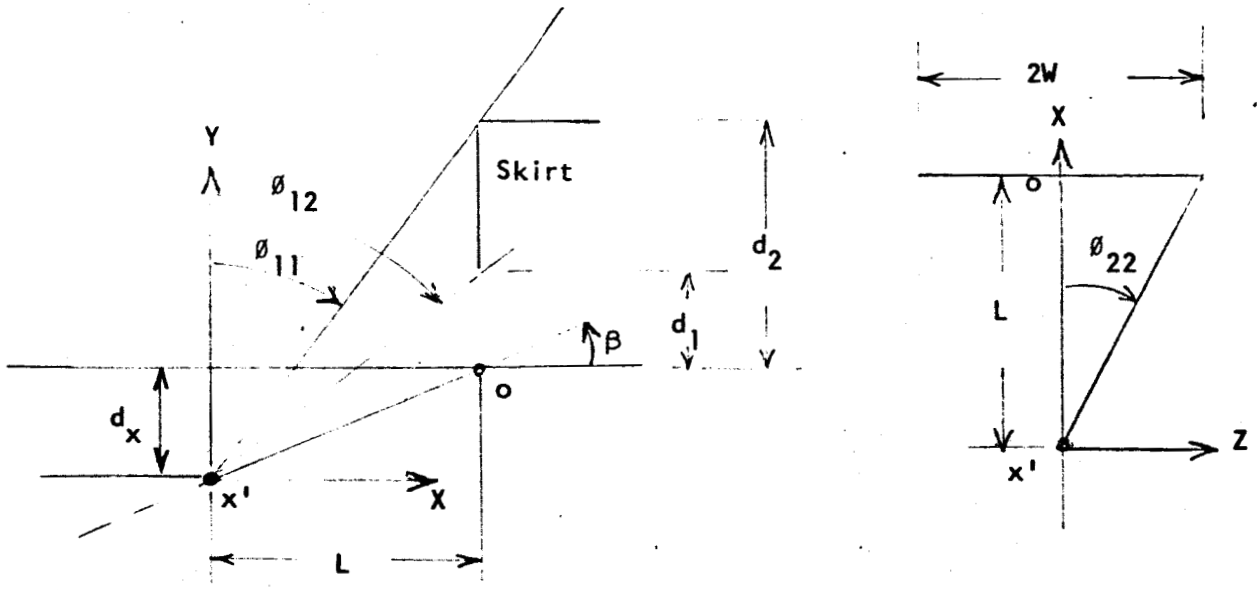

FIG. 13

$$\phi_{11} = \tan^{-1}\left[\frac{\frac{L}{d_2}}{1 + \frac{d_x}{d_2}}\right] \qquad (2.4.47a)$$

and

$$\phi_{12} = \tan^{-1}\left[\frac{\frac{L}{d_2}}{\frac{d_1}{d_2} + \frac{d_x}{d_2}}\right] \qquad (2.4.47b)$$

Let

W = the half width of the skirt

Then from Fig. 13(B)

$$\phi_{22} = \tan^{-1}\left\{\frac{W}{L}\right\} \qquad (2.4.47c)$$

Since

$$L = x'_o \cos\beta \qquad (2.4.48)$$

and

$$d_x = x'_o \sin\beta \qquad (2.4.49)$$

$$d_x = L \tan\beta \qquad (2.4.50)$$

Equations (2.4.47a) and (2.4.47b) can be written as

$$\phi_{11} = \tan^{-1}\left[\frac{\frac{L}{d_2}}{1 + \frac{L}{d_2}\tan\beta}\right] \qquad (2.4.51a)$$

$$\phi_{12} = \tan^{-1}\left[\frac{\frac{L}{d_2}}{\frac{d_1}{d_2} + \frac{L}{d_2}\tan\beta}\right] \qquad (2.4.51b)$$

The distance from the skirt, L, may be expressed in terms of position in the penumbra, $\frac{a'x'}{a'b'}$, as

$$L = \left\{\frac{a'o}{a'b'} - \frac{a'x'}{a'b'}\right\} a'b'\cos\beta \qquad (2.4.52)$$

Using Eqs. (2.4.7), (2.4.9) and (2.4.17) and noting that

$$a'b' = a'o + ob'$$

$$a'b' = \frac{ao}{\cos\beta}\left[\frac{1 + \frac{D}{2}\tan\beta + \frac{d_1}{d_2}\left\{1 - \frac{D}{2}\tan\beta\right\}}{1 - \left\{\frac{D}{2}\tan\beta\right\}^2}\right] \qquad (2.4.53)$$

but

$$ao = d_2\,\frac{D}{2} \qquad (2.4.54)$$

so that from Eq. (2.4.52), (2.4.53) and (2.4.54)

$$\frac{L}{d_2} = \frac{D}{2}\left[\frac{1 + \frac{D}{2}\tan\beta + \frac{d_1}{d_2}\left\{1 - \frac{D}{2}\tan\beta\right\}}{1 - \left\{\frac{D}{2}\tan\beta\right\}^2}\right]\left\{\frac{a'o}{a'b'} - \frac{a'x'}{a'b'}\right\} \qquad (2.4.55)$$

$$0 \leq \frac{a'x'}{a'b'} \leq \frac{a'o}{a'b'}$$

with $\frac{a'o}{a'b}$ given in Eq. (2.4.13)

The angles ϕ_{11} and ϕ_{12} in Eq. (2.4.51) can be evaluated for any point in the penumbra using Eq. (2.4.55). The azimuth angle, ϕ_{22}, may be expressed as

$$\phi_{22} = \tan^{-1}\left[\frac{\frac{W}{d_2}}{\frac{L}{d_2}}\right] \tag{2.4.56}$$

with $\frac{L}{d_2}$ given by Eq. (2.4.55) and $\frac{W}{d_2}$ being a constant for any particular skirt.

The method of solution for the diffuse skirt is as follows:

(1) For a given D, d_1/d_2 and incident angle, β, calculate L/d_2 as a function of position in the penumbra from Eq. (2.4.55)

(2) Using L/d_2 determined in Step (1), calculate ϕ_{11} and ϕ_{22} from Eq. (2.4.51)

(3) For a given W/d_2, calculate ϕ_{22} from Eq. (2.4.56) using L/d_2 from Step (1)

(4) Substitute ϕ_{11}, ϕ_{12} and ϕ_{22} from Steps (2) and (3) into Eq. (2.4.46) and evaluate Q' using D and β from Step (1). Q' is the relative energy flux density in the penumbra contributed by diffuse reflection from the skirt.

2.5. Method of Analysis - Double Knife Edge

The shaded surface considered is schematically represented in Fig. 14.

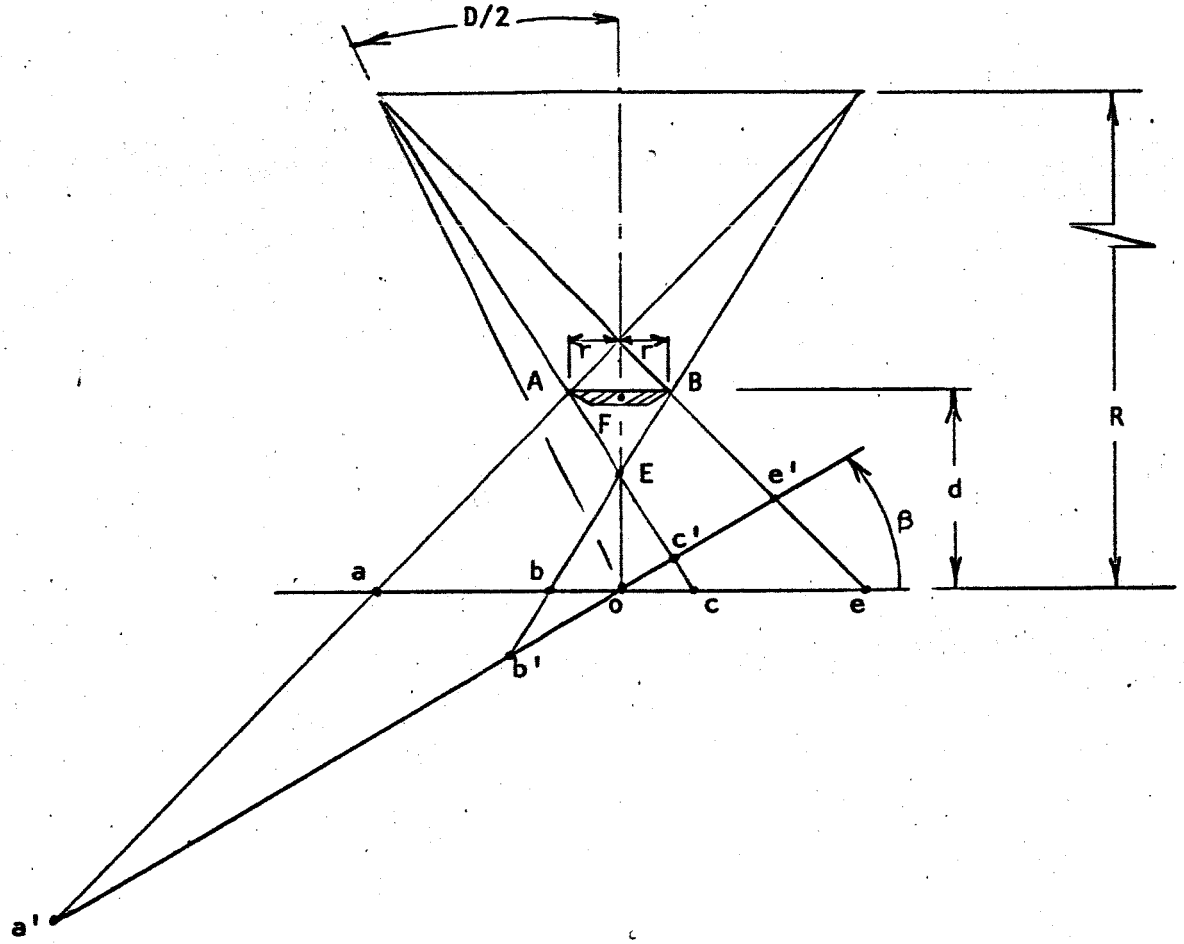

FIG. 14

The energy flux density for the double knife edge is obtained by superposition of the distributions corresponding to single knife edges at A and B in Fig. 14. The penumbra region a'c' is caused by a knife edge at A. While the penumbra region b'e' is obtained by considering a knife edge at B. For certain values of d/r the two penumbrae will overlap.

giving a region of increased intensity or a "reinforced penumbra". The characteristics of the penumbra as dictated by the d/r ratio will be:

$\text{ctn}^{-1}\left(\frac{d}{r}\right) > \frac{D}{2}$: Two distinct penumbra regions separated by a distinct umbra region.

$\text{ctn}^{-1}\left(\frac{d}{r}\right) < \frac{D}{2}$: No umbra region. Penumbra due to knife edges at A and B overlap resulting in a "reinforced penumbra".

Let

$\frac{a'x'}{L_i}$ = Position in penumbra for a single knife edge at i

The position in the penumbra for the double knife edge may be expressed in terms of $\frac{a'x'}{L_A}$ as

$$\frac{a'x'}{a'e'} = \frac{a'x'}{L_A}\frac{L_A}{a'e'} \qquad (2.5.1)$$

$$0 \leq \frac{a'x'}{L_A} \leq 1.0$$

Referring to Fig. 1 .

$$L_A = a'c' \qquad (2.5.2)$$

For $R \gg d$

$$a'c' = \frac{ao\left[\left(1 + \frac{D}{2}\tan\beta\right) + \frac{oc}{ao}\left(1 - \frac{D}{2}\tan\beta\right)\right]}{\cos\beta\left\{1 - \left(\frac{D}{2}\tan\beta\right)^2\right\}} \qquad (2.5.3)$$

and

$$a'e' = 2ao \frac{1}{\cos\beta\left\{1 - \left(\frac{D}{2}\tan\beta\right)^2\right\}} \qquad (2.5.4)$$

Substituting Eq. (2.5.2), (2.5.3) and (2.5.4) into Eq. (2.5.1) and solving for $\frac{a'x'}{L_A}$ yields

$$\frac{a'x'}{L_A} = \frac{a'x'}{a'e'}\left[\frac{2}{(1 + \frac{D}{2}\tan\beta) + (\frac{oc}{ao})(1 - \frac{D}{2}\tan\beta)}\right] \qquad (2.5.5)$$

but due to symmetry

$$\frac{oc}{ao} = \frac{2oc}{2ao} = \frac{bc}{ae} \qquad (2.5.6)$$

If $R \gg d$, then using similar triangles

$$bc \simeq (d - EF)D \qquad (2.5.7)$$

and also

$$\frac{2r}{EF} \simeq D \qquad (2.5.8)$$

so that

$$bc = 2r(\frac{d}{r}\frac{D}{2} - 1) \qquad (2.5.9)$$

Referring to Fig. 14.

$$ae = ac + be - bc \qquad (2.5.10)$$

Since for $R >> d$

$$ac = be = dD$$

$$ae = 2r\left(\frac{d}{r}\frac{D}{2} + 1\right) \tag{2.5.11}$$

and

$$\frac{bc}{ae} = \frac{\frac{d}{r}\frac{D}{2} - 1}{\frac{d}{r}\frac{D}{2} + 1} \tag{2.5.12}$$

Substituting Eq. (2.5.12) into Eq. (2.5.5)

$$\frac{a'x'}{L_A} = \frac{a'x'}{a'e'}\left[\frac{1 + \frac{D}{2}\frac{d}{r}}{\frac{D}{2}\left\{\frac{d}{r} + \tan\beta\right\}}\right] \tag{2.5.13}$$

$$0 \leq \frac{a'x'}{a'e'} \leq \frac{a'c'}{a'e}$$

where

$$\frac{a'c'}{a'e'} = \text{fraction of total penumbra due to knife edge at A.}$$

and from Eq. (2.5.2), (2.5.3), (2.5.4) and (2.5.11)

$$\frac{a'c'}{a'e'} = \frac{\frac{D}{2}\left\{\frac{d}{r} + \tan\beta\right\}}{1 + \frac{D}{2}\frac{d}{r}} \tag{2.5.13a}$$

In Eq. (2.5.13) $\frac{a'x'}{a'e'}$ is the actual position in the penumbra and $\frac{a'x'}{L_A}$ is the equivalent position in the penumbra of a single edge at A.

Now consider the penumbra due to a knife edge at B. The portion of the actual penumbra of interest is then

$$\frac{a'b'}{a'e'} \leq \frac{a'x}{a'e'} \leq 1.0$$

The position in the penumbra is expressed as

$$\frac{a'x'}{a'e'} = 1 - \frac{e'x'}{L_B}\left\{\frac{L_B}{a'e'}\right\}$$

$$0 \leq \frac{e'x'}{L_B} \leq 1.0 \qquad (2.5.14)$$

where in Eq. (2.5.14)

$$L_B = b'e' \qquad (2.5.15)$$

and

$\frac{e'x'}{L_B}$ = position in penumbra due to a single knife edge at B as measured from point e'.

Solving Eq. (2.5.14) for $\frac{e'x'}{L_B}$ yields

$$\frac{e'x'}{L_B} = \left\{1 - \frac{a'x'}{a'e'}\right\} \frac{a'e'}{b'e'}$$

$$\frac{a'b'}{a'e} \leq \frac{a'x'}{a'e'} \leq 1.0 \qquad (2.5.16)$$

By analogy to the solution for

$$0 \leq \frac{a'x'}{a'e'} \leq \frac{a'c'}{a'e'} \quad \text{i.e., Eq. (2.5.3)}$$

$$b'e' = \frac{oe\left\{\frac{bo}{oe}\left(1 + \frac{D}{2}\tan\beta\right) + 1 - \frac{D}{2}\tan\beta\right\}}{\cos\beta\left\{1 - \left(\frac{D}{2}\tan\beta\right)^2\right\}} \qquad (2.5.17)$$

The expression for a'e' is given in Eq. (2.5.4) so that since oe = ao and bo = oc

$$\frac{a'e'}{b'e'} = \frac{1 + \frac{D}{2}\frac{d}{r}}{\frac{D}{2}\left\{\frac{d}{r} - \tan\beta\right\}} \qquad (2.5.18)$$

Substituting Eq. (2.5.18) into Eq. (2.5.16) yields

$$\frac{e'x'}{L_B} = \left\{1 - \frac{a'x'}{a'e'}\right\}\left[\frac{1 + \frac{d}{r}\frac{D}{2}}{\frac{D}{2}\left\{\frac{d}{r} - \tan\beta\right\}}\right] \qquad (2.5.18a)$$

$$\frac{a'b'}{a'e'} \leq \frac{a'x'}{a'e'} \leq 1.0$$

with

$$\frac{a'b'}{a'e'} = \frac{1 + \frac{D}{2}\tan\beta}{1 + \frac{d}{r}\frac{D}{2}} \qquad (2.5.19)$$

The position of the conical axis is given as

$$\frac{a'o}{a'e'} = \frac{1}{2}\left\{1 + \frac{D}{2}\tan\beta\right\} \qquad (2.5.20)$$

The technique used for determining the flux density distribution in the penumbra of a double knife edge is as follows:

(1) Calculate the fraction of total penumbra due to single knife edge at A, $\frac{a'c'}{a'e'}$ from Eq. (2.5.13a).

(2) For $0 \leq \frac{a'x'}{a'e'} \leq \frac{a'c'}{a'e'}$ with $\frac{a'c'}{a'e'}$ determined from step (1), calculate the equivalent position in the penumbra of a single knife edge, $\frac{a'x'}{L_A}$, from Eq. (2.5.13).

(3) Calculate the energy flux density corresponding to $\frac{a'x'}{L_A}$ in a manner identical to that for a single knife edge, i.e., use Eq. (2.3.21), (2.3.25), (2.3.5), (2.3.6) and (2.3.4a). This flux density is the required density at $\frac{a'x'}{a'e'}$.

(4) Calculate the starting location of the penumbra due to a single knife edge at B, $\frac{a'b'}{a'e'}$ from Eq. (2.5.19).

(5) For $\frac{a'b'}{a'e'} \leq \frac{e'x'}{b'e'} \leq 1.0$ with $\frac{a'b'}{a'e'}$ from step (4), calculate the equivalent position in the penumbra of a single knife edge at B, $\frac{e'x'}{L_B}$, from Eq. (2.5.18).

(6) Calculate the energy flux density corresponding to $\frac{e'x'}{L_B}$ from Step (3) replacing $\frac{a'x'}{L_A}$ by $\frac{e'x'}{L_B}$ and using $-\beta$ in Eq. (2.3.21).

(7) The energy flux density distribution in the penumbra of a double knife edge is obtained by summing the flux densities obtained in steps (3) and (6) for a given location in the penumbra, $\frac{a'x'}{a'e'}$.

IMPORTANT NOTE

A word of caution is in order in reference to the penumbra referred to in step (5). The single knife edge system described in Section 2.3 is not symmetric with respect to knife edge orientation and incident angle. A comparison of the knife edge system of Section 2.3 and the system implied by step (5) is shown in Fig. 15.

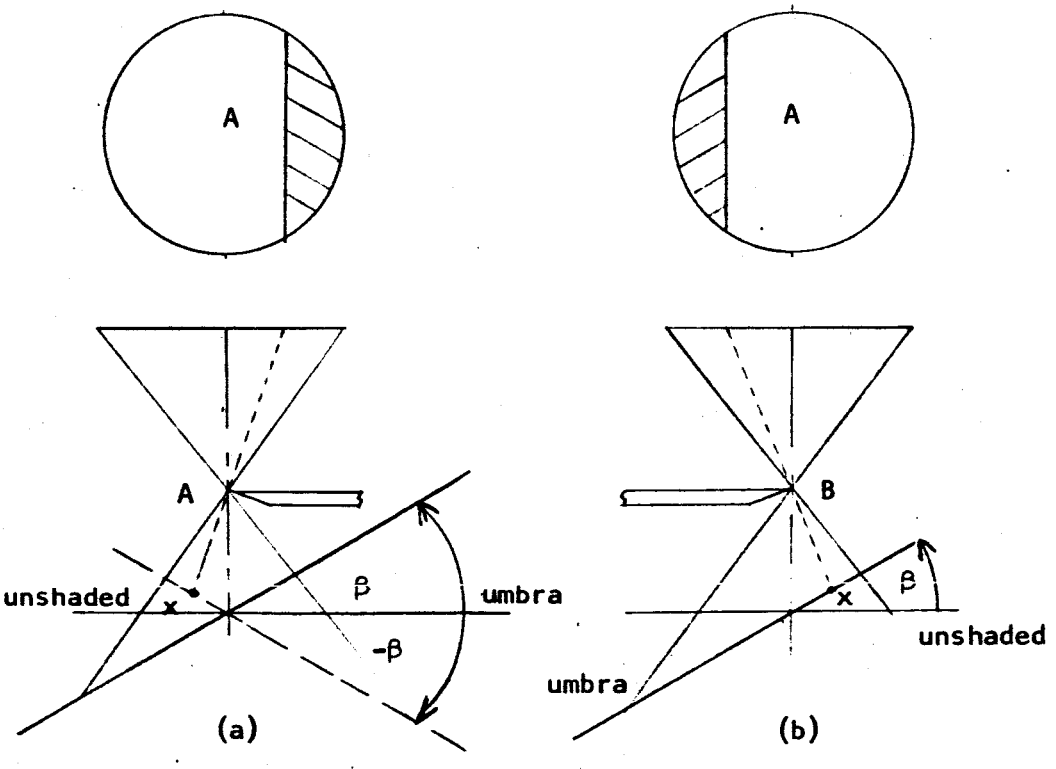

FIG. 12

From Fig. 15(a) it is apparent that the flux density distribution corresponding to Fig. 12(b) is identical to the distribution obtained in Section 2.3 with the incident angle equal to $-\beta$. Therefore, in step (6) use $-\beta$ in Eq. (2.3.21).

2.6 METHOD OF ANALYSIS - RECTANGULAR CYLINDER

2.6.1 Diffuse Rectangular Cylinder, Reflectance = 0.0

The geometry considered is shown in Fig. 16

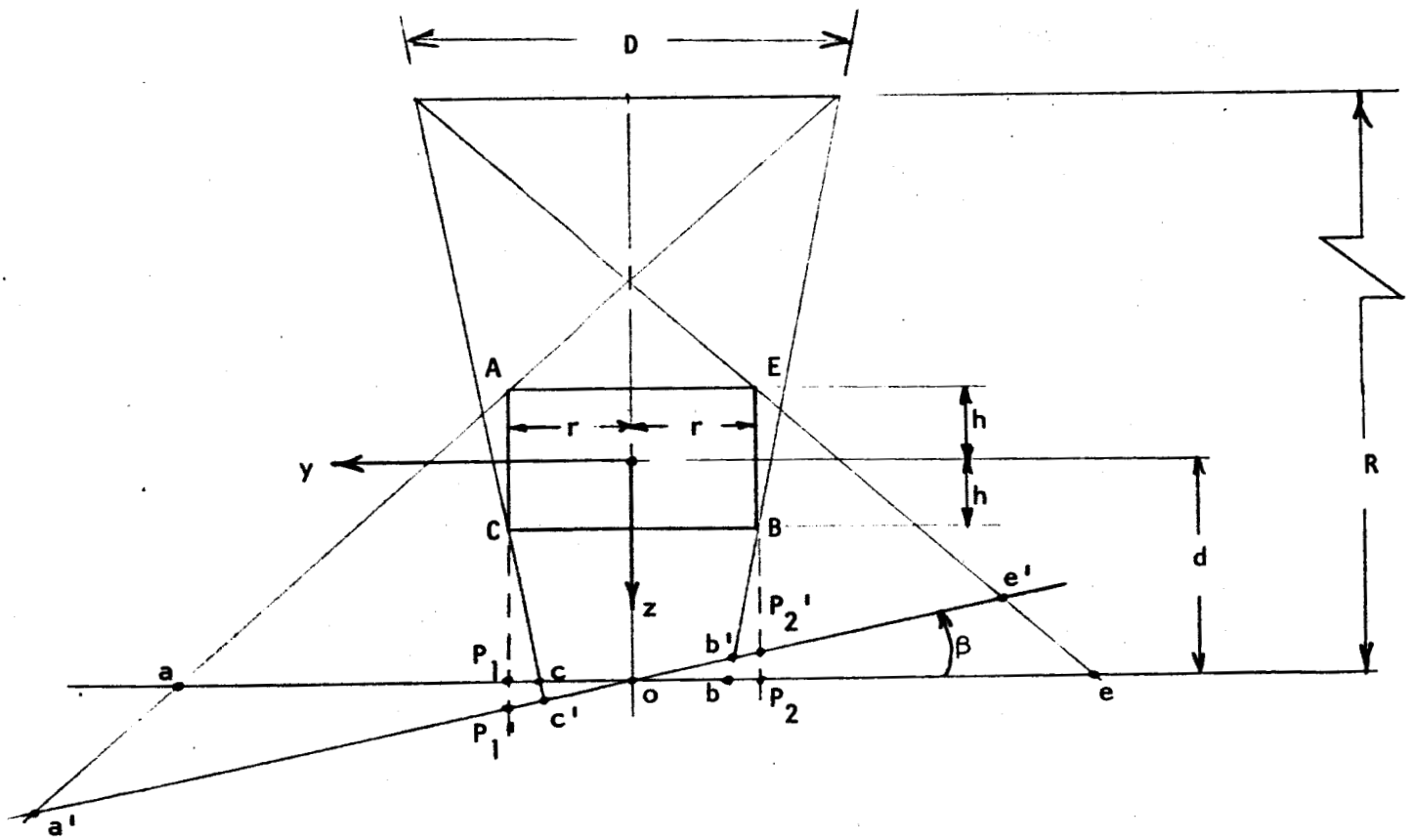

FIG. 16

The solution for a rectangular cylinder is closely related to the solutions for a knife edge with a skirt, Section 2.4. Therefore, it is possible to determine the relative energy flux density in the penumbra of a rectangular cylinder by judicial superpositions of flux density distributions in penumbrae of different single knife edges. The knife edges are considered to be located at each of the four corners of the rectangular cylinder.

The analysis of the rectangular cylinder differs from the analysis of the previous shading bodies in that a new parameter must be considered. This parameter defines the geometry of the rectangle in that it is the ratio of the height to width, $\frac{h}{r}$, and will be called the "shape factor". The characteristic of the penumbra is dictated not only by the location of the rectangular cylinder relative to the receiving surface, but also by the shape factor. From Fig. 16 for

$$\text{ctn}^{-1}\left[\frac{d}{r} - \frac{h}{r}\right] > \frac{D}{2} \qquad (2.6.1a)$$

The penumbra consists of two distinct penumbrae separated by an umbra region. For

$$\text{ctn}^{-1}\left[\frac{d}{r} - \frac{h}{r}\right] < \frac{D}{2} \qquad (2.6.1b)$$

the penumbraw due to the left and right sides of the rectangular cylinder overlap resulting in a reinforced penumbra in the overlapping region.

Temporarily consider only the left half side of the rectangular cylinder. A detailed view of this half is shown in Fig. 17.

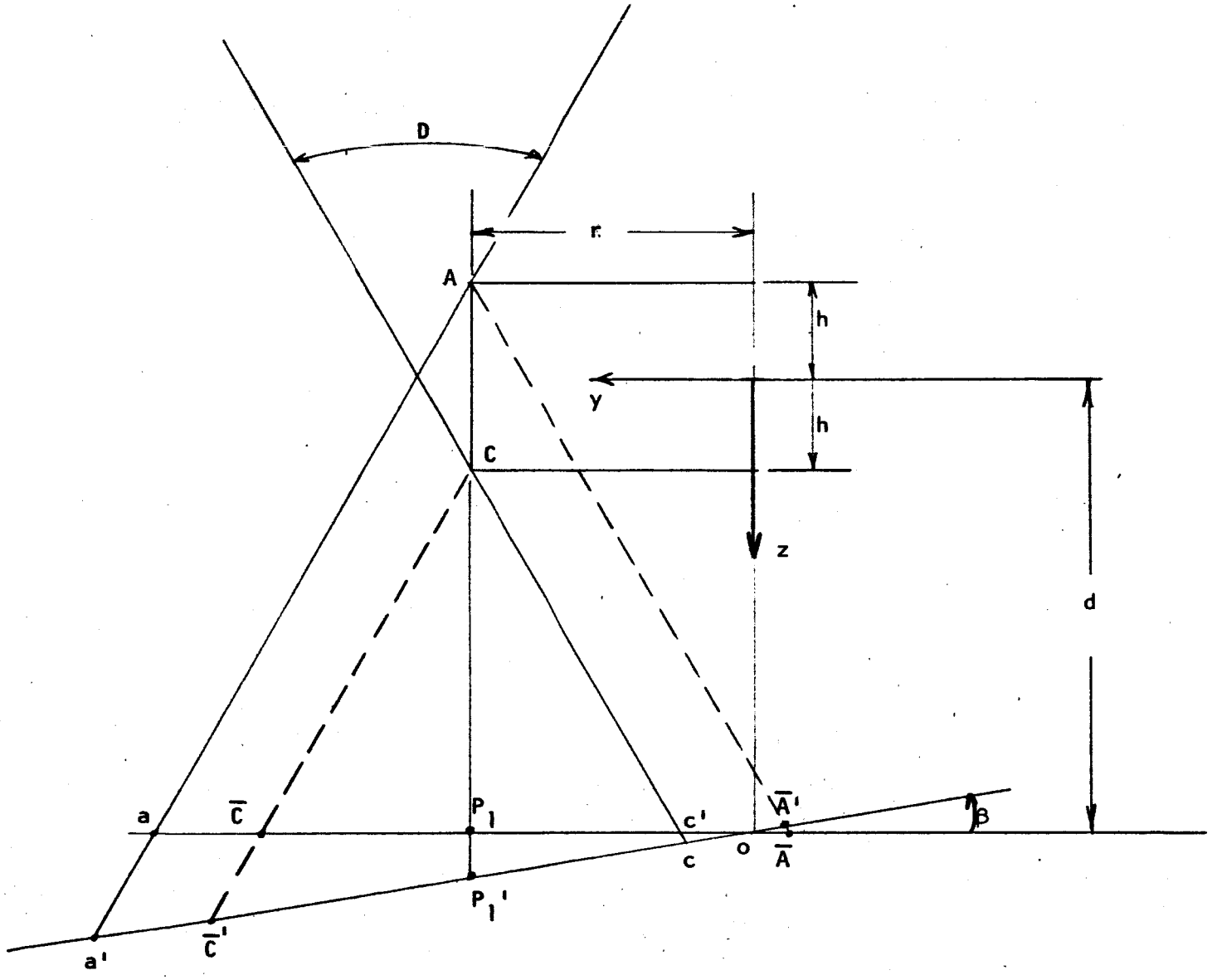

FIG. 17

In the penumbra region $a'P_1'$ the penumbra may be considered due to a knife edge at A. In the region from P_1' to c' the apparent knife edge may be considered located at C. Referring to Fig. 17, the position in the actual penumbra is expressed as

$$\frac{a'x'}{a'e'} = \frac{a'x'}{L_A}\,\frac{L_A}{a'e'} \tag{2.6.2}$$

where

$$L_A \triangleq a'\bar{A}' \tag{2.6.3}$$

and is the length of the penumbra due to an apparent knife edge at A. Therefore,

$$\frac{a'x'}{L_A} = \frac{a'x'}{a'e'}\left\{\frac{a'e'}{a'\bar{A}'}\right\}$$

$$0 \leq \frac{a'x'}{a'e'} \leq \frac{a'P_1'}{a'e'} \tag{2.6.4}$$

If $R >> d$, then from Fig. 16 and Fig. 17, trajectories $e'E$ and $\bar{A}'A$ may be considered parallel. Let an orthogonal coordinate system with its origin on the axis of the rectangular cylinder be orientated as shown in Fig. 16. The equation for a general ray is given as

$$z = my + b \tag{2.6.5}$$

Furthermore, note that the slopes of the ray trajectories are given by

$$m_{a'A} = \frac{1}{D/2} \tag{2.6.6a}$$

$$m_{e'E} = -\frac{1}{D/2} \tag{2.6.6b}$$

$$m_{\overline{A}'A} = m_{e'E} = -\frac{1}{D/2} \tag{2.6.6c}$$

Also, the coordinates of points A, C and E located on ray trajectories a'A, c'C and e'E, respectively, are given as

$$\text{Point A:} \qquad y_A = r; \qquad z_A = -h \tag{2.6.7a}$$

$$\text{Point C:} \qquad y_C = r; \qquad z_C = h \tag{2.6.7b}$$

$$\text{Point E:} \qquad y_E = -r; \qquad z_E = -h \tag{2.6.7c}$$

From Eqs. (2.6.6), (2.6.7) and (2.6.5), the required ray trajectory equations are given as

$$(z)_{a'A} = \frac{1}{D/2}\, y - r\left\{\frac{h}{r} + \frac{2}{D}\right\} \tag{2.6.8a}$$

$$(z)_{\overline{A}'A} = -\frac{1}{D/2}\, y - r\left\{\frac{h}{r} - \frac{2}{D}\right\} \tag{2.6.8b}$$

$$(z)_{e'E} = -\frac{1}{D/2}\, y - r\left\{\frac{h}{r} + \frac{2}{D}\right\} \tag{2.6.8c}$$

The equation for the receiving surface is given as

$$z = d + y \tan\beta \tag{2.6.9}$$

Combining Eq. (2.6.9) with Eq. (2.6.8) yields the y intercept of the ray trajectories on the receiving surface.

$$y_{a'} = \frac{r\frac{D}{2}\left\{\frac{d}{r} + \frac{h}{r} + \frac{2}{D}\right\}}{1 - \frac{D}{2}\tan\beta} \tag{2.6.10a}$$

$$y_{\bar{A}'} = \frac{-r\frac{D}{2}\left\{\frac{d}{r} + \frac{h}{r} - \frac{2}{D}\right\}}{1 + \frac{D}{2}\tan\beta} \tag{2.6.10b}$$

$$y_{e'} = \frac{-r\frac{D}{2}\left\{\frac{d}{r} + \frac{h}{r} + \frac{2}{D}\right\}}{1 + \frac{D}{2}\tan\beta} \tag{2.6.10c}$$

Also from Fig. 17

$$y_{P_1'} = r \tag{2.6.11}$$

From Eqs. (2.6.10a) and (2.6.10c) and Fig. 16

$$a'e' = \frac{rD}{\cos\beta}\left[\frac{\frac{d}{r} + \frac{h}{r} + \frac{2}{D}}{1 - \left\{\frac{D}{2}\tan\beta\right\}^2}\right] \tag{2.6.12}$$

and from Eqs. (2.6.10a) and (2.6.10b)

$$a'\bar{A}' = \frac{rD}{\cos\beta}\left[\frac{\frac{d}{r}+\frac{h}{r}+\tan\beta}{1-\left\{\frac{d}{2}\tan\beta\right\}^2}\right] \tag{2.6.13}$$

Also from Eqs. (2.6.10a) and (2.6.11)

$$a'P_1' = \frac{r\frac{D}{2}}{\cos\beta}\left[\frac{\frac{d}{r}+\frac{h}{r}+\tan\beta}{1-\frac{D}{2}\tan\beta}\right] \tag{2.6.14}$$

Substituting Eqs. (2.6.12), 2.6.13) and (2.6.14) into Eq. (2.6.4) yields the expression for the equivalent position in the penumbra of a single knife edge at A that will have the same energy flux density as the actual position in the penumbra due to <u>half</u> a rectangular cylinder.

$$\left.\begin{aligned}\frac{a'x'}{L_A} &= \frac{a'x'}{a'e'}\left[\frac{1+\frac{D}{2}\left\{\frac{d}{r}+\frac{h}{r}\right\}}{\frac{D}{2}\left\{\left(\frac{d}{r}+\frac{h}{r}\right)+\tan\beta\right\}}\right]\\ 0 &\le \frac{a'x'}{a'e'} \le \frac{a'P_1'}{a'e'}\end{aligned}\right\} \tag{2.6.15}$$

with

$$\frac{a'P_1'}{a'e'} = \frac{\frac{D}{4}\left\{1+\frac{D}{2}\tan\beta\right\}\left\{\frac{d}{r}+\frac{h}{r}+\tan\beta\right\}}{1+\frac{D}{2}\left\{\frac{d}{r}+\frac{h}{r}\right\}} \tag{2.6.15a}$$

For a point in the actual penumbra such that

$$\frac{a'P_1'}{a'e'} \leq \frac{a'x'}{a'e'} \leq \frac{a'c'}{a'e'} \tag{2.6.16}$$

The position in the actual penumbra may be expressed as

$$\frac{a'x'}{a'e'} = \frac{a'x'}{L_C}\frac{L_C}{a'e'} \tag{2.6.17}$$

or

$$\frac{a'x'}{a'e'} = \left\{\frac{a'P_1'}{L_C} - \frac{\bar{C}'P_1'}{L_C} + \frac{\bar{C}'x'}{L_C}\right\}\frac{L_C}{a'e'} \tag{2.6.18}$$

where

$$L_C = \bar{C}'c' \tag{2.6.19}$$

and is the length of the penumbra due to an apparent knife edge at C. Solving Eq. (2.6.18) for $\frac{\bar{C}x'}{L_C}$ yields

$$\left.\begin{aligned} \frac{C'x'}{L_C} &= \frac{a'x'}{a'e'}\left\{\frac{a'e'}{\bar{C}'c'}\right\} - \frac{a'P_1'}{\bar{C}'c'} + \frac{\bar{C}'P_1'}{\bar{C}'c'} \\ \frac{a'P_1'}{a'e'} &\leq \frac{a'x'}{a'e'} \leq \frac{a'c'}{a'e'} \end{aligned}\right\} \tag{2.6.20}$$

From Fig. 17 for $R \gg d$ the ray trajectories a'A and $\overline{C}$'C may be considered parallel. From Eqs. (2.6.6a), (2.6.7b), (2.6.5) and (2.6.9) the y intercept of ray $\overline{C}$'C with the receiving surface is given as

$$y_{\overline{C}'} = \frac{r\frac{D}{2}\left\{\frac{d}{r} - \frac{h}{r} + \frac{2}{D}\right\}}{1 - \frac{D}{2}\tan\beta} \tag{2.6.21}$$

Referring to Fig. 17

$$\overline{C}'c' = \frac{rD}{\cos\beta}\left[\frac{\frac{d}{r} - \frac{h}{r} + \tan\beta}{1 - \left\{\frac{D}{2}\tan\beta\right\}^2}\right] \tag{2.6.22}$$

and

$$\overline{C}'P_1' = \frac{r\frac{D}{2}}{\cos\beta}\left[\frac{\frac{d}{r} - \frac{h}{r} + \tan\beta}{1 - \frac{D}{2}\tan\beta}\right] \tag{2.6.23}$$

Substituting Eqs. (2.6.12), (2.6.14), (2.6.22) and (2.6.23) into Eq. (2.6.20) yields

$$\frac{\overline{C}'x'}{L_C} = \frac{a'x'}{a'e'}\left[\frac{1 + \frac{D}{2}\left\{\frac{d}{r} + \frac{h}{r}\right\}}{\frac{D}{2}\left\{\frac{d}{r} - \frac{h}{r} + \tan\beta\right\}}\right] - \left[\frac{\frac{h}{r}\left\{1 + \frac{D}{2}\tan\beta\right\}}{\frac{d}{r} - \frac{h}{r} + \tan\beta}\right] \tag{2.6.24}$$

$$\frac{a'P_1'}{a'e'} \leq \frac{a'x'}{a'e'} \leq \frac{a'c'}{a'e'}$$

with

$$\frac{a'c'}{a'e'} = \frac{\frac{D}{2}\left[\frac{d}{r} + \left\{1 + \frac{D}{2}\frac{h}{r}\right\}\tan\beta\right]}{1 + \frac{D}{2}\left\{\frac{d}{r} + \frac{h}{r}\right\}} \qquad (2.6.24a)$$

and

$$\frac{a'P_1'}{a'e'} \quad \text{given by Eq. (2.6.15a)}$$

Equations (2.6.15) and (2.6.24) define equivalent positions for apparent single knife edges associated with the left half of the rectangular cylinder.

Now consider the energy distribution in the penumbra due to the right half of the rectangular cylinder. The geometry is shown in Fig. 18.

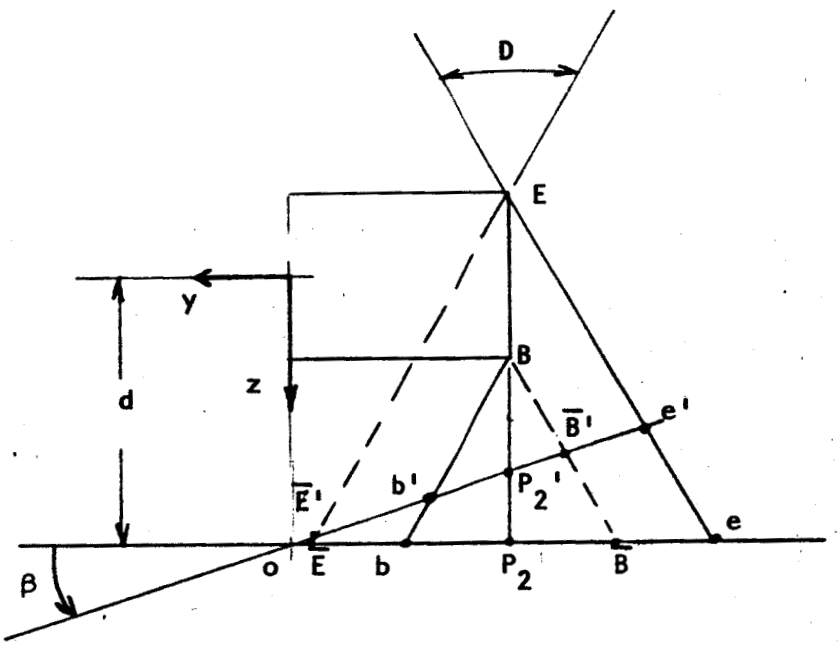

FIG. 18

For

$$\frac{a'b'}{a'e'} \leq \frac{a'x'}{a'e'} \leq \frac{a'P_2'}{a'e'} \tag{2.6.25}$$

the position in the actual penumbra may be expressed as

$$\frac{a'x'}{a'e'} = 1 - \frac{e'x'}{L_B}\frac{L_B}{a'e'} \tag{2.6.26}$$

where

$$L_B \triangleq b'\bar{B}' \tag{2.6.27}$$

and is the length of the penumbra due to an apparent knife edge at B.

Referring to Fig. 18 since

$$e'x' = e'P_2' - \bar{B}'P_2' + \bar{B}'x' \tag{2.6.28}$$

Eq. (2.6.26) may be expressed as

$$\frac{a'x'}{a'e'} = 1 - \left\{\frac{e'P_2'}{L_B} - \frac{\bar{B}'P_2'}{L_B} + \frac{\bar{B}'x'}{L_B}\right\}\frac{L_B}{a'e'} \tag{2.6.29}$$

Solving Eq. (2.6.29) for $\frac{\overline{B}'x'}{L_B}$

$$\left.\begin{aligned} \frac{\overline{B}'x'}{L_B} &= \left\{1 - \frac{a'x'}{a'e'}\right\}\frac{a'e'}{b'\overline{B}'} - \frac{e'P_2'}{b'\overline{B}'} + \frac{\overline{B}'P_2'}{b'\overline{B}'} \\ \frac{a'b'}{a'e'} &\le \frac{a'x'}{a'e'} \le \frac{a'P_2'}{a'e'} \end{aligned}\right\} \qquad (2.6.30)$$

Referring to Fig. 16 for $R \gg d$, the ray trajectory, b'B, can be considered to be parallel to the ray trajectory, a'A, and ray $\overline{B}'B$ can be considered parallel to ray e'E. Therefore from Eq. (2.6.6a) and (2.6.6b)

$$m_{b'B} = m_{a'A} = \frac{1}{D/2} \qquad (2.6.31a)$$

$$m_{B'B} = m_{e'E} = -\frac{1}{D/2} \qquad (2.6.31b)$$

The coordinates of point B on ray trajectory b'B are

$$\text{Point B:}\quad y_B = -r; \quad z_B = h \qquad (2.6.32)$$

From Eq. (2.6.31), (2.6.32) and (2.6.5), the equations for ray b'B and $\overline{B}'B$ are given as

$$(z)_{b'B} = \frac{1}{D/2}\,y + r\left\{\frac{h}{r} + \frac{2}{D}\right\} \qquad (2.6.33a)$$

$$(z)_{\overline{B}'B} = -\frac{1}{D/2}\,y + r\left\{\frac{h}{r} - \frac{2}{D}\right\} \qquad (2.6.33b)$$

Combining Eq. (2.6.33) and (2.6.9) yields the y intercept of rays b'B and $\overline{B}$'B with the receiver.

$$y_{b'} = \frac{r\frac{D}{2}\left\{\frac{d}{r} - \frac{h}{r} + \frac{2}{D}\right\}}{1 - \frac{D}{2}\tan\beta} \tag{2.6.34}$$

$$y_{\overline{B}'} = \frac{-r\frac{D}{2}\left\{\frac{d}{r} - \frac{h}{r} + \frac{2}{D}\right\}}{1 + \frac{D}{2}\tan\beta} \tag{2.6.35}$$

From Eq. (2.6.34) and (2.6.35)

$$b'\overline{B}' = \frac{rD}{\cos\beta}\frac{\left\{\frac{d}{r} - \frac{h}{r} - \tan\beta\right\}}{1 - \left\{\frac{D}{2}\tan\beta\right\}^2} \tag{2.6.36}$$

From Eq. (2.6.10c) and Fig. 18

$$e'P_2' = \frac{r\frac{D}{2}}{\cos\beta}\frac{\left\{\frac{d}{r} + \frac{h}{r} - \tan\beta\right\}}{1 + \frac{D}{2}\tan\beta} \tag{2.6.37}$$

Also from Eq. (2.6.34) and Fig. 18

$$\overline{B}'P_2' = \frac{r\frac{D}{2}}{\cos\beta}\frac{\left\{\frac{d}{r} - \frac{h}{r} - \tan\beta\right\}}{1 + \frac{D}{2}\tan\beta} \tag{2.6.38}$$

and from Eq. (2.6.10a), (2.6.34) and Fig. 18

$$a'b' = \frac{rD}{\cos\beta}\left[\frac{\frac{h}{r}+\frac{2}{D}}{1-\frac{D}{2}\tan\beta}\right] \tag{2.6.39}$$

$$a'P_2' = \frac{r\frac{D}{2}}{\cos\beta}\frac{\left\{\frac{d}{r}+\frac{h}{r}+\frac{4}{D}-\tan\beta\right\}}{1-\frac{D}{2}\tan\beta} \tag{2.6.40}$$

Substituting Eq. (2.6.12) and Eqs. (2.6.36) through (2.6.40) into Eq. (2.6.30) yields the expression for the equivalent position in the penumbra due to a knife edge at B that has the same energy flux density as the point in the actual penumbra.

$$\frac{\overline{B}'x'}{L_B} = \left\{1-\frac{a'x'}{a'e'}\right\}\left[\frac{1+\frac{D}{2}\left\{\frac{d}{r}+\frac{h}{r}\right\}}{\frac{D}{2}\left\{\frac{d}{r}-\frac{h}{r}-\tan\beta\right\}}\right]-\left[\frac{\frac{h}{r}\left\{1-\frac{D}{2}\tan\beta\right\}}{\frac{d}{r}-\frac{h}{r}-\tan\beta}\right] \tag{2.6.41}$$

$$\frac{a'b'}{a'e'} \le \frac{a'x'}{a'e'} \le \frac{a'P_2'}{a'e'}$$

with

$$\frac{a'b'}{a'e'} = \frac{\left\{1+\frac{D}{2}\frac{h}{r}\right\}\left\{1+\frac{D}{2}\tan\beta\right\}}{1+\frac{D}{2}\left\{\frac{d}{r}+\frac{h}{r}\right\}} \tag{2.6.42a}$$

and

$$\frac{a'P_2'}{a'e'} = \frac{\frac{1}{2}\left\{1+\frac{D}{2}\tan\beta\right\}\left[2+\frac{D}{2}\left\{\frac{d}{r}+\frac{h}{r}\right\}-\frac{D}{2}\tan\beta\right]}{1+\frac{D}{2}\left\{\frac{d}{r}+\frac{h}{r}\right\}} \tag{2.6.42b}$$

Finally for regions in the penumbra such that

$$\frac{a'P_2'}{a'e'} \leq \frac{a'x'}{a'e'} \leq 1 \tag{2.6.43}$$

the position in the actual penumbra may be expressed in terms of the position of an apparent knife edge at E.

$$\frac{a'x'}{a'e'} = 1 - \frac{e'x'}{L_E}\frac{L_E}{a'e'} \tag{2.6.44}$$

where

$$L_E = \overline{E}'e' \tag{2.6.45}$$

and is the length of the penumbra due to a knife edge at E.

From Eq. (2.6.44)

$$\left.\begin{aligned} \frac{e'x'}{L_E} &= \left\{1 - \frac{a'x'}{a'e'}\right\}\frac{a'e'}{\overline{E}'e'} \\ \frac{a'P_2'}{a'e'} &\leq \frac{a'x'}{a'e'} \leq 1 \end{aligned}\right\} \tag{2.6.46}$$

If $R \gg d$, then from Fig. 18 and Fig. 16 $\overline{E}'E$ and ray trajectory, a'A may be considered parallel. Then from Eq. (2.6.6a)

$$m_{\overline{E}'E} = m_{a'A} = \frac{1}{D/2} \tag{2.6.47}$$

Combining Eqs. (2.6.47), (2.6.7c) and (2.6.5) yields

$$(z)_{\overline{E'E}} = \frac{1}{D/2}\, y \; - r\left\{\frac{h}{r} - \frac{2}{D}\right\} \tag{2.6.48}$$

The y intercept of ray $\overline{E'E}$ and the receiving surface is then (from Eq. (2.6.48) and (2.6.9))

$$y_{\overline{E'}} = \frac{-r\,\frac{D}{2}\left\{\frac{d}{r} + \frac{h}{r} - \frac{2}{D}\right\}}{1 - \frac{D}{2}\tan\beta} \tag{2.6.49}$$

From Eq. (2.6.49) and Eq. (2.6.10c)

$$\overline{E'e'} = L_E = \frac{rD}{\cos\beta}\,\frac{\left\{\frac{d}{r} + \frac{h}{r} - \tan\beta\right\}}{1 - \left\{\frac{D}{2}\tan\beta\right\}^2} \tag{2.6.50}$$

Substituting Eqs. (2.6.50) and (2.6.12) into Eq. (2.6.46) yields

$$\left.\begin{aligned} \frac{e'x'}{L_E} &= \left\{1 - \frac{a'x'}{a'e'}\right\}\left[\frac{1 + \frac{D}{2}\left\{\frac{d}{r} + \frac{h}{r}\right\}}{\frac{D}{2}\left\{\frac{d}{r} + \frac{h}{r} - \tan\beta\right\}}\right] \\ \frac{a'P_2'}{a'e'} &\le \frac{a'x'}{a'e'} \le 1 \end{aligned}\right\} \tag{2.6.51}$$

with $\frac{a'P_2'}{a'e'}$ being given in Eq. (2.6.42b)

The position of the conical axis in the penumbra is given by

$$\frac{a'o}{a'e'} = \frac{y_{a'}}{a'e'} \tag{2.6.52}$$

and from Eqs. (2.6.10a) and (2.6.12)

$$\frac{a'o}{a'e'} = \frac{1}{2}\left\{1 + \frac{D}{2}\tan\beta\right\} \tag{2.6.53}$$

The technique used for determining the flux density distribution in the penumbra of a rectangular cylinder is as follows:

(1) Calculate the fraction of total penumbra due to an apparent knife edge at A, $\frac{a'P_1'}{a'e'}$, from Eq. (2.6.15a)

(2) For $0 \leq \frac{a'x'}{a'e'} \leq \frac{a'P_1'}{a'e'}$ with $\frac{a'P_1'}{a'e'}$ determined in step (1), calculate the equivalent position in the penumbra of a single knife edge, $\frac{a'x'}{L_A}$, from Eq. (2.6.15).

(3) Calculate the energy flux density corresponding to $\frac{a'x'}{L_A}$ in a manner identical to that for a single knife edge, i.e., determine $\frac{\theta_T}{D}$ from Eqs. (2.3.21) and (2.3.25) and the relative flux density from Eqs. (2.3.5), (2.3.6) and (2.3.4a). This flux density is the required density at $\frac{a'x'}{a'e'}$.

(4) Calculate the position of the end of a penumbra due to an apparent knife edge at C, $\frac{a'c'}{a'e'}$, from Eq. (2.6.24a).

(5) For $\frac{a'P_1'}{a'e'} \leq \frac{a'x'}{a'e'} \leq \frac{a'c'}{a'e'}$ with the limits defined in steps (1) and (4), calculate the equivalent position in the penumbra of a single knife edge at C, $\frac{\bar{C}'x'}{L_C}$, from Eq. (2.6.24).

(6) Calculate the energy flux density corresponding to $\frac{\bar{C}'x'}{L_C}$ from step (3) replacing $\frac{a'x'}{L_A}$ by $\frac{\bar{C}'x'}{L_C}$.

(7) Calculate $\frac{a'b'}{a'e'}$ and $\frac{a'P_2'}{a'e'}$ from Eqs. (2.6.42a) and (2.6.42b)

(8) For $\frac{a'b'}{a'e'} \leq \frac{a'x'}{a'e'} \leq \frac{a'P_2'}{a'e'}$ with the limits defined in step (7), calculate the equivalent position in a penumbra due to a knife edge at B, $\frac{\bar{B}'x'}{L_B}$, from Eq. (2.6.41).

(9) Calculate the energy flux density corresponding to $\frac{\bar{B}'x'}{L_B}$ from step (3) replacing $\frac{a'x'}{L_A}$ by $\frac{\bar{B}'x'}{L_B}$ and using $-\beta$ (see note Section 2.5, p.49) in Eqs. (2.3.25), (2.3.5), (2.3.6) and (2.3.4a)

(10) For $\frac{a'P_2'}{a'e'} \leq \frac{a'x'}{a'e'} \leq 1$ with $\frac{a'P_2'}{a'e'}$ given in step (7), calculate the equivalent position in the penumbra due to a knife edge at E, $\frac{e'x'}{L_E}$ from Eq. (2.6.51).

(11) Calculate the energy flux density corresponding to $\frac{e'x'}{L_E}$ from step (3), replacing $\frac{a'x'}{L_A}$ by $\frac{e'x'}{L_E}$ and use $-\beta$ (see note p.49) in Eqs. (2.3.25), (2.3.5), (2.3.6) and (2.3.4a).

(12) The energy flux density distribution in the penumbra of a non-reflecting rectangular cylinder is obtained by summing the flux densities determined in steps (3), (6), (9) and (11) for a given location in the penumbra, $\frac{a'x'}{a'e'}$.

2.6.2 Specular Rectangular Cylinder, Reflectance = 1.0

If the source and the rectangular cylinder have relative positions such that (see Fig. 16)

$$R \gg d + h$$

the sides of the rectangular cylinder will have the characteristics of specular skirts. Therefore, from Section 2.4.1, the effect of the specular sides is such that the rectangular cylinder may be replaced by a double knife edge located at

$$\frac{\bar{d}}{r} = \frac{d}{r} - \frac{h}{r}$$

where

$\frac{\bar{d}}{r}$ is a geometry factor associated with a double knife edge

and $\frac{d}{r}$ and $\frac{h}{r}$ are the geometry factors associated with the rectangular cylinder.

2.6.3 Diffuse Rectangular Cylinder, Reflectance = 1.0

For

$$R >> d + h$$

each side of the rectangular cylinder may be considered a diffuse skirt and the analysis of Section 2.4.3 is appropriate. Therefore, the relative flux density due to diffuse reflection from the skirt, Q', may be calculated using Eq. (2.6.46). However, the angles, ϕ_{11}, ϕ_{12} and ϕ_{22} must be redefined in terms of geometric parameters associated with the rectangular cylinder. The geometry considered is shown in Fig. 19.

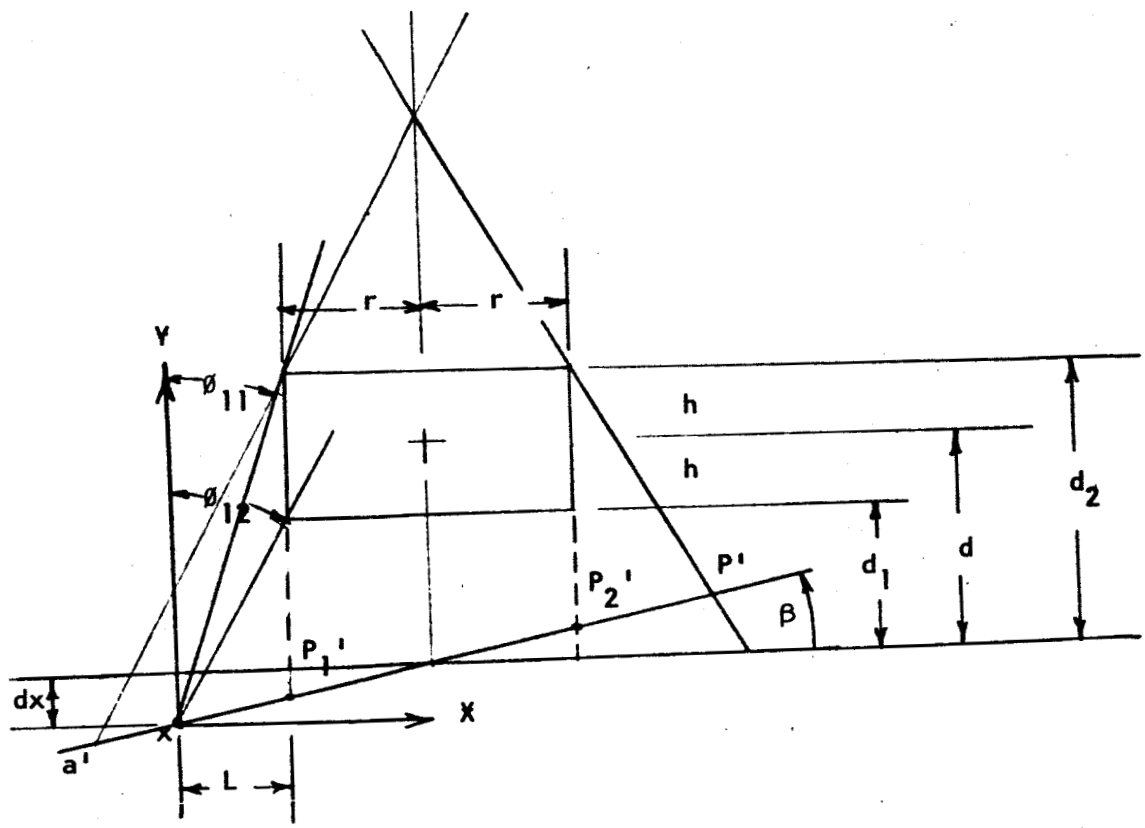

FIG. 19

From Fig. 19 for the left half of the rectangle

$$L = x'P_1'\cos\beta \tag{2.6.54}$$

$$dx = \tan\beta(L + r) \tag{2.6.55}$$

and

$$\phi_{11} = \tan^{-1}\left\{\frac{L}{d_2 + d_x}\right\} \tag{2.6.56a}$$

$$\phi_{12} = \tan^{-1}\left\{\frac{L}{d_1 + d_x}\right\} \tag{2.6.56b}$$

Substituting Eq. (2.6.55) into Eq. (2.6.56) yields

$$\phi_{11} = \tan^{-1}\left[\frac{\frac{L}{r}}{\frac{d_2}{r} + \left\{\frac{L}{r} + 1\right\}\tan\beta}\right] \tag{2.6.57a}$$

$$\phi_{12} = \tan^{-1}\left[\frac{\frac{L}{r}}{\frac{d_1}{r} + \left\{\frac{L}{r} + 1\right\}\tan\beta}\right] \tag{2.6.57b}$$

Since $x'P_1' = a'P_1' - a'x'$

$$L = \left\{\frac{a'P_1'}{a'e'} - \frac{a'x'}{a'e'}\right\} a'e'\cos\beta \tag{2.6.58}$$

Substituting $a'e'\cos\beta$ from Eq. (2.6.12) into Eq. (2.6.58) and solving for L/r

$$\frac{L}{r} = 2\left[\frac{1+\frac{D}{2}\left\{\frac{d}{r}+\frac{h}{r}\right\}}{1-\left\{\frac{D}{2}\tan\beta\right\}^2}\right]\left\{\frac{a'P_1'}{a'e'} - \frac{a'x'}{a'e'}\right\} \qquad (2.6.59)$$

$$0 \leq \frac{a'x'}{a'e'} \leq \frac{a'P_1'}{a'e'}$$

with $\frac{a'P_1'}{a'e'}$ given in Eq. (2.6.15a)

Referring to Fig. 19

$$\frac{d_2}{r} = \frac{d}{r} + \frac{h}{r} \qquad (2.6.60a)$$

$$\frac{d_1}{r} = \frac{d}{r} - \frac{h}{r} \qquad (2.6.60b)$$

so that

$$\phi_{11} = \tan^{-1}\left[\frac{\frac{L}{r}}{\left\{\frac{d}{r}+\frac{h}{r}\right\}+\left\{\frac{L}{r}+1\right\}\tan\beta}\right] \qquad (2.6.61a)$$

$$\phi_{12} = \tan^{-1}\left[\frac{\frac{L}{r}}{\left\{\frac{d}{r}-\frac{h}{r}\right\}+\left\{\frac{L}{r}+1\right\}\tan\beta}\right] \qquad (2.6.61b)$$

where $\frac{d}{r}$ and $\frac{h}{r}$ are geometry factors for the rectangular cylinder and $\frac{L}{r}$ is given in Eq. (2.6.59). The azimuth angle may be derived as

$$\phi_{22} = \tan^{-1}\left\{\frac{W}{t}\right\} = \tan^{-1}\left[\frac{\left\{\frac{W}{d_2}\right\}\left\{\frac{d}{r}+\frac{h}{r}\right\}}{\frac{L}{r}}\right] \qquad (2.6.62a)$$

or

$$\phi_{22} = \tan^{-1}\left\{\frac{\frac{W}{r}}{\frac{L}{r}}\right\} \qquad (2.6.62b)$$

where

W = half width of the skirt

and $\frac{L}{r}$ is given by Eq. (2.6.59)

For the right half of the cylinder, i.e.

$$\frac{a'P_2'}{a'e'} \leq \frac{a'x'}{a'e'} \leq 1$$

$$\phi_{11} = \tan^{-1}\left[\frac{\frac{L}{r}}{\frac{d}{r}+\frac{h}{r}-\left\{\frac{L}{r}+1\right\}\tan\beta}\right] \qquad (2.6.63a)$$

$$\phi_{12} = \tan^{-1}\left[\frac{\frac{L}{r}}{\frac{d}{r}-\frac{h}{r}-\left\{\frac{L}{r}+1\right\}\tan\beta}\right] \qquad (2.6.63b)$$

$$\phi_{22} = \tan^{-1}\left[\frac{\left\{\frac{W}{d_2}\right\}\left\{\frac{d}{r}+\frac{h}{r}\right\}}{\frac{L}{r}}\right] = \tan^{-1}\left\{\frac{\frac{W}{r}}{\frac{L}{r}}\right\} \qquad (2.6.63c)$$

with

$$\left.\begin{aligned} \frac{L}{r} &= 2\left[\frac{1+\frac{D}{2}\left\{\frac{d}{r}+\frac{h}{r}\right\}}{1-\left\{\frac{D}{2}\tan\beta\right\}^2}\right]\left\{\frac{a'x'}{a'e'}\right\} - \frac{a'P_2'}{a'e'} \\ \frac{a'P_2'}{a'e'} &\le \frac{a'x'}{a'e'} \le 1 \end{aligned}\right\} \qquad (2.6.64)$$

where $\frac{a'P_2'}{a'e'}$ is given in Eq. (2.6.42b)

In evaluating Q' for the region $\frac{a'P_2'}{a'e'} \le \frac{a'x'}{a'e'} \le 1$, note that <u>$-\beta$ must be used in Eq. (2.4.46)</u>.

2.7 METHOD OF ANALYSIS - CIRCULAR CYLINDER

2.7.1 <u>Diffuse Circular Cylinder, Reflectance = 0.0</u>

The general geometry of the system being considered is shown in Fig. 20. (See following page.) In Fig. 20 the points on the cylinder identified as A, C, B and E define the points of tangency of the extreme rays with the cylinder. The total length of the penumbra is given by the intersection of rays a'A and e'E with the receiving surface. A general point in the penumbra has an obstructed view of the source. If diffraction effects are ignored, a general point in the penumbra "sees" that part of the source that is defined by a limiting ray that passes through the point and is

FIG 20

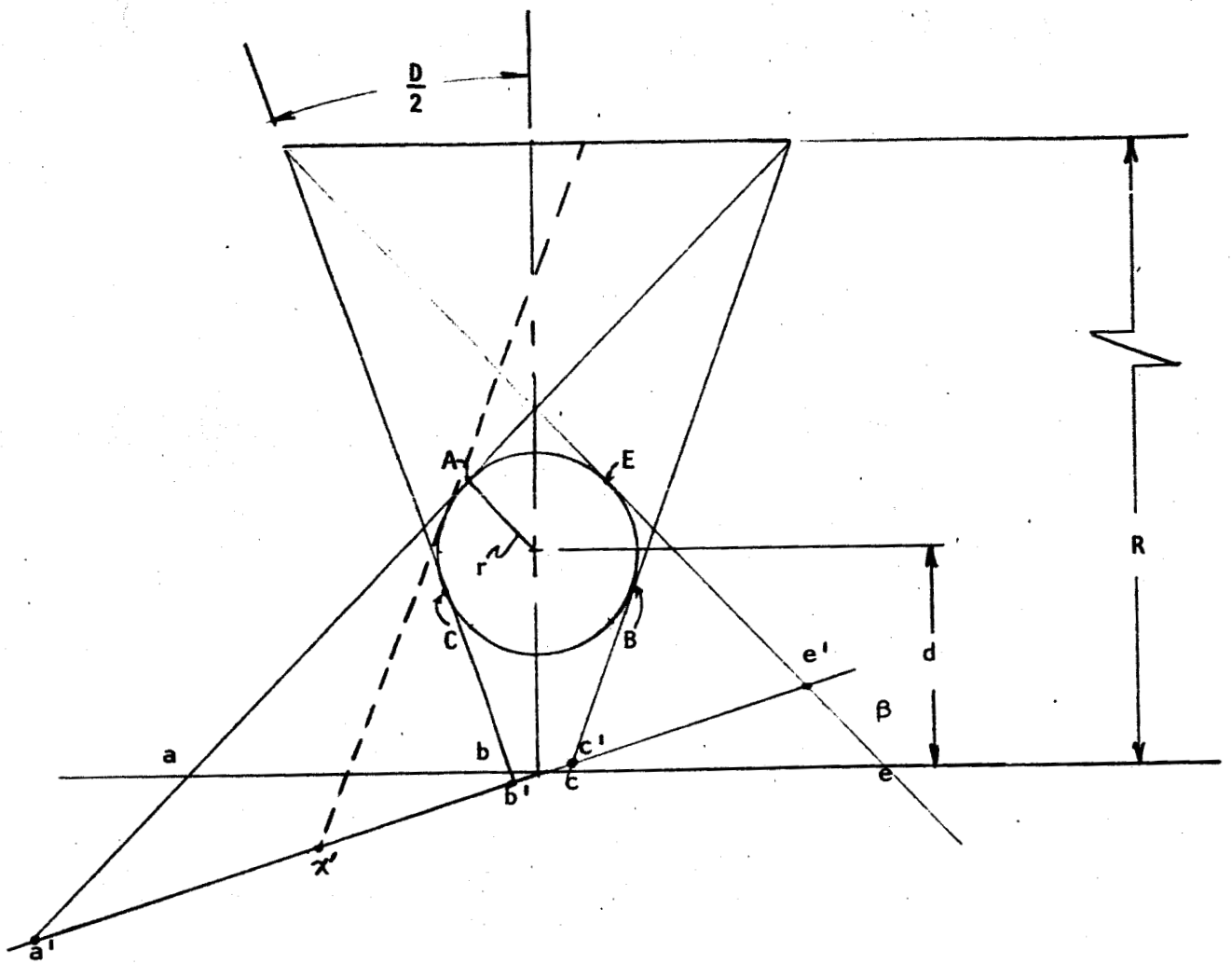

FIG. 20

tangent to the cylinder. Therefore, each point in the penumbra has an obstructed view of the source due to an apparent knife edge located at the point of tangency of the limiting ray with the cylinder. The energy flux density distribution in the penumbra of a circular cylinder may be obtained by determining the location of the apparent knife edge for each point in the penumbra and calculating the corresponding relative energy flux density at that point due to that particular apparent knife edge.

If $R \ll d$ then the rays a'A and b'B may be considered parallel. Similarly, the rays e'E and c'C amy be considered parallel and the geometry used in the analysis of the circular cylinder is as shown in Fig. 21. p.74a.

Consider the part of the cylinder generating the penumbra region a'c'. For any point in the penumbra from a' to c', a ray trajectory to the point and tangent to the cylinder will have a point of tangency between A and C on the cylinder. Referring to Fig. 21, p.74a, locate an orthogonal coordinate system (Y-Z) on the cylinder such that the origin of the coordinate system is coincident with the axis of the cylinder. Define

$\theta_X \triangleq$ angle measured from the positive Y axis (positive counterclockwise to any radius line perpendicular to a ray x'X that is tangent to the cylinder.

From Fig. 21, the characteristic of the penumbra will be such that for $\theta_X = \theta_c$

$$\text{ctn}^{-1}\left[\frac{d - r\sin\theta_{c'}}{r\cos\theta_{c'}}\right] \approx \text{ctn}^{-1}\left[\frac{\frac{d}{r} - \frac{D}{2}}{1 - \frac{D^2}{8}}\right] > \frac{D}{2} \qquad (2.7a)$$

there will be two penumbrae separated by an umbra region, and for

$$\text{ctn}^{-1}\left[\frac{\frac{d}{r} - \frac{D}{2}}{1 - \frac{D^2}{8}}\right] < \frac{D}{2} \qquad (2.7b)$$

the penumbrae due to the left and right portion of the cylinder will overlap resulting in a reinforced penumbra in the overlapping region.

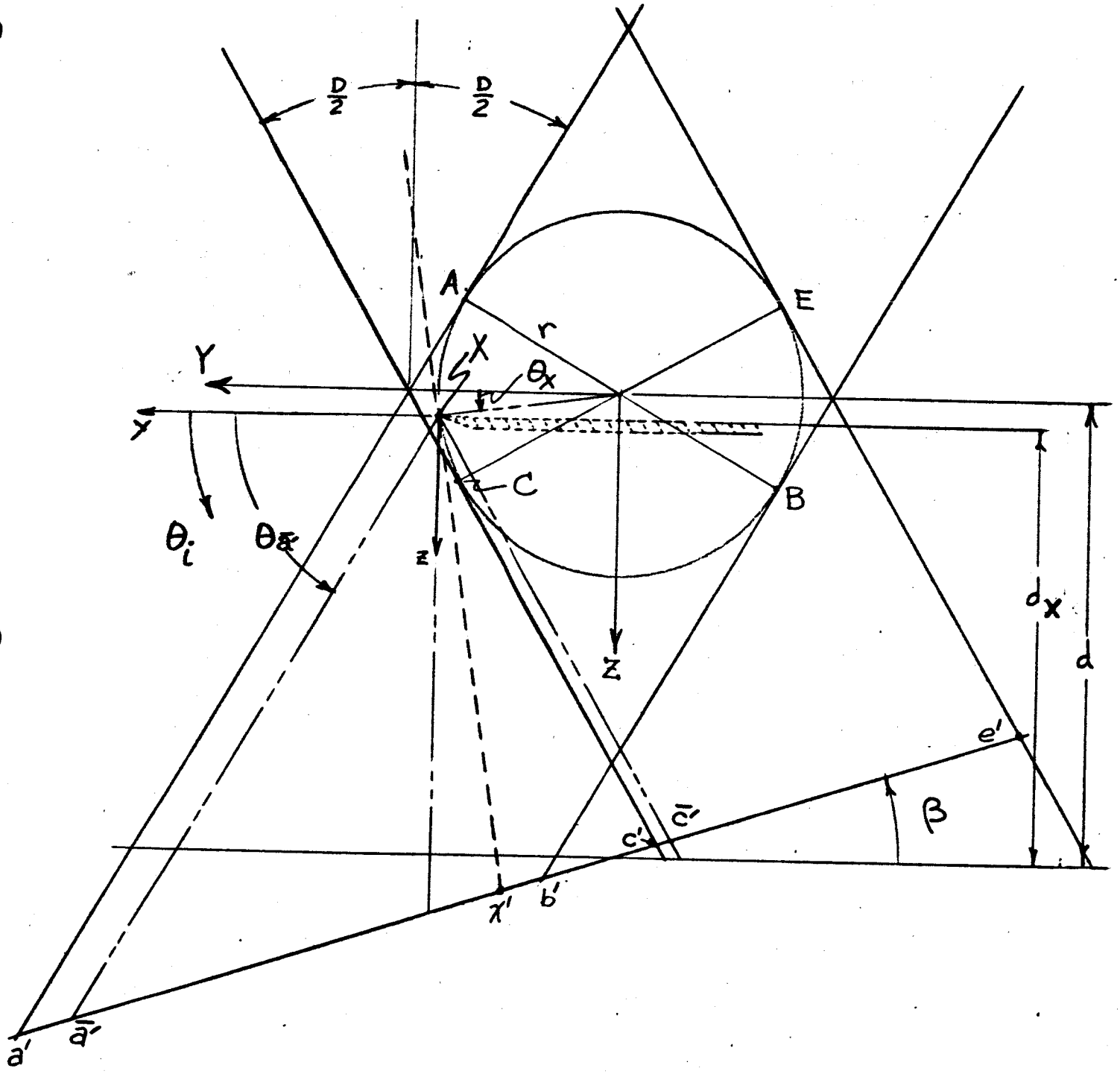

FIG. 21

The general equation for any ray given as

$$Z = mY + b \tag{2.7.1}$$

If the ray is tangent to the cylinder, the slope of the ray will be

$$m = -\frac{1}{\tan\theta_X} \tag{2.7.2}$$

Furthermore, the coordinate of the tangent points will be

$$Y_X = r\cos\theta_X \tag{2.7.3a}$$

$$Z_X = r\sin\theta_X \tag{2.7.3b}$$

From Eqs. (2.7.2), (2.7.3) and (2.7.1) the general equation for a ray tangent to the cylinder is given as

$$Z = -\frac{1}{\tan\theta_X} Y + \frac{r}{\sin\theta_X} \tag{2.7.4}$$

The equation of the receiving surface is given as

$$Z = d + Y\tan\beta \tag{2.7.5}$$

Substituting Eq. (2.7.5) into Eq. (2.7.4) and solving for Y gives the Y intercept on the receiver of a general ray tangent to the cylinder

$$Y_{x'} = \frac{r\left\{1 - \frac{d}{r}\sin\theta_X\right\}}{\cos\theta_X + \sin\theta_X\tan\beta} \qquad (2.7.6)$$

Now consider a general point, x, in the penumbra region a'c'. The point x "sees" an apparent knife edge at X, the tangent point of ray x'X and the cylinder. In fact, the incident energy on x' is the same as that received in the penumbra of a single knife edge a distance d_x above the surface (measured at the conical axis) at a location $\frac{\overline{a'x'}}{\overline{a'c'}}$ in the penumbra due to the knife edge. The position in the penumbra of a knife edge at d_x may be expressed as

$$\left.\begin{aligned} \frac{\overline{a'x'}}{\overline{a'c'}} &= \frac{a'x'}{a'e'}\left\{\frac{\overline{ax'}}{a'x'}\right\}\left\{\frac{a'e'}{\overline{a'c'}}\right\} \\ 0 \le \frac{a'x'}{a'e'} &\le \frac{a'c'}{a'e'} \end{aligned}\right\} \qquad (2.7.7)$$

For rays a'A

$$\theta_X = \theta_{a'} = -\frac{D}{2} \qquad (2.7.8)$$

Since

$$a'x' = \frac{1}{\cos\beta}\left(Y_{a'} - Y_{x'}\right) \qquad (2.7.9)$$

Use of Eqs. (2.7.8) and (2.7.6) yields

$$a'x' = \frac{r}{\cos\beta}\left[\frac{\cos\theta_X - \cos\frac{D}{2} + (\sin\frac{D}{2} + \sin\theta_X)\tan\beta + \frac{d}{r}\sin(\frac{D}{2} + \theta_X)}{\left\{\cos\frac{D}{2} - \sin\frac{D}{2}\tan\beta\right\}\left\{\cos\theta_X + \sin\theta_X\tan\beta\right\}}\right] \tag{2.7.10}$$

For ray e'E

$$\theta_X = \theta_{e'} = \pi + \frac{D}{2} \tag{2.7.11}$$

so that from Eq. (2.7.11) and (2.7.10), the total length of the penumbra due to the cylinder is

$$a'e' = \frac{r}{\cos\beta}\left[\frac{2\cos\frac{D}{2}\left\{1 + \frac{d}{r}\sin\frac{D}{2}\right\}}{\left\{\cos\frac{D}{2}\right\}^2 - \left\{\sin\frac{D}{2}\tan\beta\right\}^2}\right] \tag{2.7.12}$$

For ray c'C

$$\theta_X = \theta_{c'} = \frac{D}{2} \tag{2.7.13}$$

and from Eq. (2.7.10)

$$a'c' = \frac{r}{\cos\beta}\left[\frac{2\sin\frac{D}{2}\tan\beta + \frac{d}{r}\sin D}{\left\{\cos\frac{D}{2}\right\}^2 - \left\{\sin\frac{D}{2}\tan\beta\right\}^2}\right] \tag{2.7.14}$$

The fraction of the total penumbra due to the section of cylinder AC is obtained from Eqs. (2.7.12) and (2.7.14) as

$$\frac{a'c'}{a'e'} = \frac{\tan\frac{D}{2}\tan\beta + \frac{d}{r}\sin\frac{D}{2}}{\left\{1 + \frac{d}{r}\sin\frac{D}{2}\right\}} \tag{2.7.15}$$

Referring to Fig. 21, p.74a, consider another orthogonal coordinate system (y,z) parallel to the Y,Z coordinate system and origined at X. The equation for a general ray trajectory associated with the apparent knife edge at X will be

$$(z)_{iX} = y_{iX}\tan\theta_i \tag{2.7.16}$$

The equation for the receiving surface in the y,z coordinate system is

$$z = d_X + (r\cos\theta_X + y)\tan\beta \tag{2.7.17}$$

The y intercept of a general ray and the receiving surface is obtained by combining Eq. (2.7.16) and (2.7.17) as

$$y_i = \frac{d_X + r\cos\theta_X\tan\beta}{\tan\theta_i - \tan\beta} \tag{2.7.18}$$

For the ray x'X reference to Fig. 21 indicates

$$\theta_i = \theta_x = 90 + \theta_X \tag{2.7.19}$$

so that Eq. (2.7.18) may be written as

$$y_{x'} = \frac{-(d_X + r\cos\theta_X\tan\beta)\tan\theta_X}{1 + \tan\theta_X\tan\beta} \tag{2.7.20}$$

Also for the hypothetical ray, $\bar{a}'X$, parallel to ray a'A

$$\theta_i = \theta_{\bar{a}'} = 90 - \frac{D}{2} \tag{2.7.21}$$

and

$$y_{\bar{a}'} = \frac{(d_X + r\cos\theta_X\tan\beta)\tan\frac{D}{2}}{1 - \tan\frac{D}{2}\tan\beta} \tag{2.7.22}$$

From Eqs. (2.7.20) and (2.7.22) and the fact that

$$d_X = r\left\{\frac{d}{r} + \sin\theta_X\right\} \tag{2.7.23}$$

$$\bar{a}'x' = \frac{r}{\cos\beta}\left[\frac{\left\{\frac{d}{r} - \sin\theta_X + \cos\theta_X\tan\beta\right\}\left\{\tan\frac{D}{2} + \tan\theta_X\right\}}{\left\{1 - \tan\frac{D}{2}\tan\beta\right\}\left\{1 + \tan\theta_X\tan\beta\right\}}\right] \tag{2.7.24}$$

For the hypothetical ray $\bar{c}'X$ parallel to c'C

$$\theta_i = \theta_{\bar{c}'} = 90 + \frac{D}{2} \tag{2.7.25}$$

From Eqs. (2.7.25), (2.7.18) and (2.7.22)

$$\bar{a}'\bar{c}' = \frac{2r}{\cos\beta}\left[\frac{\tan\frac{D}{2}\left\{\frac{d}{r} - \sin\theta_X + \cos\theta_X\tan\beta\right\}}{1 - \left\{\tan\frac{D}{2}\tan\beta\right\}^2}\right] \tag{2.7.26}$$

Substituting Eqs. (2.7.24), (2.7.10), (2.7.12) and (2.7.26) into Eq. (2.7.17) gives an expression for the equivalent position in a penumbra due to an apparent knife edge at X for a point in the actual penumbra due to the cylinder

$$\frac{\bar{a}'x'}{\bar{a}'\bar{c}'} = \frac{a'x'}{a'e'}\left[\frac{\cos\theta_X\left\{1+\frac{d}{r}\sin\frac{D}{2}\right\}\left\{\tan\frac{D}{2}+\tan\theta_X\right\}}{\tan\frac{D}{2}\left\{\cos\theta_X-\cos\frac{D}{2}+\left(\sin\frac{D}{2}+\sin\theta_X\right)\tan\beta+\frac{d}{r}\sin\left(\frac{D}{2}+\theta_X\right)\right\}}\right] \tag{2.7.27}$$

$$0 \le \frac{a'x'}{a'e'} \le \frac{a'c'}{a'e'}$$

with $\frac{a'c'}{a'e'}$ given by Eq. (2.7.15)

It should be noted that by the definition of θ_X, θ_X is a function of $\frac{a'x'}{a'e'}$.

For

$$0 \le \frac{a'x'}{a'e'} \le \frac{a'c'}{a'e'}$$

$$\theta_A \le \theta_X \le \theta_c \tag{2.7.28}$$

$$-\frac{D}{2} \le \theta_X \le \frac{D}{2} \qquad (D \le 15^o) \tag{2.7.28a}$$

Small angle approximations may be used in evaluating Eq. (2.7.27). Let

$$\sin\theta_X = \theta_X \tag{2.7.29a}$$

$$\cos\theta_X = 1 - \frac{\theta_X^2}{2} \tag{2.7.29b}$$

$$\sin\frac{D}{2} = \frac{D}{2} \tag{2.7.29c}$$

$$\cos\frac{D}{2} = 1 - \frac{D^2}{8} \tag{2.7.29d}$$

Substituting Eq. (2.7.29) into (2.7.27) expanding and eliminating all 3rd order terms (i.e., terms proportional to D^3, $D\theta_X^2$, $D^2\theta_X$, θ_X^3) yields an expression for the equivalent position in the penumbra of a single knife as

$$\frac{a'x'}{\overline{a'c'}} = \frac{a'x'}{a'e'} \frac{1 + \frac{d}{r}\frac{D}{2}}{\frac{D}{2}\left\{\frac{d}{r} + \tan\beta\right\}} \tag{2.7.30}$$

A comparison of Eq. (2.7.30) with Eq. (2.5.13) in the Double Knife Edge Section indicates that the expression for equivalent positions in penumbrae due to the left half of the cylinder (Eq. (2.7.30)) is identical to the expression for the equivalent position in the penumbra of a single knife edge which corresponds to the left edge of the double knife edge Eq. (2.5.13)). Therefore, for the calculation of relative energy flux density, it is concluded that for small solar field angle ($D < 15^o$) the curvature of the cylinder may be ignored and the cylinder reduces to a double knife edge located at the diameter of the cylinder.

2.7.2 Specular Cylinder, Reflectance = 1.0

The case of the nonreflecting cylinder has been covered in a previous section and was shown to be equivalent to a double knife edge in so far as the accuracies being considered here are concerned. The addition of a specular surface to the cylinder has the effect of increasing the energy flux density both inside and outside the penumbra.

A point on the receiver in the penumbra will see an image of that portion of the source which is directly visible in the cylinder. The problem of finding the flux density augmentation due to the specular cylinder reduces to that of finding the ratio of the angle subtended by the specular image to that of the angle subtended by the directly visible image. This ratio is ϕ/θ_T, as defined in Fig. 22, p. 82a. The defining relationship for ϕ/θ_T has been derived using some small angle approximations having for their basis the previously used approximation that the sine or tangent of half the solar field angle, $\frac{D}{2}$, is equal to the angle itself. θ_T will never be greater than the solar field angle, and ϕ and ψ will always be less than θ_T.

Referring to Fig. 22

$$\delta_t = r \sin\psi \doteq r\psi \tag{2.7.31}$$

$$\delta_r = r(1 - \cos\psi) \doteq r\left\{1 - \left(1 - \frac{\psi^2}{2}\right)\right\} = \frac{r\psi^2}{2} \tag{2.7.32}$$

$$\phi \doteq \frac{\delta_r}{V'} = \frac{\delta_r}{V - \delta_t} = \frac{\frac{r\psi^2}{2}}{V - r\psi} \tag{2.7.33}$$

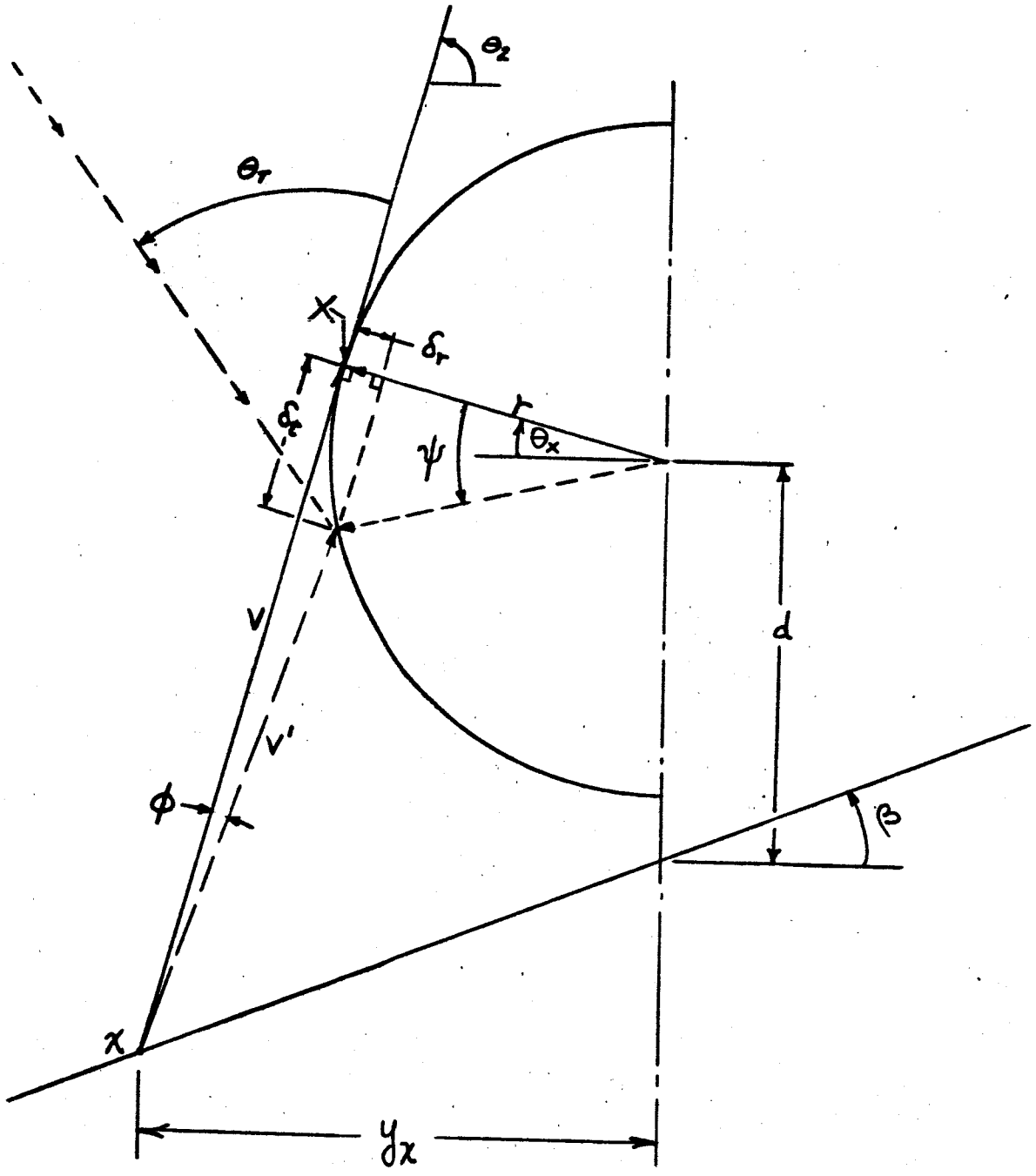

FIG. 22

Equation (2.7.33) relates ϕ, ψ and V. The next requirement is to find a relationship between these quantities and θ_T. Define γ_i to be the angle between an incident ray and the tangent to the cylinder at the point of impingement on the cylinder and γ_ρ to be the angle between the tangent and the reflected ray. It follows that

$$\theta_T = \psi + \gamma_i \tag{2.7.34}$$

$$\gamma_\rho = -\phi - \psi \tag{2.7.35}$$

$$\gamma_i = -\gamma_\rho = \phi + \psi \tag{2.7.36}$$

Substituting Eq. (2.7.36) into Eq. (2.7.34)

$$\theta_T = 2\psi + \phi \tag{2.7.37}$$

Substituting for ϕ from Eq. (2.7.33)

$$\theta_T = 2\psi + \frac{r\psi^2}{2(V - r\psi)} \tag{2.7.38}$$

This expression may be rewritten as

$$\psi^2 - \frac{2}{3}\left\{\theta_T + \frac{2V}{r}\right\}\psi + \frac{2V\theta_T}{3r} = 0 \tag{2.7.39}$$

Solving for ψ

$$\psi = \frac{\frac{2}{3}\left\{\theta_T + \frac{2V}{r}\right\} \pm \sqrt{\left\{\frac{2}{3}\right\}^2 \left\{\theta + \frac{2V}{r}\right\}^2 - (4)\frac{2V\theta_T}{3r}}}{2} \qquad (2.7.40)$$

The algebraic sign of the radical is chosen by noting that as either r or V become very large, $\psi \rightarrow 0$, and, therefore, the minus sign is appropriate

Now, solve Eq. (2.7.37) for ϕ/θ_T and substitute for 2ψ from Eq. (2.7.40) which gives the final expression

$$\frac{\phi}{\theta_T} = \frac{1}{3}\left\{1 - (2)\frac{2V}{r\theta_T} + 2\sqrt{\left\{1 + \frac{2V}{r\theta_T}\right\}^2 - (3)\frac{2V}{r\theta_T}}\right\} \qquad (2.7.41)$$

As $\frac{V}{r} \rightarrow 0$, $\frac{\phi}{\theta_T} \rightarrow 1$, in which case, the cylinder appears as a plane mirror. As $\frac{V}{r} \longrightarrow \infty$, $\frac{\phi}{\theta_T} \longrightarrow 0$.

The relationship between $\frac{V}{r\theta_T}$ and the position in the penumbra will now be derived. From the definition of θ_X given on p.74 and Fig. 22.

$$V = \frac{d - r\sin\theta_X + y_x\tan\beta}{\cos\left\{\frac{\pi}{2} - \theta_2\right\}} \qquad (2.7.42)$$

since

$$-\frac{D}{2} \leq \theta_X \leq \frac{D}{2} \qquad (D \leq 15^o)$$

Small angle approximation may be used so that

$$\frac{y_x}{r} \doteq \frac{1 - \frac{d}{r}\theta_X}{1 + \theta_X \tan\beta} \tag{2.7.43}$$

Also

$$\theta_2 = \frac{\pi}{2} + \theta_X \tag{2.7.44}$$

and

$$\theta_T = \frac{D}{2} + \left\{\frac{\pi}{2} - \theta_2\right\} = \frac{D}{2} - \theta_X \tag{2.7.45}$$

Substituting Eqs. (2.7.43), (2.7.44) and (2.7.45) into Eq. (2.7.42) expanding and eliminating 3rd order term in $\frac{D}{2}$ and θ_X yields

$$\frac{1}{\theta_T}\frac{V}{r} = \frac{\frac{d}{r} - \theta_X\left\{\frac{1 - \frac{d}{r}\theta_X}{1 + \theta_X\tan\beta}\right\}\tan\beta}{\frac{D}{2} - \theta_X} \tag{2.7.46}$$

θ_X is obtained by combining Eqs. (2.7.10) and (2.7.12) to form $\frac{a'x'}{a'e'}$ and solving for θ_X. Following this procedure and using small angle approximation gives

$$\left.\begin{aligned} \theta_X &= \frac{\frac{D}{2}\left\{2\frac{a'x'}{a'e'} - \frac{a'c'}{a'e'}(1 + \tan\beta)\right\}}{\frac{a'c'}{a'e'}(1 + \tan\beta) - (D\tan\beta)\frac{a'x'}{a'e'}} \\ 0 &\le \frac{a'x'}{a'e'} \le \frac{a'c'}{a'e'} \end{aligned}\right\} \tag{2.7.47}$$

with $\frac{a'c'}{a'e'}$ given by Eq. (2.5.13a) and, for convenience, repeated below

$$\frac{a'c'}{a'e'} = \frac{\frac{D}{2}\left\{\frac{d}{r} + \tan\beta\right\}}{1 + \frac{D}{2}\frac{d}{r}}$$

The interpretation of the result is that the portion of the source seen by reflection in the cylinder is being viewed at a low angle, i.e., that portion of the source appears rotated relative to the receiver about an axis parallel to that of the cylinder. The cylinder thus renders the image highly astigmatic.

Figure 23, p.86a is a graphical ray trace for a large source close to the cylinder. The ray trace indicates that the image is curved and close to the cylinder. If the source in Fig. 23 is reduced to a size consistent with those under consideration and is placed at a great distance from the cylinder, the curvature is reduced. It seems reasonable to ignore the small amount of image curvature in any calculations. Figure 24, p.86b depicts the appearance of the image. Since circular sources are being considered here, the image will appear to be a portion of an ellipse.

The energy received by reflection may be found either by considering that the area of the source has been reduced, or that the source is being viewed by the receiver at a low angle so that the energy received is reduced by the cosine of the angle between the receiver and the normal to the source. The area of an ellipse is πab, where a and b are the major and minor axes of the ellipse, respectively. The area of a circle is πa^2. The ratio of the area is

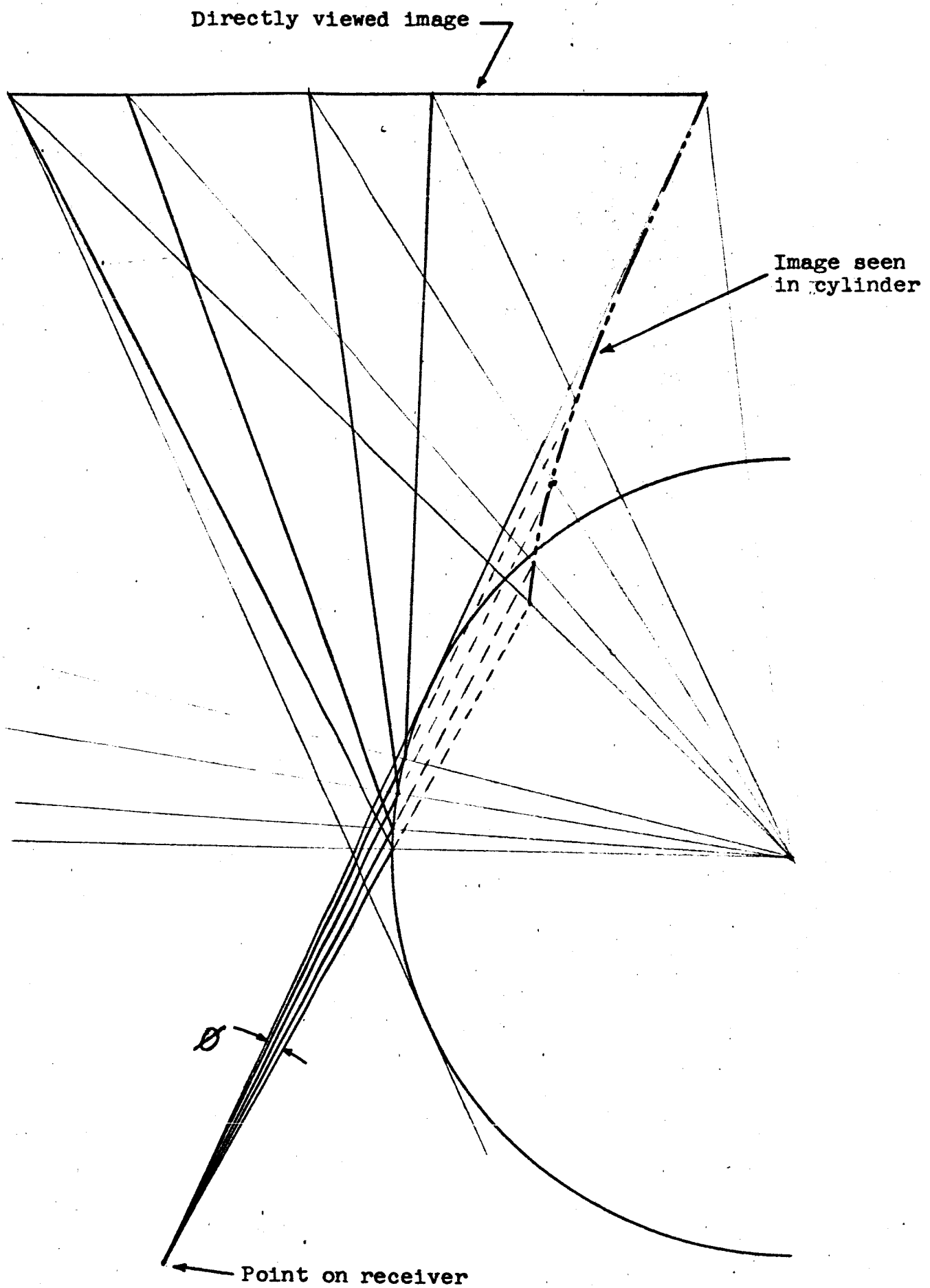
Directly viewed image
Image seen in cylinder
Point on receiver

FIG. 23

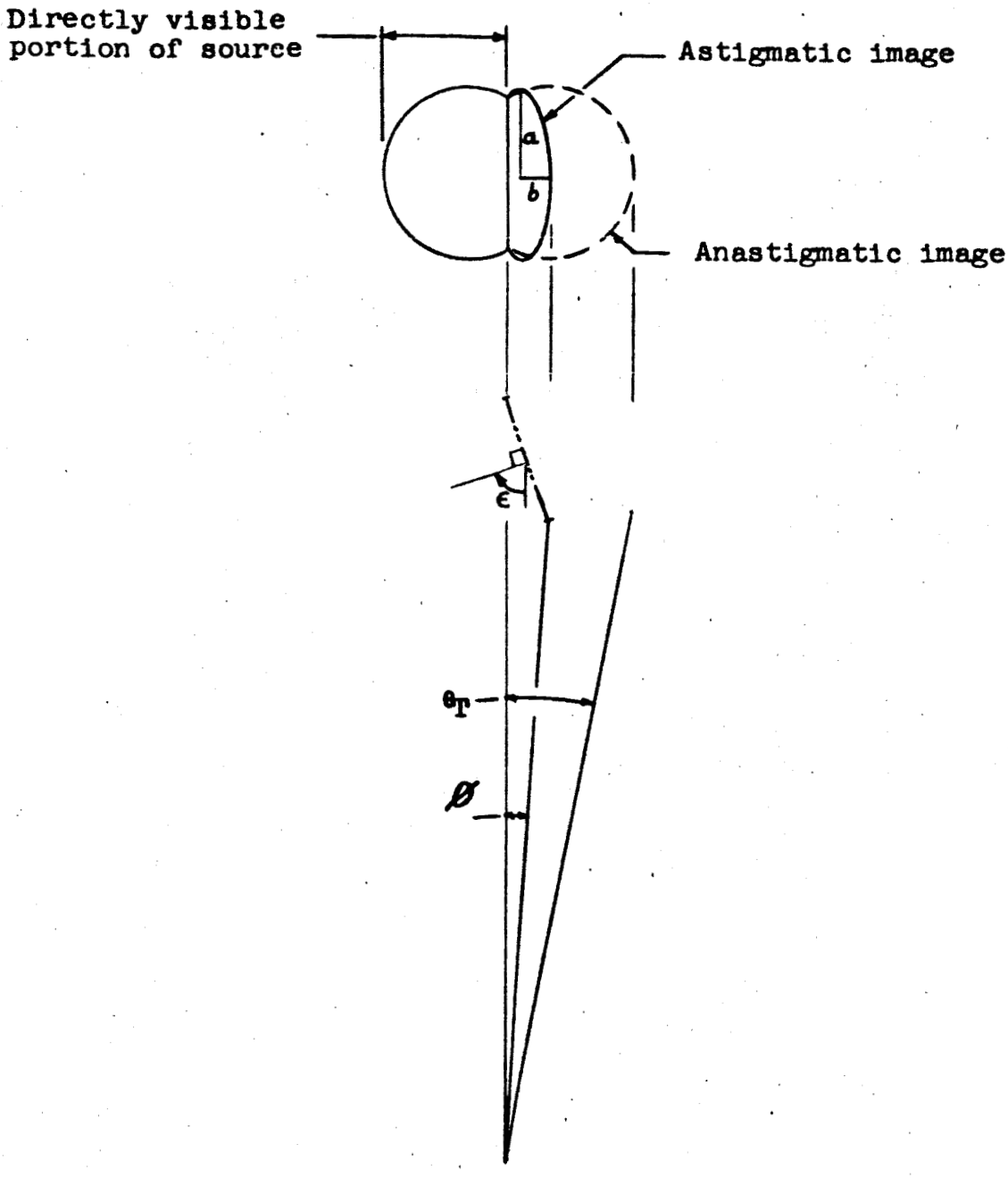
Directly visible
portion of source
Astigmatic image
a
b
Anastigmatic image
ϵ
θ_T
Ø

FIG. 24

$$\frac{A_e}{A_c} = \frac{\pi ab}{\pi a^2} = \frac{b}{a} \qquad (2.7.48)$$

Referring to Fig. 24, p.86b, it may be seen that

$$\cos\epsilon = \frac{b}{a} = \frac{A_e}{A_c} \qquad (2.7.49)$$

Also

$$\frac{\theta_T}{2} = \frac{a}{L} \qquad (2.7.50)$$

$$\frac{\phi}{2} = \frac{b}{L} \qquad (2.7.51)$$

$$\frac{\phi}{\theta_T} = \frac{b}{a} = \cos\epsilon = \frac{A_e}{A_c} \qquad (2.7.52)$$

Therefore, the augmentation in energy flux density due to reflection is found by multiplying the energy flux density arriving at the receiver directly by the factor $\frac{\phi}{\theta_T}$.

2.7.3 Diffuse Cylinder, Reflectance = 1.0

The diffuse cylinder is more analytically formidable than the diffuse skirt. The reason for this is that the cylinder is not uniformly illuminated by the source, whereas the flat skirt is uniformly illuminated. In order to determine the augmentation of relative energy flux density in the penumbra due to the diffuese circular cylinder, the integral of Eq. (2.4.44) must be evaluated with the inclusion of a function of $\emptyset$ which mathematically describes the varying illumination of the cylinder. The inclusion of this function makes the analytical evaluation of the integral tedious, and consequently, a numerical integration technique was used. This consisted of treating the cylinder as being uniformly illuminated on finite lengthwise strips.

Obtaining a solution to this problem consists of defining the illumination of the cylinder and then finding a numerical solution utilizing this information.

Referring to Fig. 25, Eq. (2.1.7) can be evaluated and rearranged as

$$\frac{dq_{12}}{dA_2} = \cos\gamma \int_{A_1} \frac{I_1 dA_1}{r^2} \qquad (2.7.53)$$

Where the subscript, 2, refers to the cylinder.

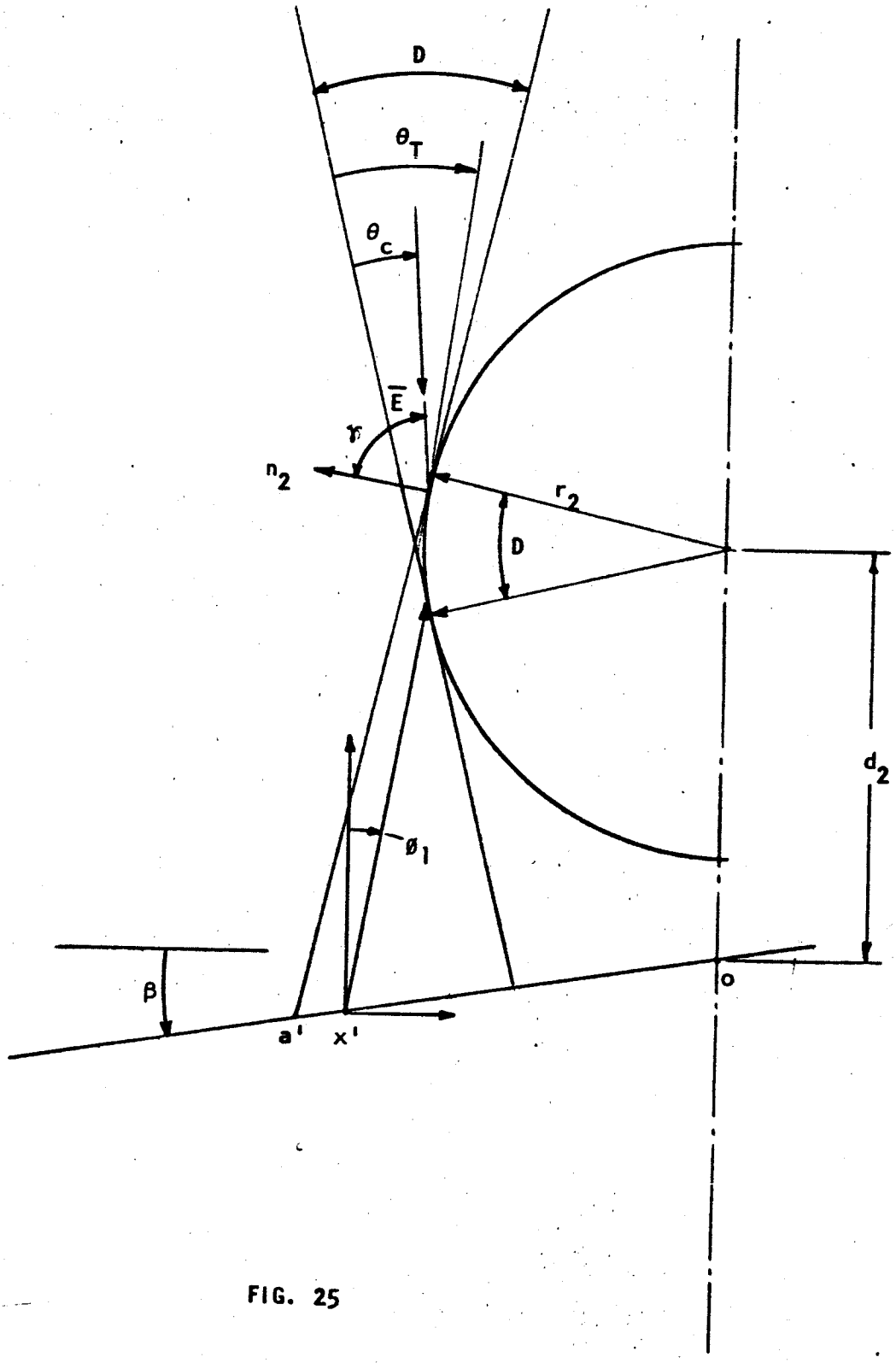

FIG. 25

Note that the only portion of the cylinder which is of interest is that defined by the limiting rays from the source, and that this portion has an included angle equal to the solar field angle, D.

$$\cos \gamma = \cos \left\{ \frac{\pi}{2} - (\theta_T - \theta_c) \right\}$$

$$= \sin (\theta_T - \theta_c) \qquad (2.7.54)$$

Since,

$$0 \leq (\theta_T - \theta_c) \leq \frac{D}{2},$$

Eq. (2.7.54) will be approximated as

$$\cos \gamma = (\theta_T - \theta_c) \qquad (2.7.55)$$

Therefore,

$$\frac{dq_{12}}{dA_2} = (\theta_T - \theta_c) \int_{A_1} \frac{I_1 dA_1}{r^2} \qquad (2.7.56)$$

Let

$$S = \int_{A_1} \frac{I_1 dA_1}{r^2} \qquad (2.7.57)$$

$$\frac{dq_{12}}{dA_2} = D\left\{\frac{\theta_T}{D} - \frac{\theta_c}{D}\right\}\left\{\frac{A}{A_t}\right\} S \qquad (2.7.58)$$

Utilizing Eq. (2.4.44), the relative energy flux density on the receiver may be written as

$$Q' = \frac{1}{\pi}\int_{o}^{\phi_{22}}\int_{\phi_{11}}^{\phi_{12}} D\left\{\frac{\theta_T}{D} - \frac{\theta_c}{D}\right\}\left\{\frac{A}{A_t}\right\} \sin\phi_1(\cos\phi_1 - \tan\beta\sin\phi_1\cos\phi_2)d\phi_1 d\phi_2 \qquad (2.7.59)$$

$\frac{\theta_c}{D}$ is computed from Eq. (2.3.5) and (2.3.6). $\frac{A}{A_t}$ is obtained from Eq. (2.3.4a) and (2.3.4b) as

$$\frac{A}{A_t} = \frac{1}{\pi}\left\{\alpha - \frac{1}{2}\sin 2\alpha\right\} \qquad (2.7.60)$$

Numerical evaluation by means of uniformly illuminated finite elements permits Eq. (2.7.59) to be evaluated as

$$Q' = \frac{D}{\pi}\sum_i \left\{\frac{\theta_T}{D} - \frac{\theta_c}{D}\right\}_i \left\{\frac{A}{A_t}\right\}_i \left\{\frac{\phi_{22}}{2}\left[\sin^2\phi_1\right]_{\phi_{11i}}^{\phi_{12i}} - \tan\beta\sin\phi_{22}\left[\frac{\phi_1}{2} - \frac{\sin 2\phi_1}{4}\right]_{\phi_{11i}}^{\phi_{12i}}\right\} \qquad (2.7.61)$$

3.0 METHOD OF ANALYSIS - MODULE SOLAR SIMULATION MODELS

The type of module solar model being considered in this study is shown in Fig. 26

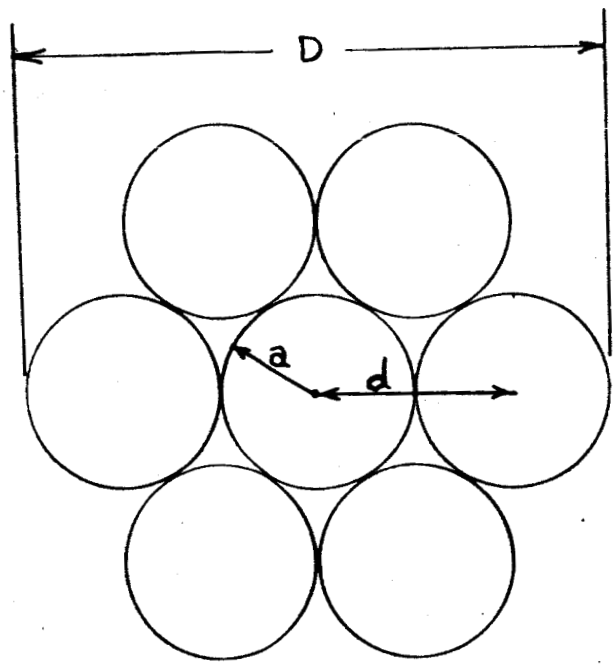

FIG. 26

Each module can be considered a separate source having 1/7 the intensity of the total source. The incident energy at any point in the receiver may be expressed as (see Eq. (2.1.8) and (2.1.9))

$$dq = -\overline{dA}\cdot\overline{E} = -\overline{dA}\cdot\sum_i \int_{S_i} \overline{dE} \qquad (3.1)$$

where $\sum\int \overline{dE}$ must include only the areas of direct (and, if applicable, reflected) illumination.

The actual solutions pertaining to module solar models are implemented by use of solutions obtained for surfaces illuminated by a uniformly radiating circular disc (Sections 2.3 - 2.7).

To illustrate the procedure consider a surface shaded by a knife edge and illuminated by a module source such as that shown in Fig.26 For this example let $\frac{a}{d} = .5$ and

$\left.\begin{matrix} \theta_T \\ D \\ A \\ A_T \\ \theta_C \end{matrix}\right\}$ = Parameters associated with the total source. (See Section 2.3 for definitions)

Define

$\left.\begin{matrix} (\theta_T)_i \\ (\bar{D})_i \\ (\bar{A})_i \\ (\bar{A_T})_i \\ (\bar{\theta_C})_i \end{matrix}\right\}$ = Parameters associated with the ith module

Fig 26

From Fig. 26 for any module

$$a = \frac{D}{6} \tag{3.2}$$

or

$$\frac{a}{D} = \frac{1}{6} \tag{3.3}$$

Let

$$\overline{D}_i = 2a = \frac{D}{3} \tag{3.4}$$

so that

$$\frac{(\overline{D})_i}{D} = \frac{1}{3} \tag{3.5}$$

Referring to Fig. 26 , in the region

$$0 \leq \frac{\theta_T}{D} \leq \frac{a}{D} \left(= \frac{1}{6}\right) \tag{3.6}$$

$$\frac{\theta_T}{(\overline{D})_N} = \frac{1}{2\left(\frac{a}{D}\right)} \left\{\frac{\theta_T}{D}\right\} = 3\frac{\theta_T}{D} \tag{3.7}$$

The centroid of the visible area is

$$\frac{\theta_c}{D} = \frac{\theta_c}{(\overline{D})_N} \frac{(\overline{D})_N}{D} = \frac{1}{3}\frac{\theta_c}{(\overline{D})_N} \tag{3.8}$$

In the region

$$\frac{1}{6} \leq \frac{\theta_T}{D} \leq \frac{2a}{D} \left(= \frac{1}{3}\right) \tag{3.9}$$

$$\left\{\frac{\bar{\theta}_T}{\bar{D}}\right\}_N = 3\frac{\theta_T}{D} \tag{3.10a}$$

$$\left\{\frac{\bar{\theta}_T}{\bar{D}}\right\}_{P,V} = 3\left\{\frac{\theta_T}{D} - \frac{1}{6}\right\} \tag{3.10b}$$

For this region the visible area from modules N, P and V must be considered in calculating the centroid of the visible area. Since the modules are of equal and uniform intensity, the centroid is found using a weighted average with the fraction of visible area from each module being the weighting parameters.

$$\frac{\theta_c}{D} = \frac{1}{3}\left\{\frac{\left\{\frac{\bar{\theta}_c}{\bar{D}}\right\}_N \left\{\frac{\bar{A}}{\bar{A}_T}\right\}_N + \left[1 + 2\left\{\frac{\bar{\theta}_c}{\bar{D}}\right\}_{P,V}\right]\left\{\frac{\bar{A}}{\bar{A}_T}\right\}_{P,Q}}{\left\{\frac{\bar{A}}{\bar{A}_T}\right\}_N + 2\left\{\frac{\bar{A}}{\bar{A}_T}\right\}_{P,V}}\right\} \tag{3.11}$$

In the region

$$\frac{1}{3} \leq \frac{\theta_T}{D} \leq \frac{3a}{D} \; (=.5) \tag{3.12}$$

$$\left\{\frac{\bar{\theta}_T}{\bar{D}}\right\}_{P,V} = 3\left\{\frac{\theta_T}{D} - \frac{1}{6}\right\} \tag{3.13a}$$

$$\left\{\frac{\bar{\theta}_T}{\bar{D}}\right\}_R = 3\left\{\frac{\theta_T}{D} - \frac{1}{3}\right\} \tag{3.13b}$$

In determining the centroid of the visible area modules N, P, V and R must be considered. The calculation of θ_c/D is detailed in Eq. (3.14).

$$\frac{\theta_c}{C} = \frac{\frac{1}{6}(1) + \left[\frac{1}{6} + \frac{1}{3}\left\{\frac{\bar{\theta}_c}{\bar{D}}\right\}_{P,V}\right] 2\left\{\frac{\bar{A}}{\bar{A}_T}\right\}_{P,V} + \left[\frac{1}{3} + \frac{1}{3}\left\{\frac{\bar{\theta}_c}{\bar{D}}\right\}_R\right]\left\{\frac{\bar{A}}{\bar{A}_T}\right\}_R}{1 + 2\left\{\frac{\bar{A}}{\bar{A}_T}\right\}_{P,V} + \left\{\frac{\bar{A}}{\bar{A}_T}\right\}_R}$$

$$= \frac{1}{6}\left\{\frac{1 + 2\left\{\frac{\bar{A}}{\bar{A}_T}\right\}_{P,V}\left[1 + 2\left\{\frac{\bar{\theta}_c}{\bar{D}}\right\}_{P,V}\right] + 2\left\{\frac{\bar{A}}{\bar{A}_T}\right\}_R\left[1 + \left\{\frac{\theta_c}{D}\right\}_R\right]}{1 + 2\left\{\frac{\bar{A}}{\bar{A}_T}\right\}_{P,V} + \left\{\frac{\bar{A}}{\bar{A}_T}\right\}_R}\right\} \qquad (3.14)$$

$\left\{\frac{\bar{\theta}_T}{\bar{D}}\right\}_i$ and $\frac{\theta_c}{D}$ for regions such that

$$\frac{\theta_T}{D} > .5$$

are found in a similar manner.

An actual solution is obtained as follows:

(1) For a given position in the penumbra, $\frac{a'x'}{a'b'}$, calculate $\frac{\theta_T}{D}$ from Eqs. (2.3.21) and (2.3.25)

(2) Determine what region for the module source corresponds to the $\frac{\theta_T}{D}$ found in step (1) and calculate the appropriate $\left\{\frac{\theta_T}{\bar{D}}\right\}_i$ for that $\frac{\theta_T}{D}$.

(3) Calculate $\left\{\frac{\bar{A}}{\bar{A}_T}\right\}_i$ and $\left\{\frac{\bar{\theta}_c}{\bar{D}}\right\}_i$ as

$$\left\{\frac{\bar{A}}{\bar{A}_T}\right\}_i = \frac{1}{\pi}\left(\alpha - \frac{1}{2}\sin 2\alpha\right) \tag{3.15}$$

$$\left\{\frac{\bar{\theta}_c}{\bar{D}}\right\}_i = \frac{1}{2} - \frac{1}{3}\,\frac{\sin^3\alpha}{\alpha - \sin\alpha\cos\alpha} \tag{3.16}$$

with

$$\alpha = \cos^{-1}\left[1 - 2\left\{\frac{\bar{\theta}_T}{\bar{D}}\right\}_i\right] \tag{3.17}$$

(4) Calculate $\frac{\theta_c}{D}$ using the equation that is appropriate for the region determined by $\frac{\theta_T}{D}$ in step (1). (For example, if $\frac{\theta_T}{D}$ found in step (1) is such that $\frac{1}{6} \le \frac{\theta_T}{D} \le \frac{1}{3}$, use Eq. (3.11) to calculate $\frac{\theta_c}{D}$.)

(5) Calculate the relative energy flux density as

$$Q = \sum_i \left\{\frac{A}{A_T}\right\}_i \frac{\cos\left[\beta - D\left\{\frac{1}{2} - \frac{\theta_c}{D}\right\}\right]}{\cos\beta} \tag{3.17}$$

where

$\sum_i \left\{\frac{A}{A_T}\right\}_i$ = sum of normalized visible module areas

and

$\frac{\theta_c}{D}$ was determined in step (4)

4.0 RESULTS AND DISCUSSION

To assist in the following discussion and for the sake of clarification and consolidation, a consistent set of notation will be adopted in this section. The notation used is defined below and pictorially described in Fig. 27a, p.97a

AB = Length of penumbra

$\frac{AO}{AB}$ = Location of conical axis measured from outer edge of penumbra as a fraction of total penumbra length.

$\frac{AX}{AB}$ = Location of general point in penumbra measured from outer edge of the penumbra as a fraction of total penumbra length.

$\frac{XO}{AB}$ = Location of a general point in ghe penumbra measured from the conical axis as a fraction of total penumbra length

$\frac{A}{A_T}$ = Ratio of visible to total source area

BETA = Incident angle, positive counter-clockwise

D = Solar field angle

D1 = Distance measured at conical axis from receiving surface to bottom of skirt or bottom of rectangular cylinder.

D2 = Distance measured at conical axis from receiving surfact to top of skirt or centroid of rectangular cylinder.

H = Half height of rectangular cylinder.

Q = Relative energy flux density
= Flux density in penumbra/flux density outside shadow.

Q' = Relative energy flux density due to specular or diffuse reflection

R = Half width of rectangular cylinder or radius of circular cylinder

W = Half length of skirt out of the plane of the paper

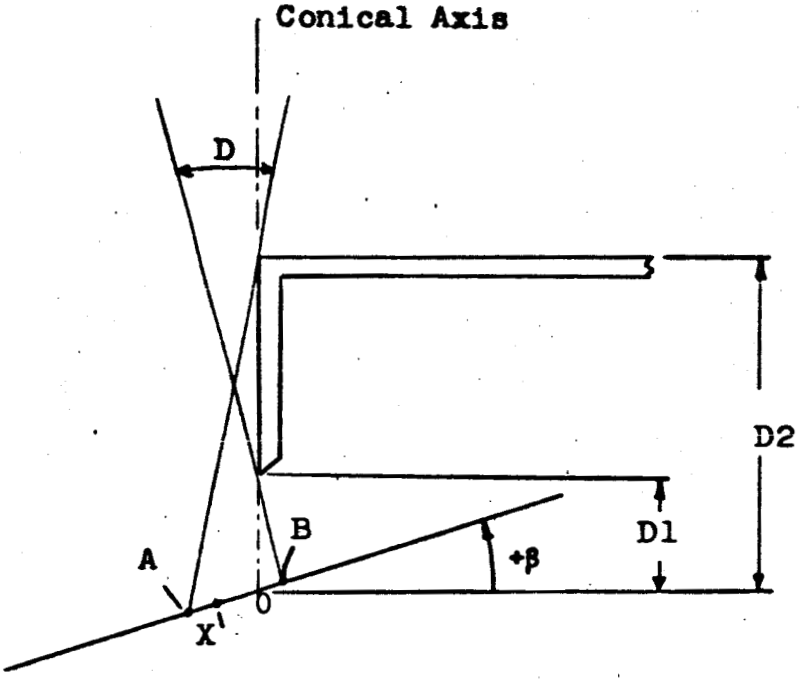

DIFFUSE SKIRT

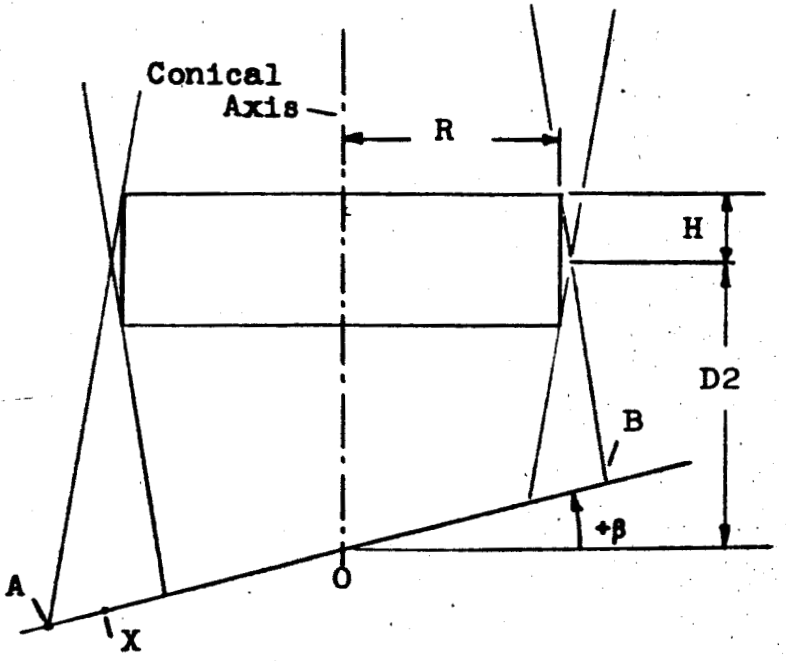

RECTANGULAR CYLINDER

FIG. 27a

FIG 27

a = Radius of module

d = Distance between adjacent module centers

$\frac{H}{R}$ = Shape factor for rectangular cylinder

β = Same definition as BETA

$\frac{\theta_c}{D}$ = Normalized angle to centroid of visible source area

$\frac{\theta_T}{D}$ = Normalized angle to limiting ray trajectory defining visible area.

ϕ_{11} = Angle measured from the zenith from a point in the penumbra to the top of the skirt

ϕ_{12} = Angle measured from the zenith from a point in the penumbra to the bottom of the skirt

ϕ_{22} = Azimuth angle measured from normal to skirt from a point in the penumbra to the outer edge of the skirt.

The shading bodies considered may conveniently be classified as either:

(a) knife edge with skirt

(b) rectangular cylinder

(c) circular cylinder

The single knife edge is a special case of the "knife edge with skirt". With D1/D2 = 1, the "knife edge with skirt" degenerates to a single knife edge. Similarly, with H/R = 0, the rectangular cylinder degenerates to a double knife edge.

4.1 KNIFE EDGE WITH SKIRT

Black Skirt - Uniform Source

Energy flux density distributions in penumbrae corresponding to what will be defined as the basic case, i.e., the case that approximates the solar environment ($D = 0.5^{\circ}$) are presented in Fig. 27 p. 110 for parametric variations in D1/D2. The effect of incident angle and solar field angle on the energy flux density distribution in the penumbra of a single knife edge (D1/D2 = 1) is shown in Figs. 28 and 29, respectively.

To assist in using the relative flux density data it will be useful to locate the position of the conical axis, $\frac{AO}{AB}$, in the penumbra. The location of a general point in the penumbra relative to the conical axis is simply

$$\frac{AX}{AB} = \frac{AO}{AB} - \frac{XO}{AB} \qquad (4.1.1)$$

with $\frac{AO}{AB}$ given by Eq. (2.4.13), and XO being the distance from the conical axis.

Figures 30 through 34, starting on p. 113, indicate the maximum deviation in relative energy flux density from the basic cases shown in Fig. 27 as a function of D and β. The symmetry of the solutions are such that negative incident angles result in negative maximum deviations of the same magnitude as that obtained for positive angles.

Figures 30 through 34 may be used in evaluating the exactness necessary for simulation of the solar field angle required in solar simulators to reduce the thermal testing errors to an acceptable magnitude. For example, referring to Fig. 30 p. 113, if a highly decollimated solar simulator, say $D = 15^{\circ}$, is to be used, flat surfaces having incident angles (β) less than 25° will have relative energy flux density distribution which deviate by no more than .05 from that obtained in an earth solar environment, and depending on the accuracy criteria being used, acceptable testing results might be obtainable. However, flat surfaces having incident angles such that $\beta > 60^{\circ}$ will have relative energy flux density distributions that deviate by a minimum of .15 from that in an earth solar environment and highly inaccurate testing results would be obtained.

Appendix B, under separate cover, contains a set of tables defining the relative energy flux density in the penumbra of a knife edge with a black skirt as a function of position in the penumbra, $\frac{AX}{AB}$, geometry of the skirt, D1/D2, incident angle, β, and solar field angle, D.

Specular Skirt - Uniform Source

The effect of adding a specular surface (reflectance = 1.0) to the skirt is such that the skirt becomes ineffective as a shading body and the relative energy density distribution can be obtained by considering a knife edge located at the lower edge of the skirt, i.e., located at D1 and using the distribution corresponding to a "knife edge with black skirt" in Appendix B with D1/D2 = 1.0

5

Diffuse Skirt - Uniform Source

In order to gain an appreciation of the magnitudes of the energy flux density arriving at a receiver from a diffuse skirt, it will be helpful to examine some extreme cases.

First, it should be noted from Eq. (2.4.46) that the energy flux density varies approximately proportional to D, the solar field angle. Consequently, decreasing the solar field angle will reduce the energy flux density received in the penumbra from the skirt.

Assume that the skirt is semi-infinite, that is, that it extends an infinite distance to each side, and from the receiver upwards to infinity. Also, assume a solar field angle of 15^{o}, $\beta = 0$, and D1/D2 = 0. Now the angles used in Eq. (2.4.46) become

$$\phi_{11} = 0$$

$$\phi_{12} = \frac{\pi}{2}$$

$$\phi_{22} = \frac{\pi}{2}$$

and

$$Q' = \frac{.2122 \times .2618}{\pi} \left(\frac{\pi}{4} \times 1. - 0\right)$$

$$= .01389$$

Thus, it can be seen that even for a semi-infinite skirt, the energy flux density received from the skirt is less than 1.4% of that being received

101

from the source outside the penumbra. In actuality, it should be noted that since ϕ_{11} will always be less than, or equal to one-half the solar field angle, the skirt, for all practical purposes, will always appear to be infinitely high relative to a point in the penumbra. If the skirt has a width which is twice its height, or more, ($W/D2 \geq 1$) the skirt will appear to the receiver to be approximately infinitely wide. This condition yields a value of $Q' = .0123$ at the outer edge of the penumbra and rises to .01389 at the skirt for the same conditions as above, except that ϕ_{11} varies from D/2 to 0, and ϕ_{22} varies from $\frac{\pi}{2} - \frac{D}{2}$ to $\frac{\pi}{2}$. Q' has thus varied by less than .002 from the semi-infinite case. This variation will be even less for smaller solar field angles. For $D1/D2 = 0$ and $\beta = 0$, a good approximation for Q' is

$$Q' = \frac{.01389\ D\ \phi_{22}}{.2618 \times \frac{\pi}{2}} = .03378\ D\ \phi_{22} \qquad (4.1.2)$$

The manner in which Q' varies with β can be seen by again referring to Eq. (2.4.46). Positive β's will reduce Q' and negative β's will increase Q'. In order to determine an upper limit for Q' when β is negative, let the skirt be inifinite in extent and set the other parameters as follows:

$$D1/D2 = 0$$
$$D = 15^{\circ}$$
$$\phi_{11} = 0$$
$$\phi_{12} = \pi$$
$$\phi_{22} = \pi/2$$
$$\beta = -(\pi/2 - D/2) = -82.5^{\circ}$$

The calculations yield

$$Q' = .01389 \times 15.1916 = .2109$$

The augmentation due to the skirt has increased by a factor of 15 compared to Q' for $\beta = 0$, and now represents a sizable percentage. An implied assumption consistent with the analysis presented in this report is that the dimension of the plate normal to the plane of interest may be considered large such that in Eq. (2.4.56), $W/D_2 \longrightarrow \infty$ and $\phi_{22} \longrightarrow \pi/2$. Investigation of the energy distribution in the penumbra as a function of incident angle, β, with $\phi_{22} = \pi/2$ and $D1/D2 = 0$ indicates that the distribution is essentially uniform. The magnitude of the relative energy flux density with $D1/D2 = 0$ and $D = 15^{o}$ as a function of β is shown in Fig.35 p.118.

If the skirt is raised from the surface, i.e., $D1/D2 > 0$, the energy received from the skirt is decreased. If the receiver is horizontal, $\beta = 0$, the energy received from the skirt becomes zero at the point directly beneath the skirt rather than reaching the maximum value of .01389 as was the case for $D1/D2 = 0$. The mathematical reason for this is that ϕ_{12} decreases to zero rather than remaining at a constant value of $\pi/2$. The physical interpretation is that a point on the receiver directly beneath the skirt can no longer see the illuminated surface of the skirt. This does not happen when $D1/D2 = 0$, since the receiver and the skirt become coincident at that point, and Q' becomes the maximum value of the relative energy flux density being radiated at the surface of the skirt.

Figure 35 p.118 indicates that for incident angles greater than - 60° ($\beta > -60^{\circ}$) less than .05 augmentation in relative energy flux density due to diffuse reflection from the skirt is possible.

As previously noted, variations in relative energy flux density due to diffuse reflection from the skirt are approximately proportional to D so that Q' in Fig. 35 represents maximum augmentations for the range of solar field angles considered in this report.

4.2 RECTANGULAR CYLINDER

Black Rectangular Cylinder - Uniform Source

As pointed out in Section 4.0, the rectangular cylinder degenerates to a double knife edge for H/R = 0. Figure 36 , p.119 shows the effect of the shape factor, H/R, on the relative energy flux density in the penumbra of a rectangular cylinder for a horizontal receiver ($\beta = 0$) and a solar field angle of 15°. Referring to Fig.36, note that for the range of shape factors (H/R) considered, the shape factor does not significantly effect the energy distribution from that corresponding to a double knife edge (H/R = 0). Therefore, in order to determine the effect of some of the other significant parameters, a double knife edge will be used. The effect of solar field angle and position of the double knife edge on the energy distribution is shown in Figs. 37 and 38 (pp.120 and 121) respectively. The effect of incident angle on the distribution is shown in Fig. 39 p.122.

To assist in using the relative flux density data, it will be useful to locate the position of the conical axis in the penumbra, $\frac{AO}{AB}$. The location of a general point in the penumbra in terms of the distance from the conical axis is given by Eq. (4.1.1) with $\frac{AO}{AB}$ given by Eq. (2.6.53).

Appendix B, under separate cover, contains a set of tables defining the relative energy flux density in the penumbra of a black rectangular cylinder as a function of position in the penumbra, $\frac{AX}{AB}$, shape factor, H/R, location of the rectangle relative to the receiver, D2/R, incident angle, β, and solar field angle, D.

Specular Rectangular Cylinder - Uniform Source

The effect of adding a specular surface (reflectance = 1.0) is such that the sides of the rectangle become ineffective as shading surfaces, i.e., results are independent of H/R and the relative energy density can be obtained by considering a double knife edge at D1, the lower edge of the rectangular cylinder. The energy distribution corresponding to a specular rectangular cylinder may be determined using Appendix B and the distribution for a black rectangular cylinder with H/R = 0 and D2/R = D1/R.

Diffuse Rectangular Cylinder - Uniform Source

Each diffuse side of the rectangular cylinder will have the characteristics of a diffuse skirt (see Section 4.1). Therefore, for positive incident angles ($\beta \geq 0$) the energy augmentations due to the left diffuse face of the rectangle will be negligible (less than 1.4%). A similar

condition exists for $\beta < 0$ in reference to the right diffuse face of the rectangle. Furthermore, from Fig. 35, p.118 for $-60^{o} < \beta < +60^{o}$ less the .05 augmentation due to diffuse reflection from either face is possible.

4.3 CIRCULAR CYLINDER

Black Circular Cylinder - Uniform Source

The analysis of Section 2.7.1 indicated that the circular cylinder degenerated to a double knife edge located at the diameter of the cylinder in as far as the energy distribution in the penumbra was concerned. This result is really not too surprising since, by reference to Fig. 21, p. 74a, the effective portion of the cylinder (ACBE) can be approximated by a rectangular cylinder with a shape factor given by

$$\frac{H}{R} = \frac{R\frac{D}{2}}{R} = \frac{D}{2}$$

Since $D \leq 15^{o}$ (.2618 radians)

$$\frac{H}{R} \leq .1309$$

An indication of the effect of this shape factor is given in Fig. 36, p.119 where it is seen that the cylinder closely approximates the double knife edge.

Specular Cylinder - Uniform Source

In the analysis of the specular cylinder it has been assumed that the geometry of the cylinder and receiving surface is such that the incident angle is limited by

$$0 > \beta > -\cos^{-1}(R/D2) \qquad (4.3.1)$$

The development of Section 2.7.2 indicates that the percent augmentation in energy is directly proportional to the factor ϕ/θ_T. From Eq. (2.7.41) and Fig. 22 it is seen that the critical parameter for any given point in the penumbra is the position of the cylinder relative to that point. Unless the point at which the flux density is of interest is nearly tangent to the reflecting surface, the increase in energy will be negligible. For example, a horizontal receiver ($\beta = 0$) illuminated by a uniform source with $D = 15^\circ$ will experience a maximum increase in energy flux density of about 3% at a distance of one cylinder radius ($D2/R = 1$). If the cylinder is raised from the surface such that $D2/R = 10$, and the surface remains horizontal, the augmentation decreases to about 1%. Furthermore, with $D2/R = 10$, unless the receiver has an attitude such that β is less than -83°, less than 3% augmentation is possible. A comparison of the relative energy flux density distribution due to specular reflection and direct irradiation is shown in Fig. 40, p. 123.

The reason for the relatively small energy augmentation due to specular reflection from the cylinder as compared to the specular skirt is the positive curvature of the cylinder and the resulting divergence of the reflected rays.

Diffuse Cylinder - Uniform Source

It is apparent from Eq. (2.4.44) and (2.7.59) that it is the angles subtended by the diffuse source relative to the receiver that is of primary importance in determining the extent of relative energy flux density augmentation in the penumbra. It is to be expected then, that just as the augmentation is relatively high in the case of the diffuse skirt when the receiver is rotated to large negative angles, the augmentation is also going to be significant under similar circumstances for the diffuse cylinder. When the receiver is at an attitude of -82.5° and is tangent to the cylinder, the augmentation is approximately 11%. This calculation, which resulted in the upper limit in terms of specular augmentation, was made assuming that the cylinder is infinitely long, that the solar field angle is 15°, and for 5 uniformly illuminated strips on the pertinent portion of the cylinder. Hypothetically, if the receiver could be placed closer to the vertical portion of the cylinder, the augmentation would approach that of the flat skirt, 21%. The lower augmentation for the cylinder reflects the effect of the curvature of the cylinder surface. The greater illumination of the upper portion of the cylinder is compensated for by the fact that the receiver sees that portion of the cylinder at low angles while the illumination of the lower portion of the cylinder decreases to zero. Therefore, only a small portion of the cylinder is effective in radiating energy to the penumbra.

Another calculation was made for a receiver angle of $\beta = -70^{\circ}$. The augmentation proved to be approximately 0.3% for this case. Thus, the

augmentation decreases very rapidly as the receiver angle decreases. This is to be expected, since the angle subtended by the portion of the cylinder which is radiating to the penumbra decreases rapidly, at first, as the receiver is moved away.

Therefore, it is concluded that for all but the cases in which the receiver is tangent to the reflecting portion of the cylinder, the increase in relative flux density due to specular reflection will be negligible.

4.4 SINGLE KNIFE EDGE - MODULE SOLAR SOURCE

Using the principle of the replacement of a source by an equivalent point source located at the centroid of the visible area, the module source may be represented by a vector having a magnitude of A/A_T and direction θ_c/D. The variation of area ratio, A/A_T, and angular centroid shift, θ_c/D, for the module solar model considered in this report is shown in Figs. 41 and 42, pp. 124 and 125.

A comparison of relative energy flux density distributions corresponding to uniform and module solar simulation models is presented in Fig. 43 and 44 on pp. 126 and 127.

As one would expect, the solution for the module solar models represent perturbation about the solutions corresponding to a uniform source. However, even for the extreme case of a/d = .25, the maximum deviation in the distributions corresponding to uniform and module solar models is less than .07 in relative energy flux density.

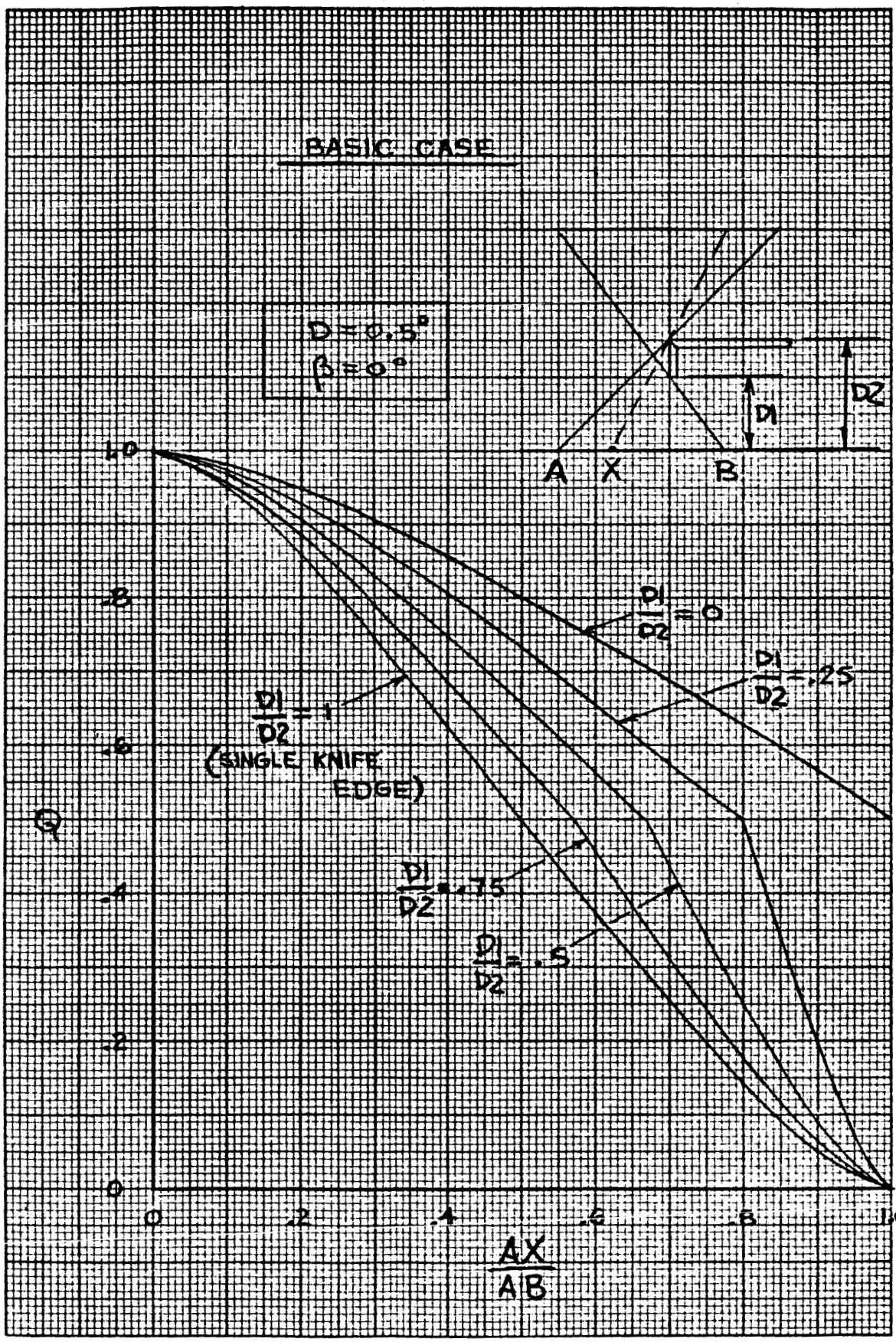

FIG. 27 Effect of Skirt Geometry on the Relative Intensity in the Penumbra of a Knife Edge With a Black Skirt Illuminated by a Uniform Solar Simulator Source

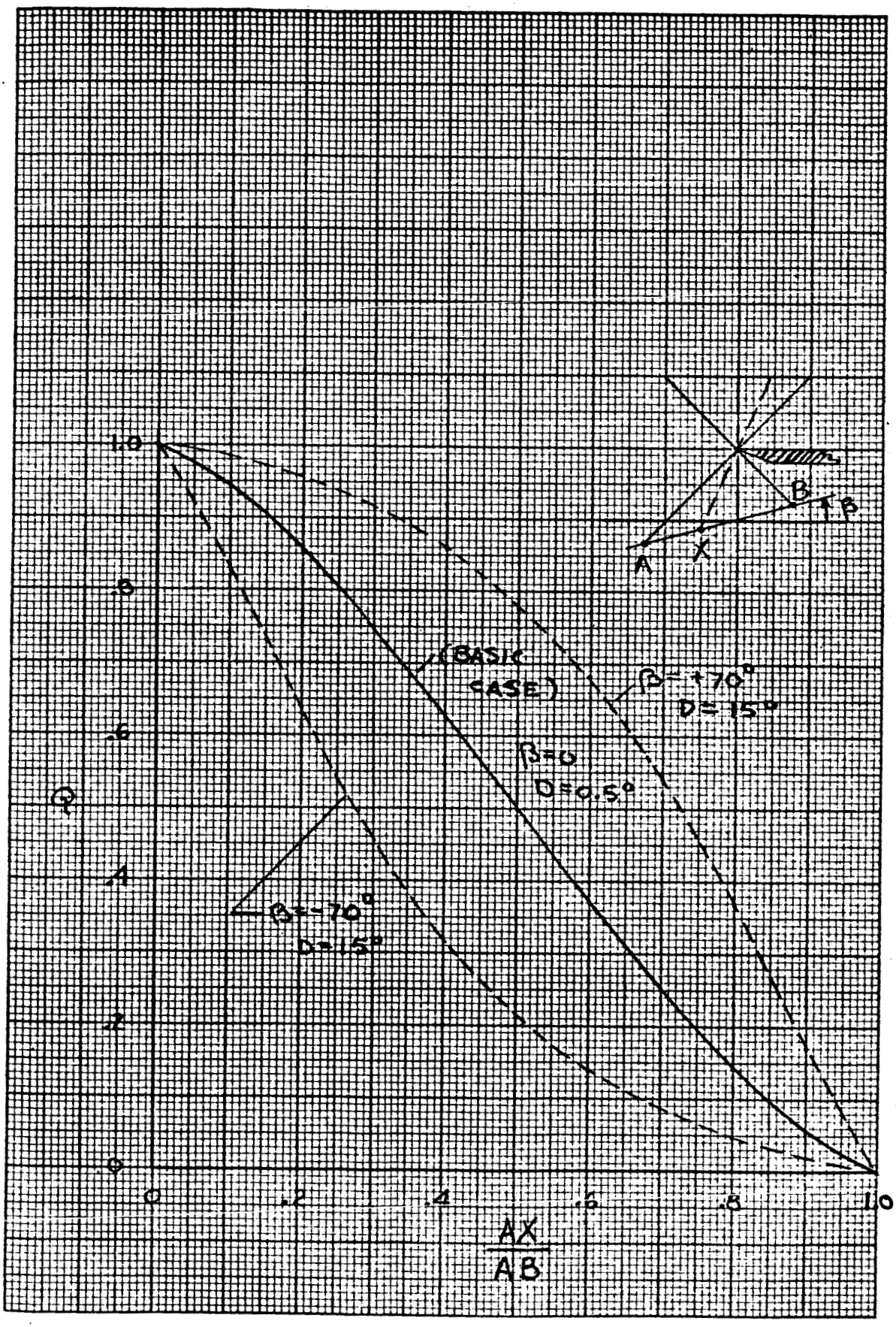

Fig. 28. Relative Intensity in the Penumbra of a Single Knife Edge Illuminated by a Uniform Ideal Solar Simulator Source

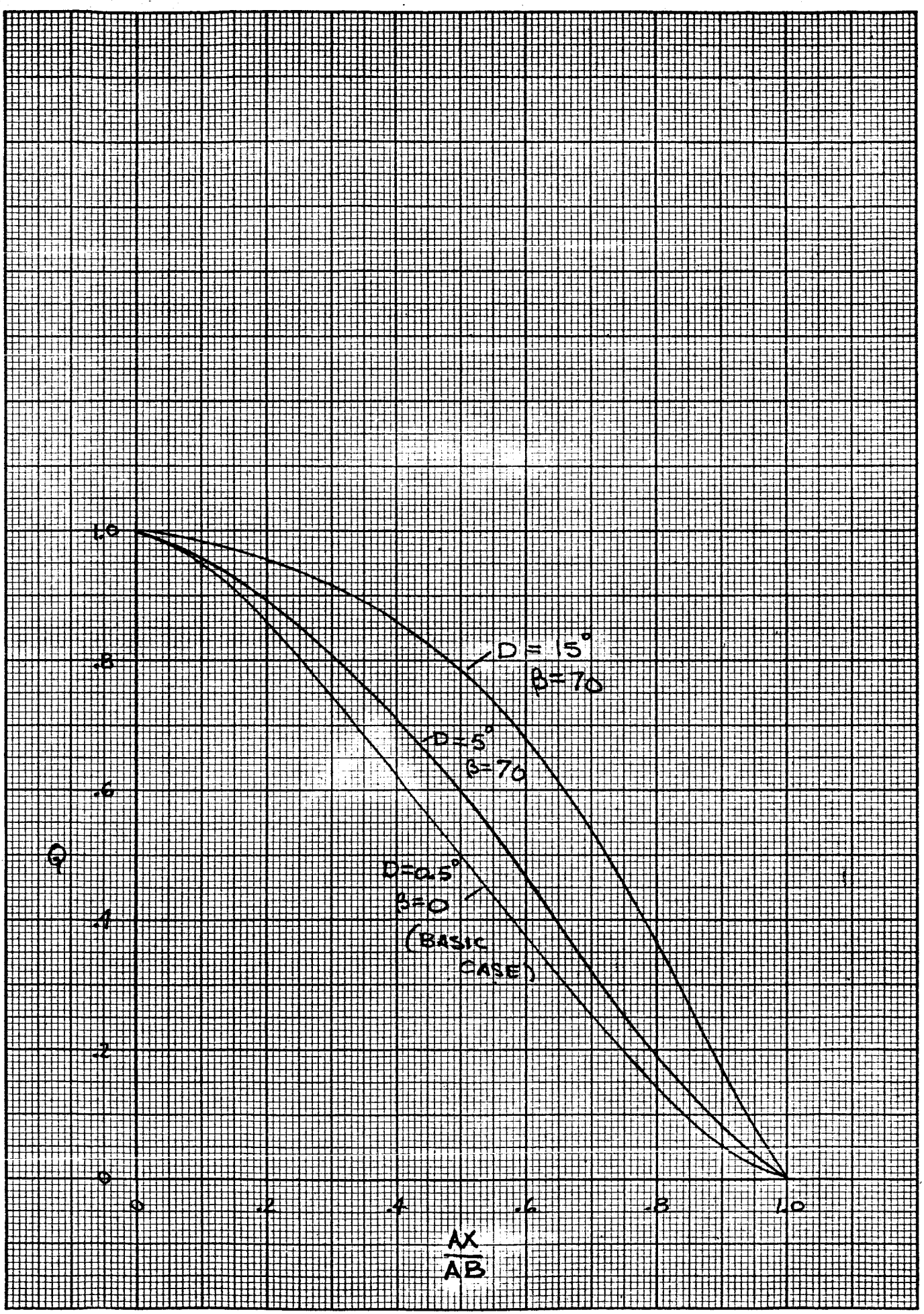

Fig. 29. Effect of Field Angle of the Solar Simulator Source on Intensity in the Penumbra of a Single Knife Edge Illuminated by a Uniform Ideal Solar Simulator Source

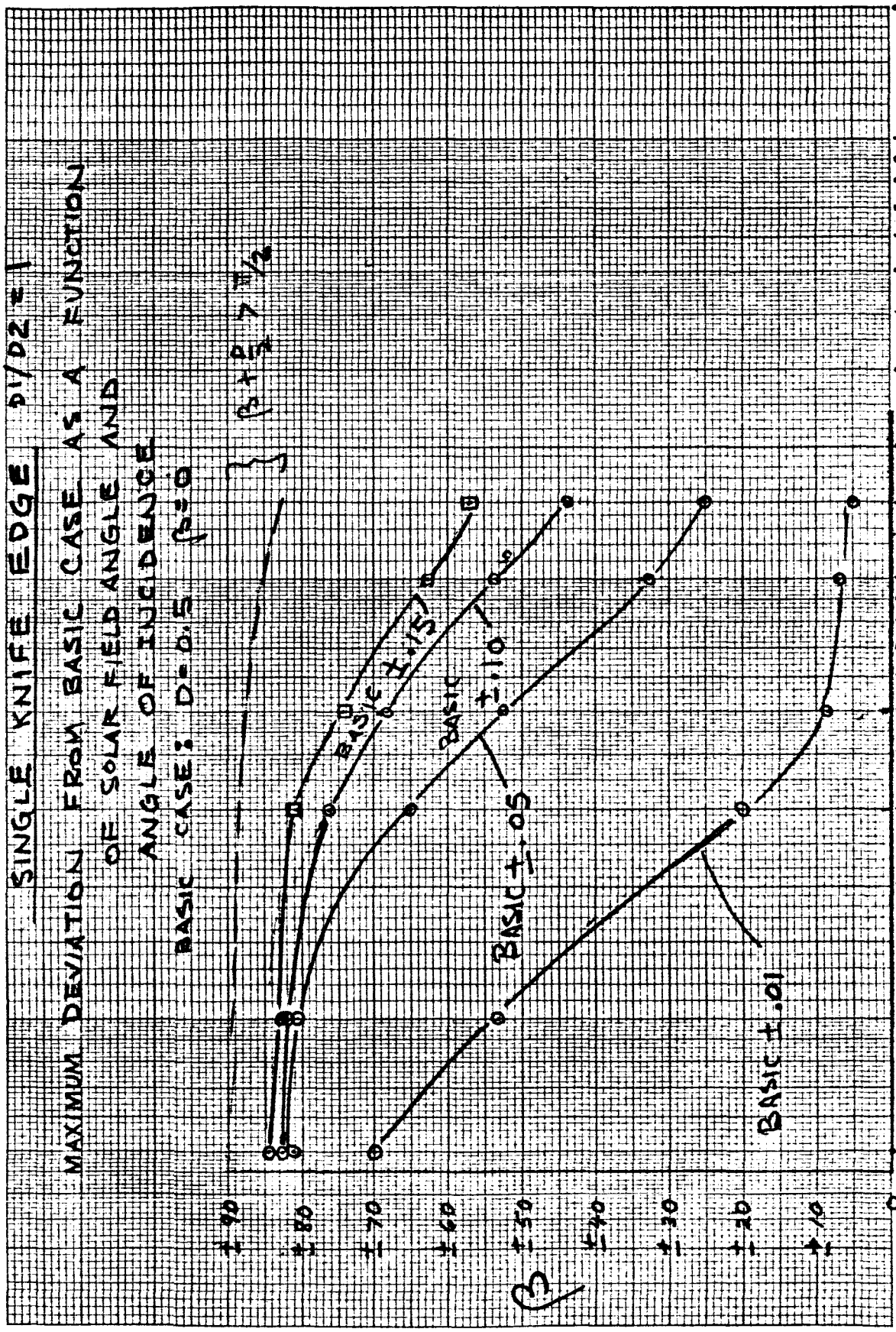

FIG. 30

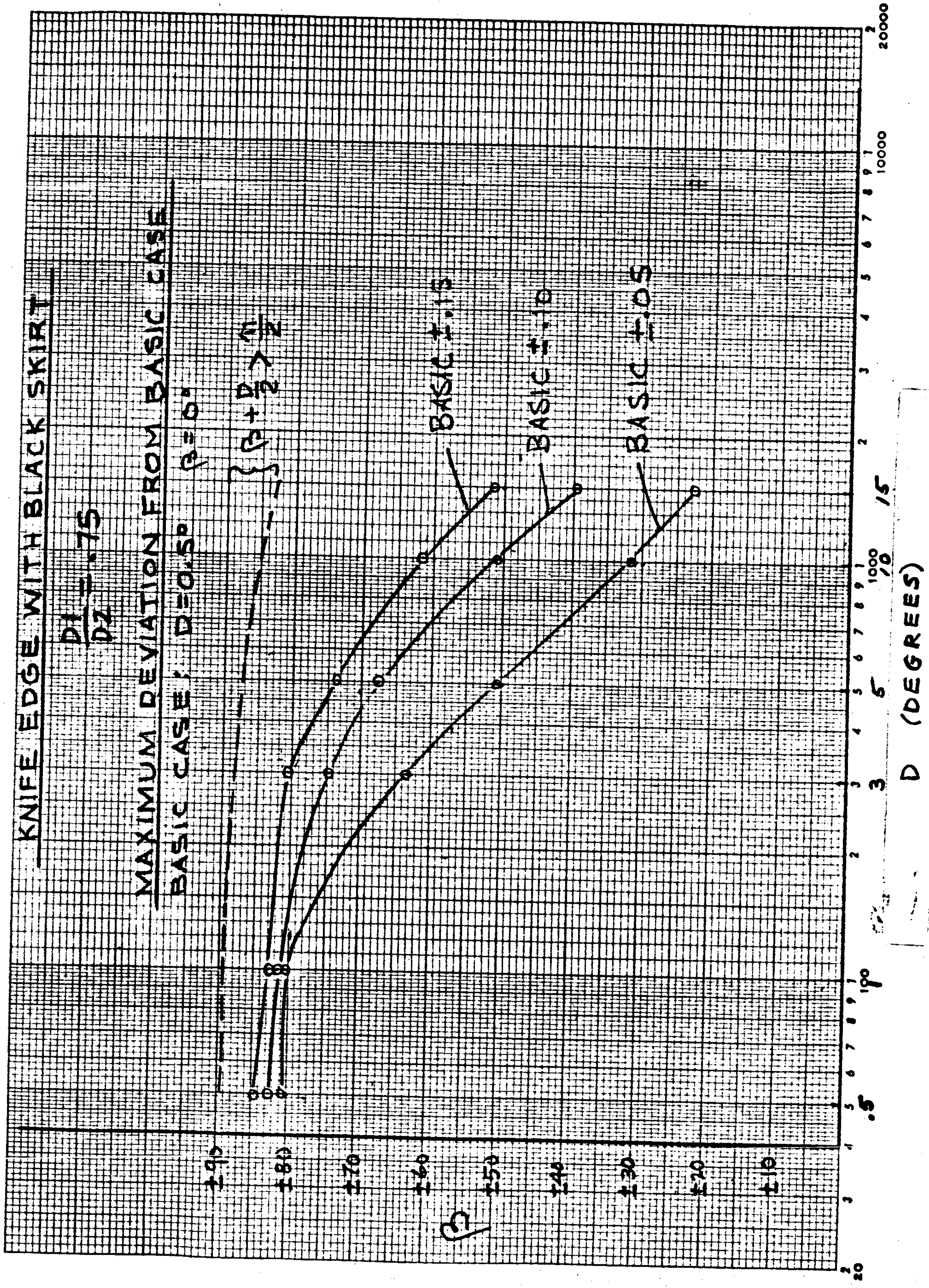

FIG. 31

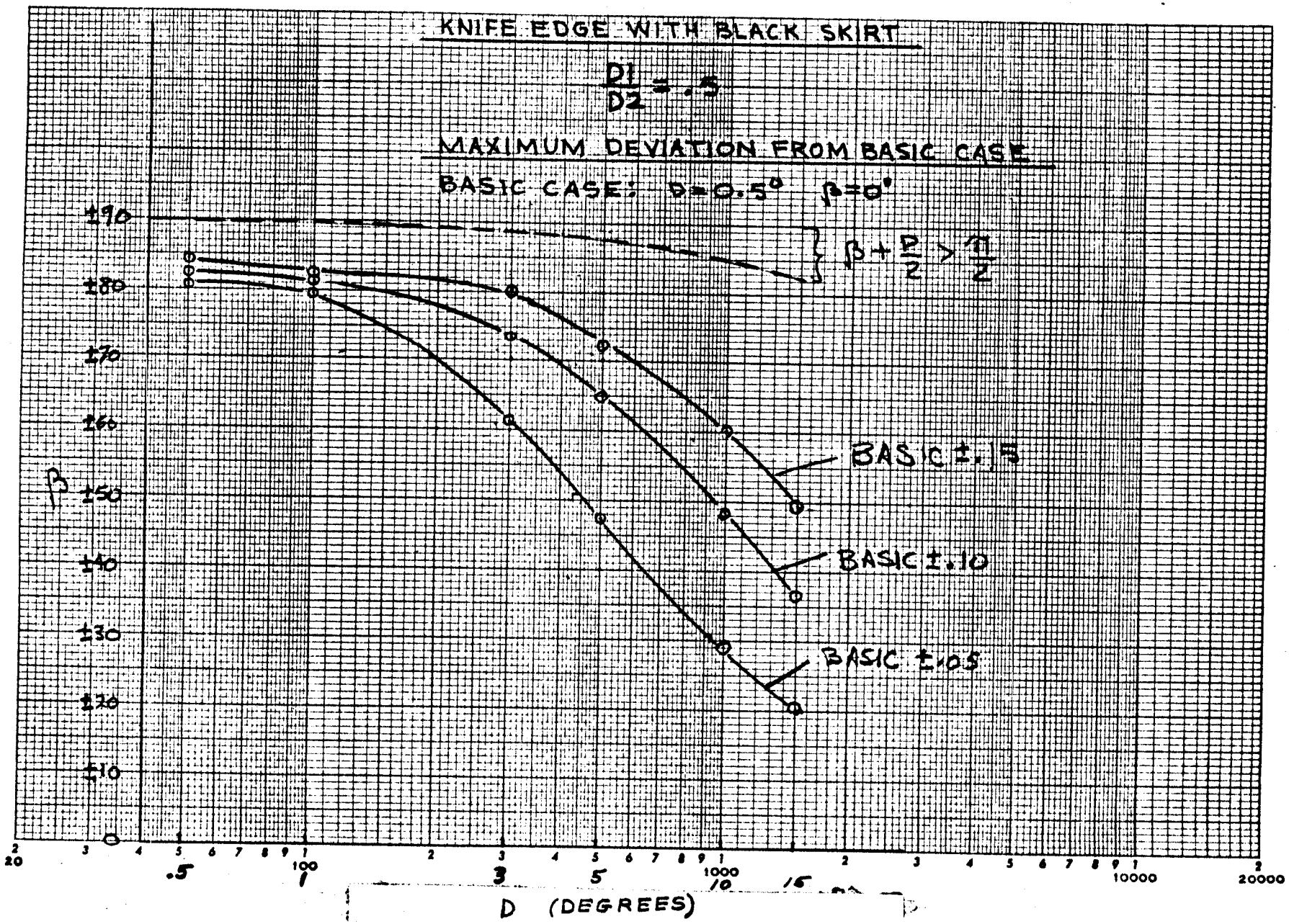

FIG. 32

CLEARPRINT PAPER CO. NO. C1. FREQUENCY X 8

CLEARPRINT CHARTS
PRINTED IN U.S.A. ON CLEARPRINT TECHNICAL PAPER NO. 1018

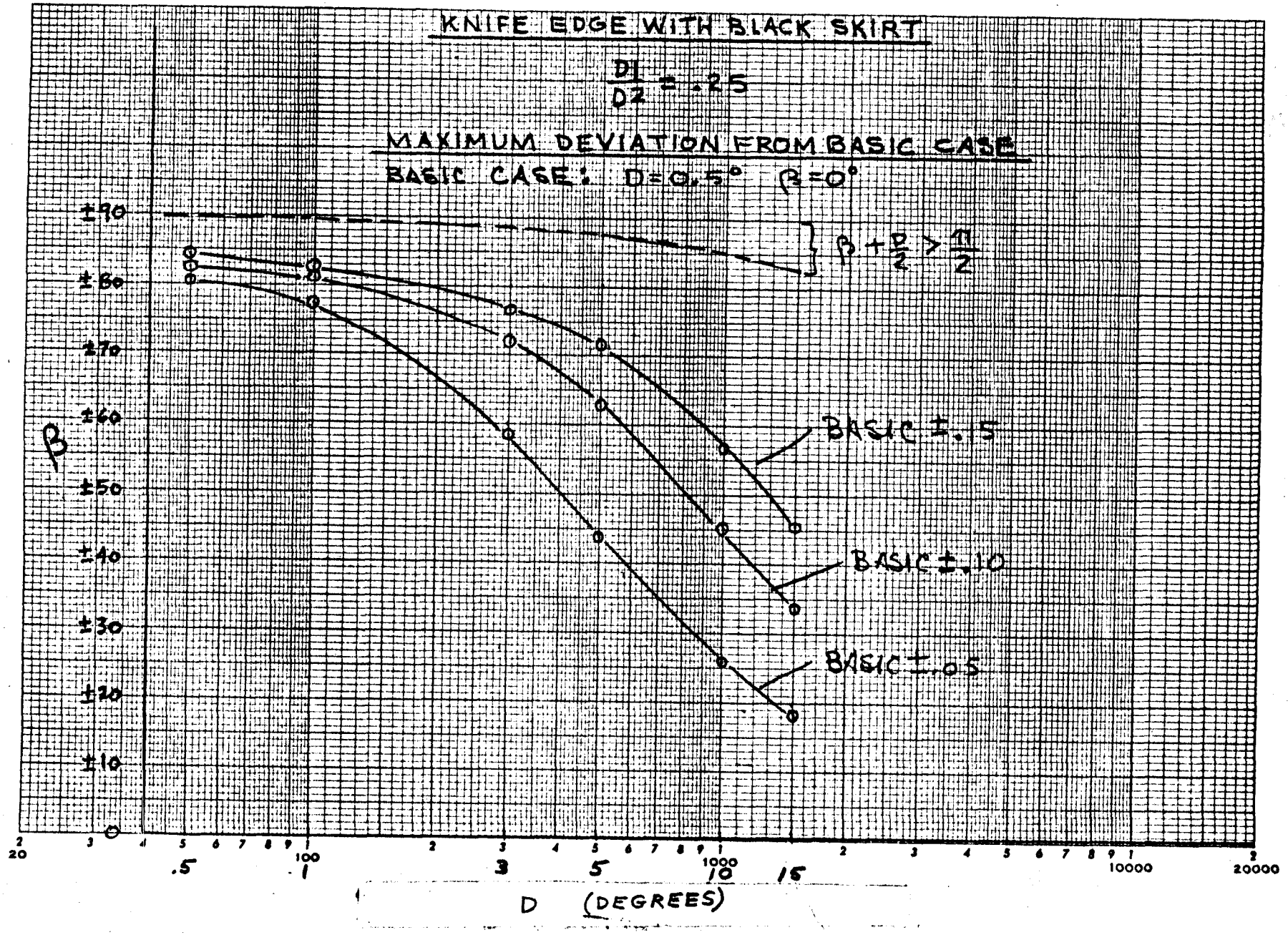

FIG. 33

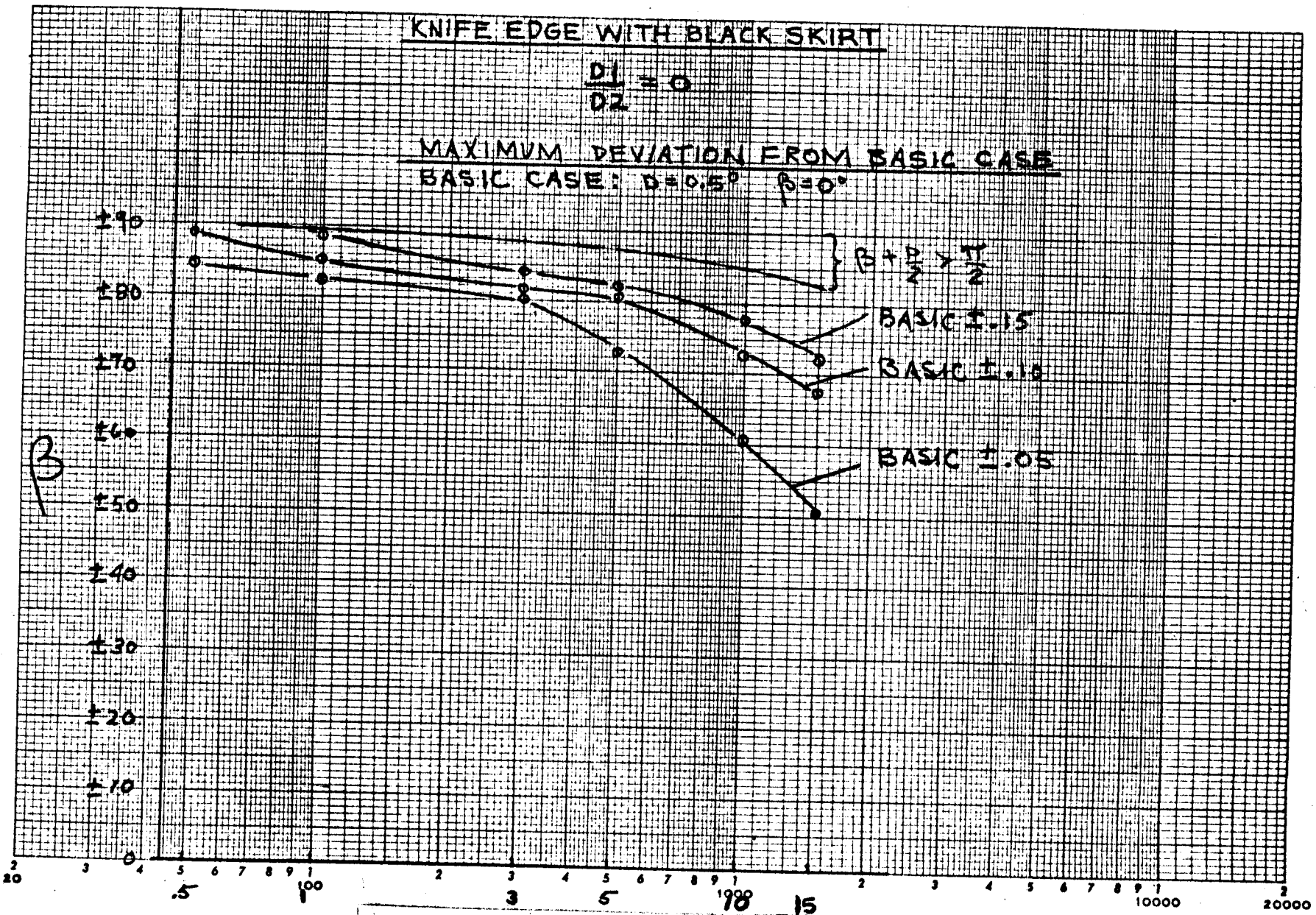
KNIFE EDGE WITH BLACK SKIRT
D1/D2 = 0
MAXIMUM DEVIATION FROM BASIC CASE
BASIC CASE: D=0.5° β=0°
β + D/2 > π/2
BASIC ±.15
BASIC ±.10
BASIC ±.05
±90
±80
±70
±60
±50
±40
±30
±20
±10
0
B
2 3 4 5 6 7 8 9 1 2 3 4 5 6 7 8 9 1 2 3 4 5 6 7 8 9 1 2
20 .5 100 3 5 1000 18 15 10000 20000
D (DEGREES)

FIG. 34

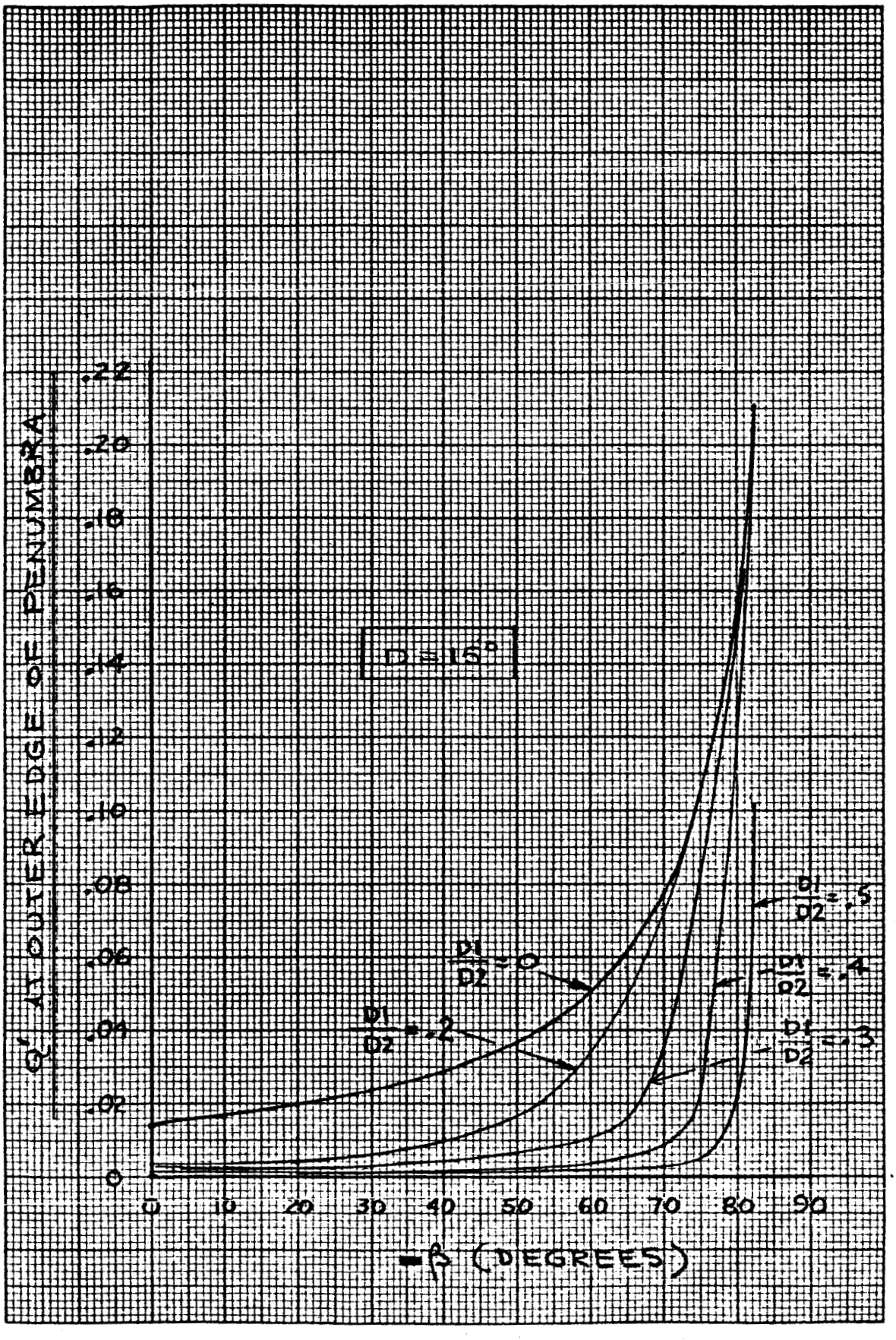

Fig.35. Effect of Skirt Geometry on the Relative Energy Flux Density Augmentation Due to a Diffuse Skirt with Reflectance = 1.0

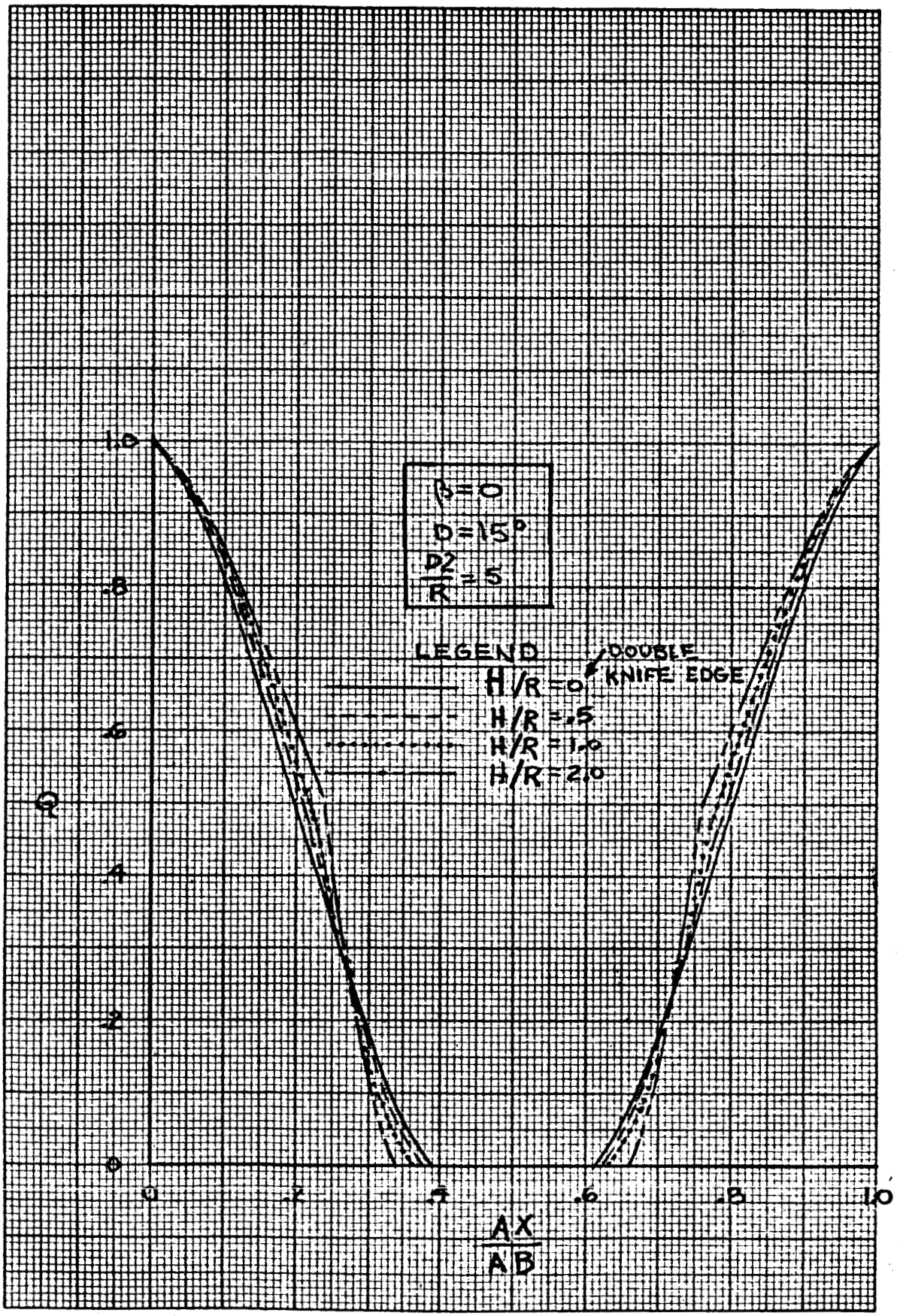

FIG. 36
Effect of Shape Factor, H/R, on the Relative Intensity in the Penumbra of a Rectangular Cylinder Illuminated by a Uniform Solar Simulator Source

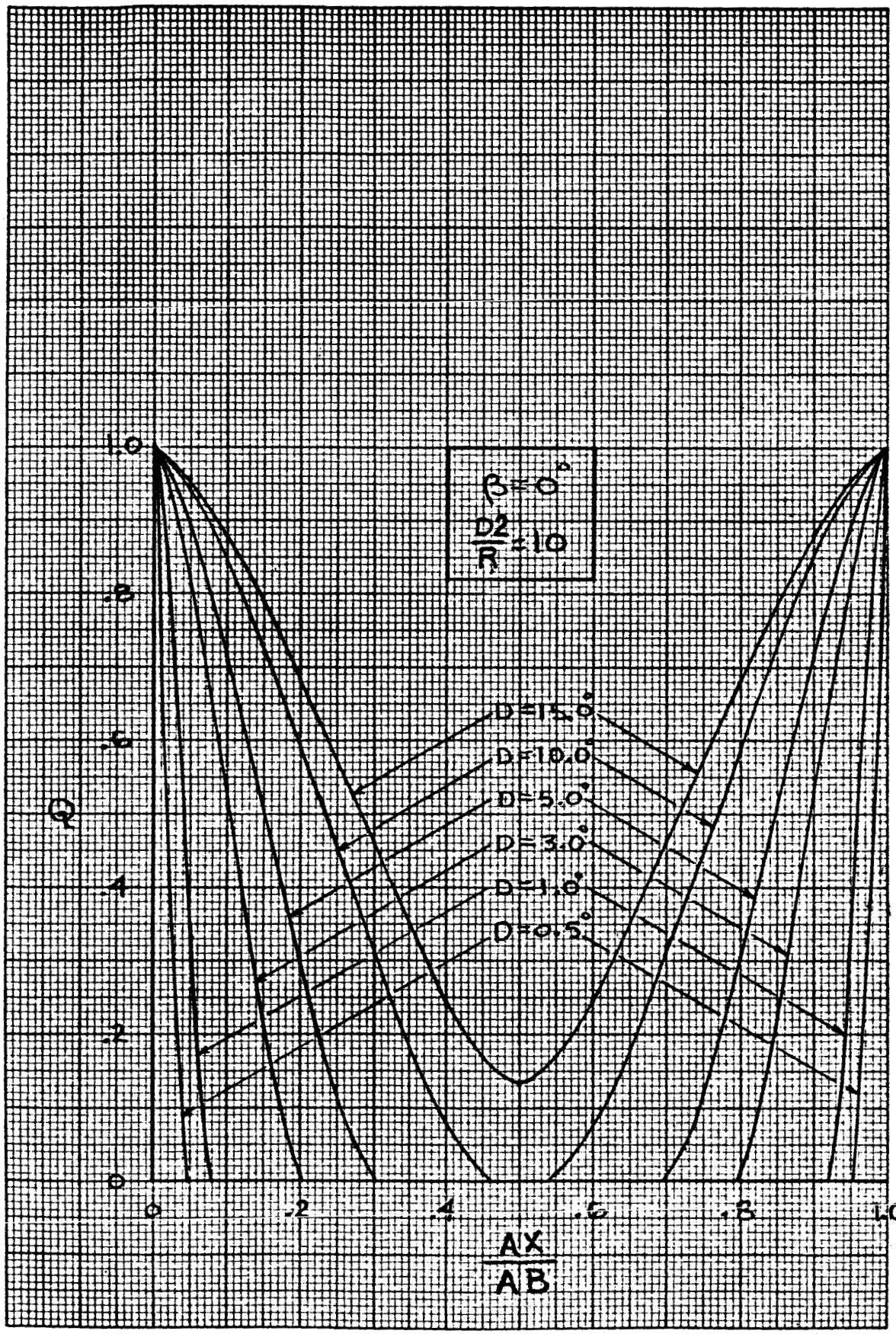

FIG. 37 Effect of Solar Field Angle on the Relative Intensity in the Penumbra of a Double Knife Edge Illuminated by a Uniform Solar Simulator Source

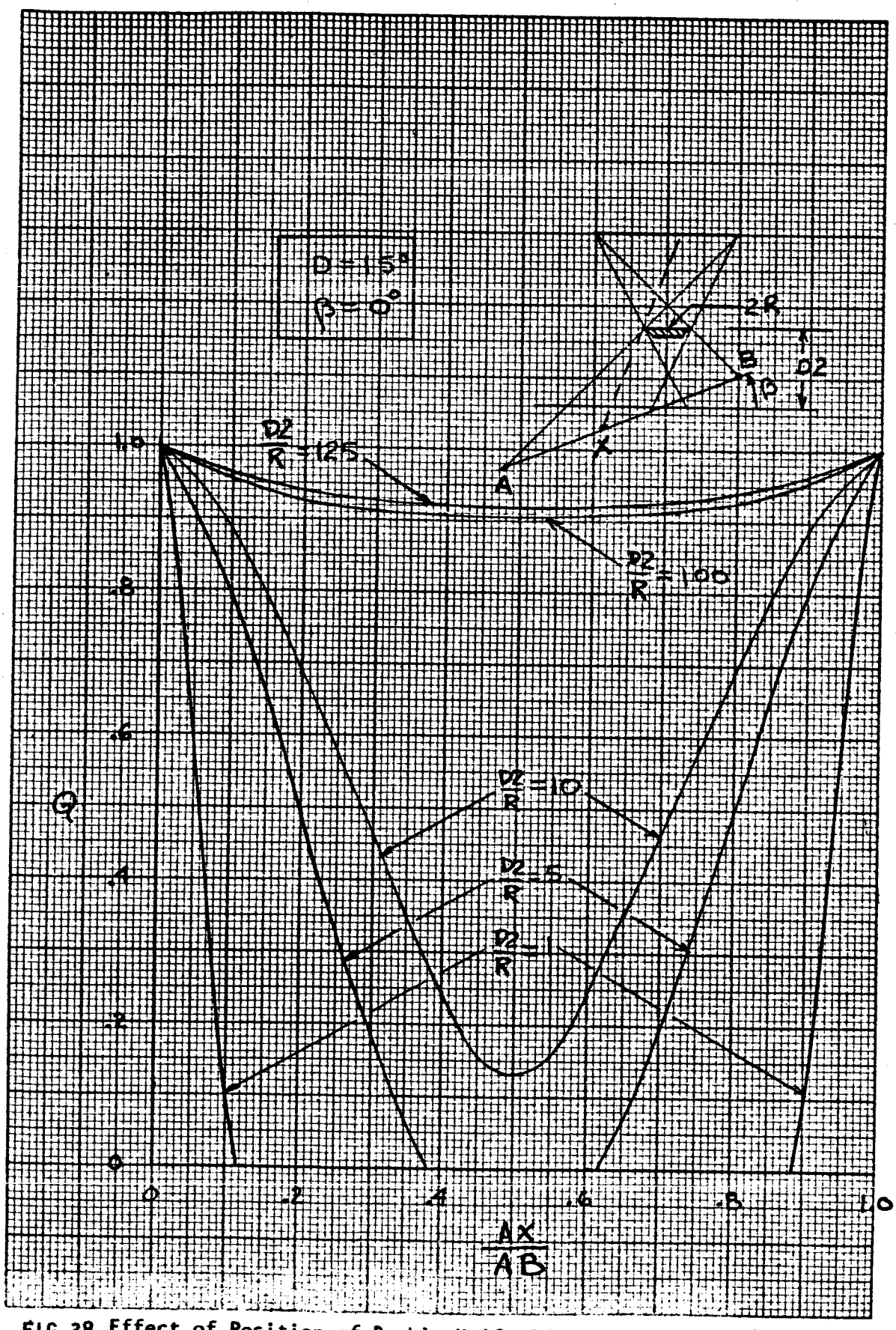

FIG. 38 Effect of Position of Double Knife Edge on the Relative Intensity in the Penumbra of a Double Knife Edge Illuminated by a Uniform Ideal Solar Simulator Source

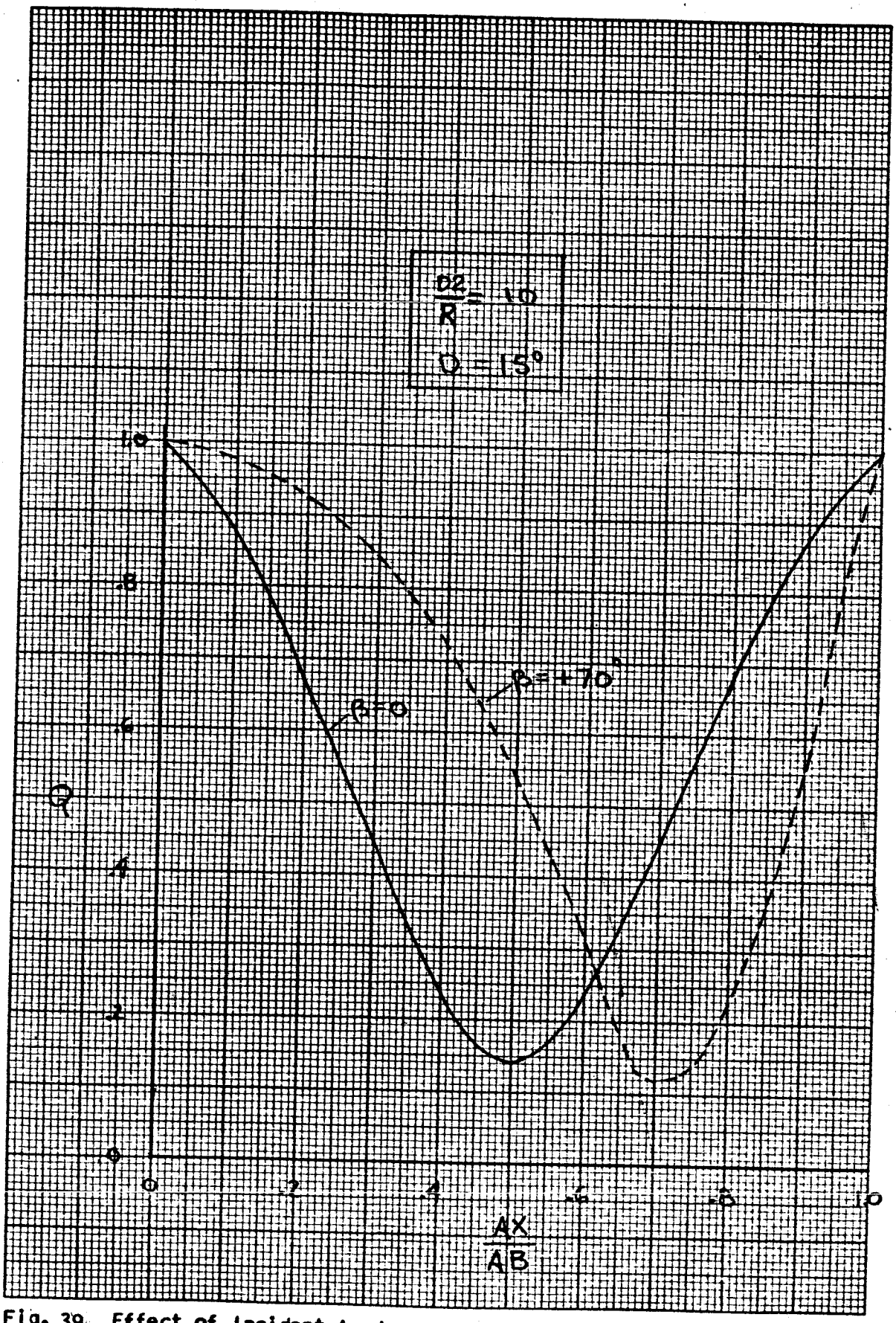

Fig. 39. Effect of Incident Angle on the Relative Intensity in the Penumbra of a Double Knife Edge Illuminated by a Uniform Ideal Solar Simulator Source

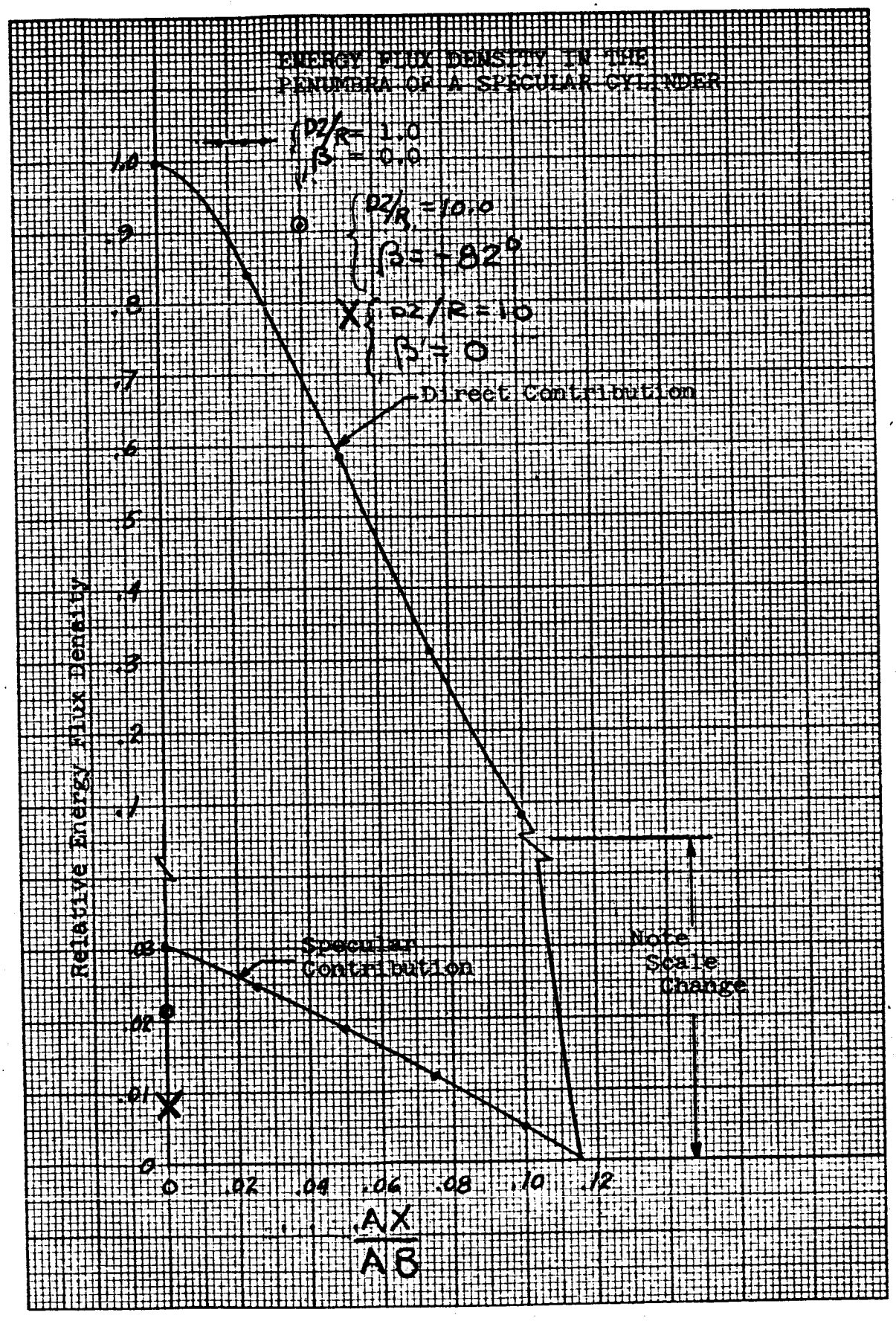
ENERGY FLUX DENSITY IN THE PENUMBRA OF A SPECULAR CYLINDER
D2/R = 1.0
β = 0.0
D2/R = 10.0
β = +82°
D2/R = 1.0
β' = 0
Direct Contribution
Specular Contribution
Note Scale Change
Relative Energy Flux Density
1.0
.9
.8
.7
.6
.5
.4
.3
.2
.1
.03
.02
.01
0
0
.02
.04
.06
.08
.10
.12
ΔX/Δβ

FIG. 40

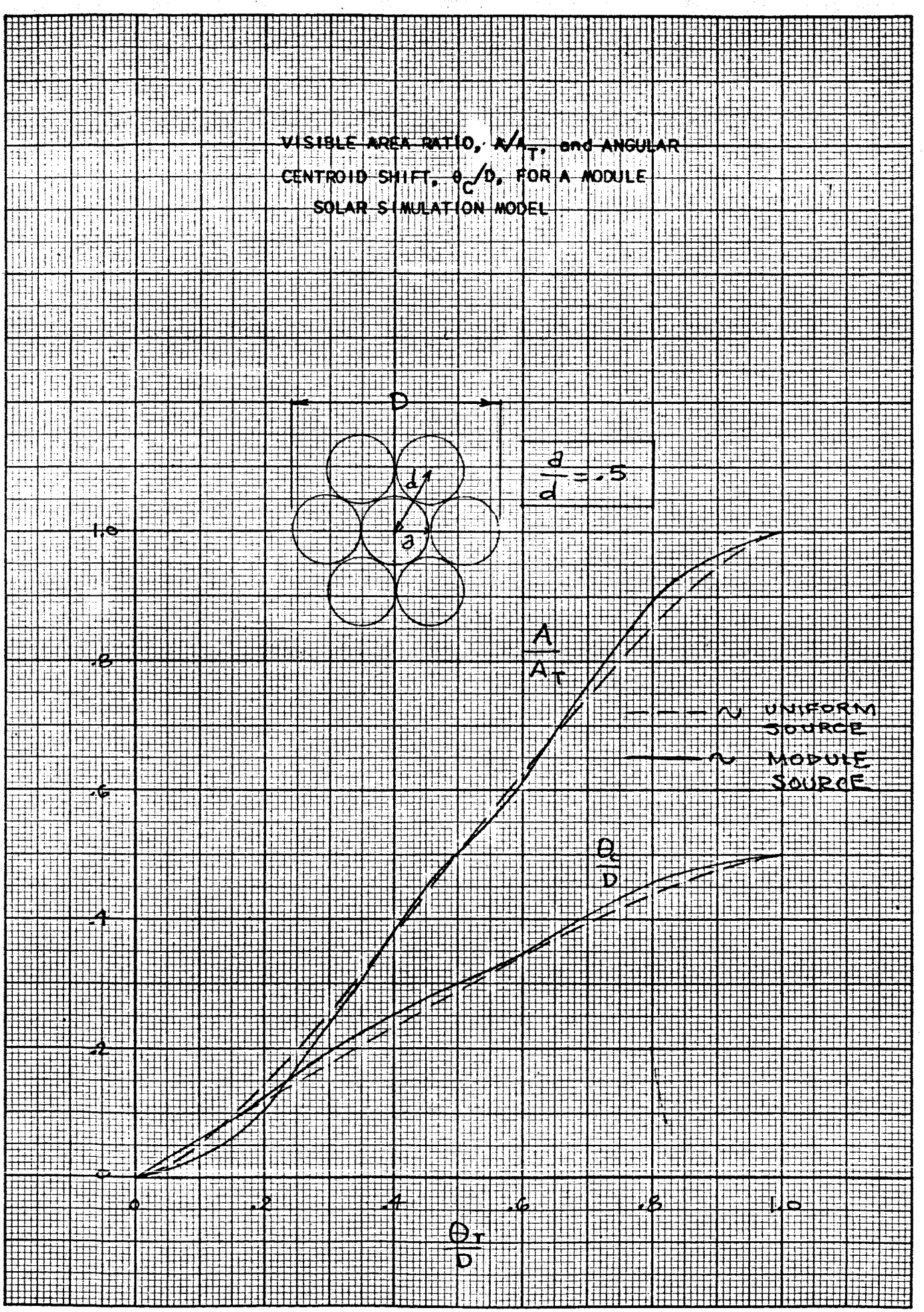

FIG. 41. Comparison of Visible Area and Angular Centroid Shift for Module and Uniform Solar Models, a/d = .5

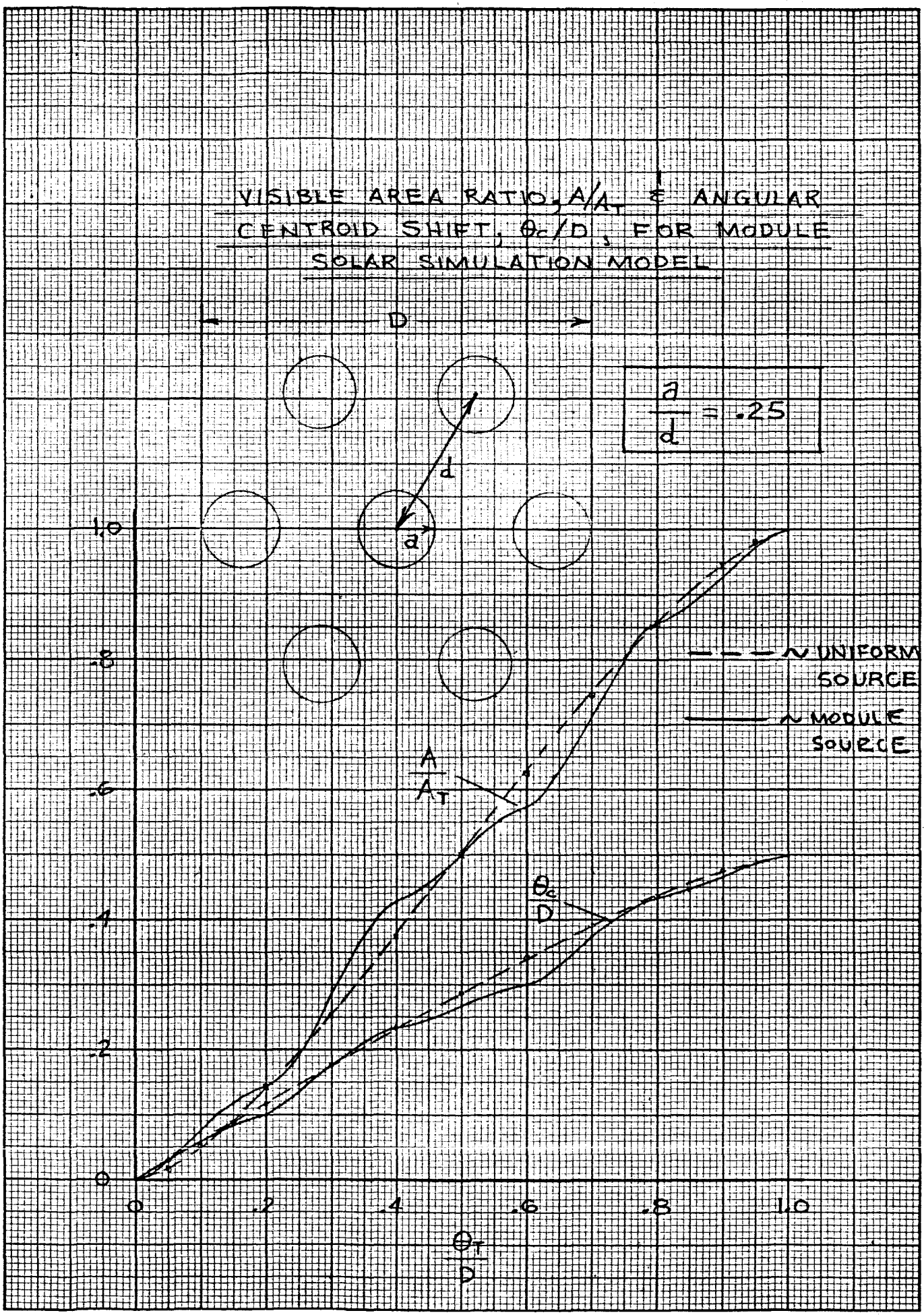

FIG. 42. Comparison of Visible Area and Angular Centroid Shift for Module and Uniform Solar Models, a/d = .25

125

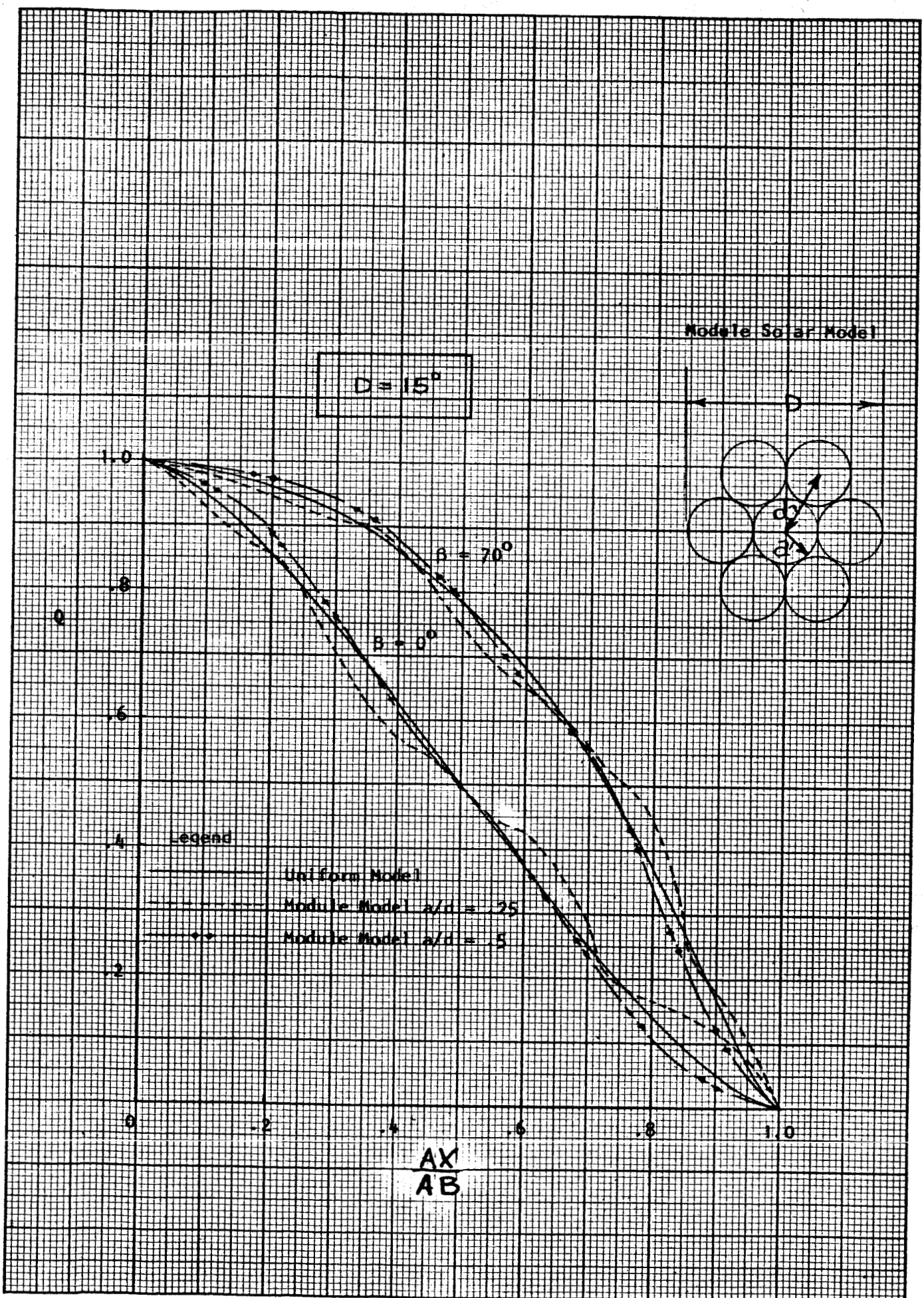

FIG. 43 Comparison of the Relative Intensity in the Penumbra of a Single Knife Edge Illuminated by Uniform and Module Solar Simulation Models. D = 15°

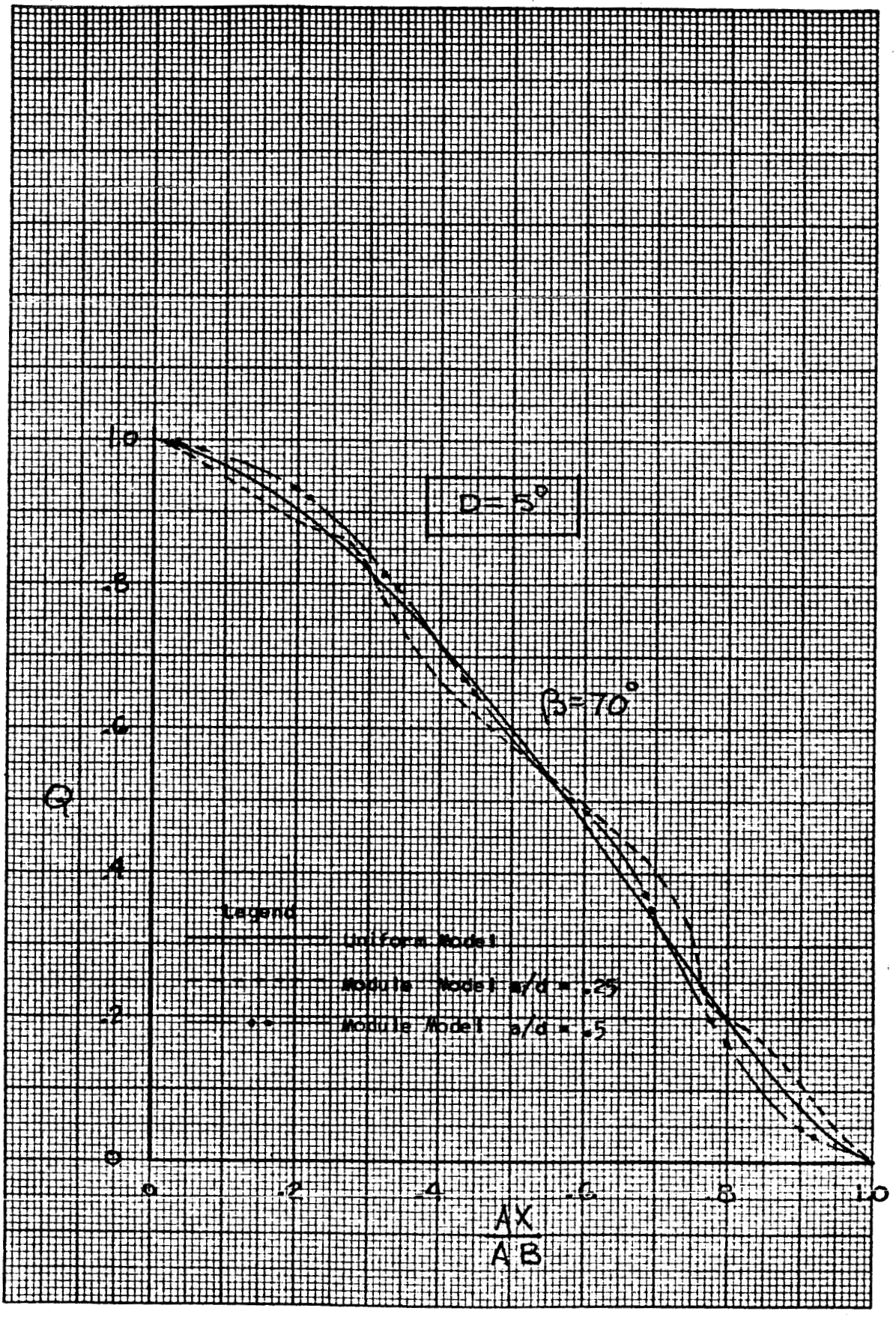

FIG. 44

Comparison of the Relative Intensity in the Penumbra of a Single Knife Edge Illuminated by Uniform and Module Solar Simulation Models D = 5°

REFERENCES

1. McAdams, William H. HEAT TRANSMISSION, Third Edition, McGraw-Hill Book Company, Inc. New York, N.Y. 1954, p.64.

2. Krieth, Frank, PRINCIPLES OF HEAT TRANSMISSION, International Textbook Company. Scranton, Pa., 1962. p.186.

APPENDIX A

EFFECT ON SOLUTIONS OF A KNIFE EDGE FIXED AT THE CONICAL AXIS AS COMPARED TO A VARIABLE POSITION KNIFE EDGE

In the solution of shaded surface problems, use has been made of equations pertaining to a single knife edge (Eqs. (2.3.1) through (2.3.6)). The solutions obtained using these equations correspond to relative energy flux density at a point in the penumbra as the knife edge is moved across the receiver. However, for other shaded surfaces, the knife edge is considered fixed at the conical axis and energy flux density distributions in the penumbra are determined.

The use of the single knife edge equations will introduce an error because of the angular differences involved for solutions corresponding to a fixed point in the penumbra as compared to a moving point in the penumbra. A comparison of the two conditions is shown in Fig. A1. (See next page.)

From Fig. A1, point P and point x "see" exactly the same fraction of the total source area. However, the angle between the power vector and surface normal vector are different. Referring to Fig. A1, the angles between the power vectors and surface normal vectors are given as

$$\psi_1 = \tan\left[\frac{\left\{\frac{D}{2} - \theta_c\right\} R}{R}\right] \qquad \text{(A1)}$$

$$\psi_2 = \tan\left[\frac{\left\{\frac{D}{2} - \theta_c\right\} R + ox}{R}\right] \qquad \text{(A2)}$$

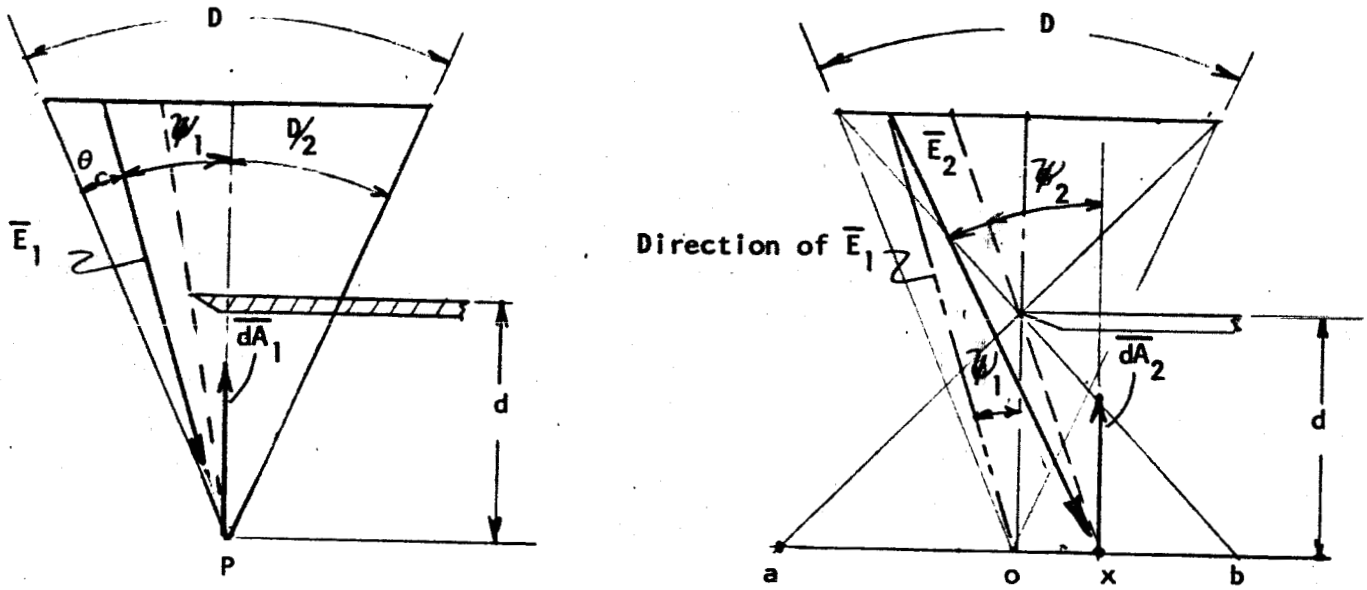

FIG. A1

From geometry

$$ox = ab - ao - xb \qquad \text{(A3)}.$$

For $R >> d$

$$ab = \frac{d\,\frac{D}{2}}{1 - \frac{d}{R}} \qquad \text{(A4)}$$

$$ao = \frac{ab}{2} \qquad \text{(A5)}$$

and

$$xb = \frac{A}{A_T} ab \tag{A6}$$

where $\frac{A}{A_T}$ is the fraction of the total source area seen by x.

Substituting Eqs. (A4), (A5) and (A6) into Eq. (A3) and combining Eq. (A3) and (A2) yields

$$\psi_2 = \tan^{-1}\left[\left\{\frac{D}{2} - \theta_c\right\} + \frac{d\,\frac{D}{2}\left\{.5 - \frac{A}{A_T}\right\}}{R\left\{1 - \frac{d}{R}\right\}}\right] \tag{A7}$$

Since $0 \leq \frac{A}{A_T} \leq 1$

$$\frac{D}{2}\left\{.5 - \frac{A}{A_T}\right\} < 1 \qquad (D \leq 15^o)$$

and for $R >> d$, Eq. (A7) reduces to

$$\psi_2 = \tan^{-1}\left\{\frac{D}{2} - \theta_c\right\} = \psi_1 \tag{A8}$$

Therefore, for $R \gg d$, the angular differences associated with solutions for a fixed point in the penumbra as compared to a moving point are negligible and the cosine of the angle between E and dA can be taken as

$$\cos\left[\beta - D\left\{\frac{1}{2} - \frac{\theta_c}{D}\right\}\right] \tag{A9}$$

where $\frac{\theta_c}{D}$ corresponds to a given $\frac{A}{A_T}$ for the single knife edge.

APPENDIX B

RELATIVE ENERGY FLUX DENSITIES IN THE PENUMBRAE OF VARIOUS SHADOWING OBJECTS

(Under Separate Cover)